POTENTIAL USE OF ^{52}FE PORPHYRINS   AS   TUMOR   SCANNING   AGENTS

by

ROY   ALAN   THALLER

B.Sc., The University of British Columbia, 1978

A THESIS SUBMITTED IN PARTIAL FULFILMENT OF

THE REQUIREMENTS FOR THE DEGREE OF

MASTER OF SCIENCE

in

THE FACULTY OF GRADUATE STUDIES

THE FACULTY OF PHARMACEUTICAL SCIENCES

DIVISION OF PHARMACEUTICAL CHEMISTRY

We accept this thesis as conforming

to the required standard

THE UNIVERSITY OF BRITISH COLUMBIA

September   1980

Department of Pharmaceutical Sciences

The University of British Columbia
2075 Wesbrook Place
Vancouver, Canada
V6T 1W5

Date Nov. 10, 1980

-6

ABSTRACT

Radioiron labelled prophyrins were tested for tumor uptake using tissue culture and animal models. The following porphyrins were tested: hematohemin; protohemin; photo-protohemin; 2-formyl-4-vinyl, 2-vinyl-4 formyl, and 2,4-diformyl deuterohemin derivatives; meso-tetra (4 carboxyphenyl) hemin (TCP); tetra-Na-meso-tetra (4-sulfonatophenyl) hemin (TPPS); and meso-tetra-(4-N-methylpyridyl) hemin tetraiodide (TMPI). ^{52}Fe was produced at TRIUMF by high energy proton spallation of a nickel target. The ^{52}Fe was separated from the other spallation products by solvent extraction with methyl isobutyl acetone and ion exchange chromatography when required. Tissue culture studies using P815 mouse tumor cells showed good uptake with protohemin, TCP, or TMPI. Mouse distribution and excretion studies indicated that the target organ for TMPI was the liver (and spleen) and its biological half-life was 270 days. Animal scans using rats with breast carcenomas with ^{52}Fe labelled protohemin, TCP and TMPI showed no tumor uptake at all. The radiation dose to a human was also calculated.

TABLE OF CONTENTS

LIST OF FIGURES

LIST OF TABLES

ACKNOWLEDGEMENT

I   INTRODUCTION

In the past, porphyrins have been used to detect external
and gastrointestinal tract tumors in humans. Exposure of
the tumor to ultraviolet light causes the porphyrin and
the tumor to fluoresce a red light. Because the tumor has
to be exposed to ultraviolet light and observed visually
this limits this type of tumor detecting agent to certain
accessible parts of the body.

The purpose of this research was to determine if radio-
actively labeled porphyrins were still taken up by tumors
and if this radiopharmaceutical could be used as a tumor
scanning agent in nuclear medicine. A number of porphyrins
were synthesized, labeled with radionuclides and tested for
tumor uptake. The radionuclide of major interest was radio-
active iron because the iron-porphyrin complex was very stable
both in vivo and in vitro.

II   LITERATURE REVIEW

A   Tumor Structure and Physiology

A tumor or neoplasm is defined as an abnormal mass of tissue,

the growth of which exceeds and is uncoordinated with that of

normal tissue. (1)   It can be classified as a benign or malig-

nant tumor according to its clinical and morphological features.

A benign tumor is a tumor which grows slowly and stops growing

when it reaches a certain size.   It is composed of well-

differentiated mature tissue imitating normal tissue.   Death

only results if the tumor interfers with a vital organ.

A malignant tumor usually grows very fast.   It grows by

expansion but also by infiltration and invasion of surrounding

tissue.   It is unencapsulated and poorly demarcated.   However,

it is possible that a malignant tumor may be encapsulated and

localized.   A malignant tumor tends to metastasize and spread

to other parts of the body.   Removal of the primary tumor

usually results in the recurrence of a tumor at the same site.

Necrosis and ulceration is very common.   Death results from

this rapid cell expansion even if a vital organ is not involved.

Cells are undifferentiated and lack adequate maturation.

Metastases from the primary tumor can spread to other parts of

the body by the lymphatics, blood stream and by implantation.
Metastic tumors are common in the lungs, liver, bones, kidneys,
lymph nodes, and adrenal glands but rare in the spleen and
skeletal muscles.

No single agent is responsible for causing cancer and one agent
may cause cancer of one organ while another agent is required
to cause cancer of another organ. Viruses cause sarcomas in
animals but there is no direct evidence of this in man. Over
90% of all carcinogens are mutagens. It is believed that
greater than 80% of all cancers are caused by environmental
carcinogens. Chemical carcinogens are able to alter the cell's
DNA or RNA structure, resulting in new or disrupted protein
production. The new proteins may transform normal cells into
cancer cells by activating latent viruses or changing the cell's
environment (hormonal balance). Radiant energy (ultra-violet)
and ionizing radiation may produce cancer by altering the DNA
structure of a normal cell.

Carcinogenesis and tumor growth can be divided into three phases:
malignant transformation, tumor development, and tumor evolution.
A transformed cell continues to divide to form a clone of trans-
formed cells. If a clone does not acquire a blood stream, it
will not continue to divide and may die. Other factors which
will determine the fate of a clone includes the body's immune

system and chalones. The established clone is then controlled by hormones, growth factors, and immune system blocking factors produced by the body. The tumor may differentiate into a benign tumor or dedifferentiate into a malignant tumor.

During transformation, the plasma membrane of the cell changes completely. All processes involving the membrane such as growth, regulation, metabolism, differentiation, etc. are altered. The levels of carbohydrate, glycoprotein, glycolipid, and glycosaminoglycan may increase or decrease depending on the type of cancer. The level of complex glycolipids may decrease but more are exposed on the cell surface so that they can interact with antibodies, enzymes, and lectins. Important glycoproteins required for control and regulation may also disappear while new glycoproteins preventing immune killing may appear on the cell surface.

Increased transport of sugars, some amino acids, and phosphates occur in transformed cells. Increased transport of sugars is due to the increased maximum velocity of the transport enzymes and not due to faster inside trapping by phosphorylation. Small changes in transport activity could dramatically affect cell growth when marginal nutrient concentrations are available in the surrounding environment.

B   The Role of Tumor-Imaging Radiopharmaceuticals in Oncology

Many techniques are available to diagnose and localize tumors
in the body. These include nuclear techniques, ultrasound,
thermography, zeroadiography, angiography and other radiological
procedures. This dissertation will limit itself to the use of
Nuclear Medicine. Nuclear medicine techniques are fast, sensitive,
noninvasive, and provide an indication of tumor and body metabolism.
Nuclear medicine scanning procedures should not replace other
diagnostic procedures, such as physical examination, laboratory
tests, and X-ray studies. However, in some instances they sould
be used before other invasive techniques.

Tumor scanning agents can be divided into three groups: non-
specific, limited use agents; specific limited use agents; or
specific general use agents.

Nonspecific limited use agents identify space-occupying lesions
or displacement or alteration of normal tissue only. There is
no specific uptake in tumors. They are usually limited to one
organ or system. Multiple scans and other diagnostic procedures
are required to determine the presence of a tumor.

Specific limited use agents are specific for one type of tumor or
tumors limited to one organ. Radioiodine for thyroid tumors,
iodocholesterol for adrenal tumors, or radiolabeled tumor anti-

bodies to one type of tumor fit into this group.

Specific general use agents should be taken up by all tumors and not limited to one type of organ. ^{67}Ga-citrate and ^{111}In-labeled bleomycin are general use agents but not too specific and are taken up by nonmalignant processes.

The choice of radiopharmaceutical and/or radionuclide to be used in nuclear medicine is determined by:(2)

1) Physical properties of the radionuclide
   a) Energy and intensity of photons or particles emitted
   b) Half-live
   c) Purity
   d) Availability
2) Biophysical and chemical properties of the agent affecting distribution and turnover in the body.
3) Tissue transmission and scattering
   a) Depth of the site of interest
   b) Absorption coefficients of local tissue
4) Characteristics of the imaging system:
   a) Sensitivity to local and distributed sources
   b) Energy discrimination
   c) Intrinsic resolution for given photon energy
   d) Resolution time
   e) Focal distance

C   Tumor Imaging Radiopharmaceuticals

Tumor imaging radiopharmaceuticals fall into the following

catagories: Metabolite Related Agents, Radionuclides and other

Agents, Radiolabeled Antitumor Agents and Radioiodinated Agents.

1 Metabolite Related Agents

a) ^{11}C-Aspartic acid

Increased uptake was observed in an implanted Walker carcinoma

in the thigh of a rat. (3) Tumor uptake may be due to in-

creased rate of protein synthesis.

b) ^{11}C-Carboxyl 1-aminocyclopentane-carboxylic acid (ACPC)

This agent showed very rapid and uniform blood clearance, only

25% remained in the blood after five minutes. Urinary excretion

was only 1.1% indicating that it was not lost by decarboxylation.

The organ of greatest uptake was the liver, followed by the

spleen. Other organs such as blood vessels, heart, salivary

glands, nasopharynx, kidneys and breasts were also imaged.

In one clinical study using single photon detection, more

lesions were detected with this agent than with ^{67}Ga-citrate. (3)

However, the number of malignant lesions was not determined.

Infectous lesions and areas of previous surgery were visualized

faintly. Based on target to nontarget ratios, ^{67}Ga was better,

but the agent may be useful in imaging abdominal lesions.

c) ^{11}C-Methylated polyamine analogs

Increased uptake was observed in mouse tumors and the prostate gland of a dog was imaged. Methylated putrescine was nontoxic and had lower kidney activity than methylated spermine or spermidine. (4)

d) ^{18}F-S-flurouracil

Animal studies showed some tumor uptake but also high background levels. (5-6) Uptake may be due to increased RNA synthesis by tumors.

e) ^{13}N-Ammonia

This radiopharmaceutical was taken up by the liver, brain, kidney, heart, salivary glands and bladder. (7) The very rapid blood clearance allowed very fast dynamic studies to be done. (8) Tumor uptake may be due to ion exchange or it may be incorporated into other metabolites. (7) Implants of Morris hepatoma in the flank of rats were well visualized in 30-40 minutes. (9)

f) ^{13}N-Glutamine and ^{13}N-Glutamic acid

Tissue distribution was similar to ^{13}N-ammonia except that it was heavily concentrated in the liver with no cardiac uptake. Tumor uptake varied from 53% of liver uptake in mice with fibrosarcoma to 123% of liver uptake in mice with polyoma. (10)

g) ^{75}Se-L-selenomethionine

Due to the physical properties of ^{75}Se, high energy gamma

ray emission and long T½, only small doses barely sufficient

for reasonable imaging can be given without excessive patient

irradiation. Multiple window cameras must be used due to the

low abundance, multi-energy photon emission characteristics of

^{75}Se. The metabolic activities of methionine and ^{75}Se-L-seleno-

methionine is similar but not identical. (11) Tumor localization

with this agent was due to an increased rate of protein synthesis

(12-13) and DNA synthesis. (14) Uptake via DNA synthesis was

assumed but not proven. There was some relationship between

uptake and vascularity with liver tumors. (14) However,

pancreatic tumors having a greater vascular supply and increased

rate of protein synthesis accumulated less agent than less

developed tumors. (15)

^{75}Se-L-selenomethionine was orginally developed as a pancreatic

and parathyroid scanning radiopharmaceutical. (16-18) It was

first used as a tumor scanning agent when heavy uptake was seen

in a lymphosarcoma during a routine pancreatic scan. It also

has been used to diagnose and localize the following conditions:

neuroblastoma (19), hepatoma (20), staging of Hodgkin's disease

(24), lymphoma (13, 21-22), thynoma (23), thyroid lesions (24)

and metastatic melanoma (25). Since it has poor specificity and

unsuitable gamma ray emission it is no longer used as a general

tumor scanning agent. However, it is still used routinely to image the pancreas and pancreatic neoplasms which usually give rise to cold spots and rarely hot spots. (26)

2 Radionuclides and Other Agents

a) Arsenic

^{74}As was used to detect brain tumors but the high energy emmission make imaging difficult and expose the patient to high radiation doses. (26)

b) Bismuth

^{206}Bi acetate gave very high tumor to background ratios but the radiation dose to the kidneys was very high. (27-29) Imaging with conventional devices was difficult due to high energies. Bi may react with sulfhydryl groups in tumor tissues. (30)

c) Copper

^{64}Cu-citrate was similar to ^{57}Co-bleomycin with less accumulation in inflamatory tissue by 24 hours. (31-32)

d) Cesium

The exact mechanism of uptake was not known but was believed to be similar to potassium and rubidium. (33-34) Early uptake was due to the increased vascularity of the tumor because

initial distribution was proportional to fractional organ blood flow. (35-37) Metabolic processes of the tumor may account for some of the uptake. (34, 38-39) High uptake was observed in the liver and to a lesser extent in the kidneys, fundus of the stomach and spleen.

^{131}Cs was used to image malignant superficial and supra-diaphragmatic tumors. (35) When combined with ^{131}I it was used to detect thyroid tumors. (40-41) ^{129}Cs has been used to detect thyroid tumors and to image pulmonary tumors. (42) Increased Cs uptake in normal tissue made it difficult to detect tumors below the diaphram. Cs was not taken up by tuberculosis lesions as ^{67}Cu was. (42)

e) Cobalt

^{58}Co-citrate and ^{58}Co-bleomycin seem to have the same tumor specificty and tumor/normal tissue ratios. (43)

f) Gold

^{198}Au-chloride bound strongly to proteins in the blood and showed very high uptake by tumors but no clinical studies have been done. (44)

g) Indium

^{111}In-chloride showed poorer tumor affinity than Ga but had

superior physical properties for imaging. (45) However,
very little was excreted into the GI or GU system making
abdominal scanning easier. ^{67}Ga was clinically superior
and gives better tumor to liver-spleen-muscle and blood
ratios. (46-47) Clinical studies have shown 100% (48)
and 79% (49) sensitivity but the agent was nonspecific.
However, it was considered to be a very good brain tumor
scanning agent that was better than bleomycin, ^{67}Ga,
all pertechnetate compounds. (50) Recent uses include
imaging of head and neck tumors (51) and soft tissue
component of bone sarcomas. (52) Facial uptake was lower
than ^{67}Ga. Tumors near high bone marrow uptake cannot be
imaged. No difference was observed between ^{111}In-chloride
and ^{111}In-citrate in clinical studies. (53) Also no difference
between ^{111}In-fluoride,-acetate,-lactate, and -HEDTA was
observed in uptake using sterile granulomas. (54)

h) Mercury

^{197}Hg-chloride has been used to detect face and neck (55-56),
breast (57-58), thyroid (59), brain (60), lung (55, 57, 61-67)
and kidney tumors. (68) Animal studies done on mice using
transplanted Ehrlich ascites cell carcinomas suggested that
this agent was much better than ^{111}In-chloride, and ^{67}Ga-
citrate. (69-70) However, clinical studies indicated that this
agent was no more specific than any other general tumor

scanning agent. (71) Benign tumors did not take up this agent but uptake by inflammatory lesions was as high as the tumor. (71-73) The very high radiation dose to the kidneys limited the use of this agent.

^{197}Hg-1-mecuri-2-hydroxypropane has been used as a spleen tumor scanning agent. Healthy spleen tissue sequestrate red cells damaged by this agent whereas tumors do not. (74)

^{197}Hg-chlormerodrin was used to image face and neck (75-76), breast (75), lung (75), eye (76), brain (78-79), and kidney (68) (cold spot) tumors. Benign and malignant tumors however, cannot be differentiated. High radiation dose to the kidneys and Compton scattering due to low energy emmission limited the usefulness of this agent.

i) Selenium

A clinical study using ^{75}Se-selenite with a number of hepatic lesions indicated that this agent was more tumor specific than gold or sulfur colloid. Negative scans were reported in 15 patients with benign lesions, while 43 patients with malignant tumors all had positive scans. (80)

j) Technetium

^{99m}Tc-pertechnetate has been used to image and detect brain

(81-85), thyroid (85-87), breast (88-89), salivary gland

(90-92), eye orbital (93), spinal (94) and extracranial (95)

tumors. Brain imaging was about 80-90% reliable with about

10% false negative. (96) Most thyroid tumors did not localize

both iodine and ^{99m}Tc as well as normal tissue (cold spot).

However, some tumors trapped but not organified showing

increased pertechnetate uptake but not iodine. (85) (97-98)

Thyroid metastases may not be imaged early with this agent,

therefore iodine must be used. Imaging of breast cancer with

this agent has low reliability and high rate of false negatives

(20%). Warthin's tumors of the salivary gland produce hot

spots while other tumor types produce cold spots. Scanning

was of no diagnostic value but helped localize the tumor

exactly before surgery.

k) Thulium

^{170}Tm is very similar to ^{169}Yb. It is not produced commercially.

^{99m}Tc compounds have replaced this agent for bone scanning but

it may still be of value for soft-tissue tumor scanning.

l) Thallium

^{201}Tl-chloride did not show any tumor uptake using animal

studies. Lung cancer was first detected with this agent during

routine myocardial imaging. A clinical study involving 15

patients showed that it was not superior to ^{67}Ga-citrate

(^{201}Tl 73.3% positive and ^{67}Ga 75% positive).

^{201}Tl was used for detecting neck and chest tumors (99) and Hodgkin's lymphoma (100). The advantages of this agent over ^{67}Ga were that scans could be done as early as 5 - 10 minutes after injection and it did not concentrate in bone or bone marrow, making tumor imaging of the mediastinum easier. The disadvantages were that it concentrated in abdominal organs like ^{67}Ga and the low energy of the mercury X-rays made deep seated tumor imaging difficult.

m) Xenon

Fatty neoplasms and liposarcomas were detected using this lipid soluble inert gas. One clinical study involving 3 patients with recurrent liposarcomas showed that the tumor could be imaged after rebreathing ^{133}Xe for 5 minutes. (101)

n) Ytterbium

Of all the radiolanthanides only ^{170}Tm, ^{169}Yb and ^{177}Lu bind strongly to plasma proteins and have tumor affinity. Higher lanthanides were taken up by the bone, while lower lanthanides were taken up by the RE system. (102-104) Uptake of ^{169}Yb-citrate by normal tissue was much lower than that of ^{67}Ga-citrate. Bone uptake was about two times higher than ^{67}Ga.

Carrier in the preparation reduced tumor affinity and increased the background. In a clinical study of over 400 patients in 10 hospitals the overall positive rate was 65.3% (33.3-89.5%) and the false positive rate was 29.2% (0-62.5%). The positive rate also varied by anotamical region-extremites and pelvic area 100%, head and neck 78.5%, lung 77.8% and abdomen 48.3%. (105-106)

o) Gallium

^{67}Ga-citrate is the most common general tumor scanning agent used in nuclear medicine today. Injected ^{67}Ga-citrate binds to transferrin and less tightly to haptoglobin, albumin, and leukocytes. The tumor takes up the transferrin-^{67}Ga complex. Uptake due to the accumulation of labeled lymphocytes, plasma cells, granulocytes, and macrophages around or in the tumor does not account for the high uptake. (107) Once the ^{67}Ga is inside the cell it binds to gallium binding granules (GBC), which are lysomal in nature. (108) This was confirmed by other people (109-110) using subcellular fractionation techniques. A microsomal fraction which binds Ga has also been discovered. (111)

Normal liver takes up Ga. Studies done have indicated that it binds to liver lysosmes. However, when the protein that bound the Ga was isolated from the lysosomes it turned out to

be transferrin. Therefore, liver uptake was due to endocytosis of the Ga-transferrin complex. (112) It is not known if tumors contain more lysosomes or have higher endocytosis activity than normal cells.

There is some form of relationship between ^{67}Ga uptake and the rate of DNA syntheses. (113) It is not known if ^{67}Ga binds or interacts with DNA.

Uptake by experimental inflammatory lesions was due to direct uptake of the ^{67}Ga by the bacteria in the lesions (114) or by ^{67}Ga labeled polymorphonuclear leukocytes (PMN). (115) PMN's had a higher affinity for ^{67}Ga than lymphocytes, while red blood cells had no affinity. However, only 20% of the total uptake was accounted for by direct uptake by bacteria and PMN's; the remaining 80% was in a soluble fraction.

The biological distribution depends on the time the scan is taken after injection and the age of the patient. The renal cortex takes up the highest amount after injection. After the first 24 hours the Ga shifts from the renal cortex to the bone and lymph nodes. After the first week it shifts from the bone and lymph nodes to the liver and spleen.

Children have increased blood flow to the epiphyseal plate areas

of growing bone with a symmetrical relative increased uptake in these regions; and increased thymic and splenic uptake. (116)

About one third of the dose is excreted during the first week after injection. About 25% of the dose is excreted by the kidneys during the first 24 hours. About 10% is excreted via the GI tract during the first week. The remaining 65% after the first week is distributed through out the body. Within 48 to 72 hours after injection about 5% of the dose concentrates in the liver, 1% in the spleen, 2% in the kidneys, and 24% in the skeleton including bone marrow. The adrenal gland, bowel, and lung concentrate a fair amount. Uptake by muscle, brain, fat, blood and skin is low. (117).

The general indication for a ^{67}Ga scan is (i) Adjunct to the diagnosis of suspected primary or metastatic malignancy, particularly bronchogenic carcinoma, Hodgkin's disease, and certain lymphomas. (ii) Staging of appropriated malignances. Scans may be of adjunctive value, or may aid in the planning of laparotomy, lymphangiography, or other staging procedures. It is particularly valuable for staging disease in patients for whom invasive procedures are contradicted. It also may be useful in locating metastases in sites not easily examined by invasive methods (skull etc.). (iii) Follow up of patients who have received surgery, radiation therapy or chemotherapy for malignant

diseases that can be imaged before therapy, and long term noninvasive follow up to ensure against asymptomatic recurrence of tumors. (iv) Search for occult malignancy when the patient presents symptoms suggestive of neoplastic disease but without demonstrable or confirmable disease by other methods. (v) Helping in diagnostic differentation between cerebral vascular lesions and brain tumors. (118)

^{67}Ga is known to accumulate in the following benign or non-malignant processes: angioimmunoblastic lymphadenopathy (AILD) (119-121), myelofibrous (120), secondary syphilis of the myocardium (122), parathyroid adenoma (123), pancreatitis (124), pseudocysts of the pancreas (125), liver benign hepatic adenoma (focal nodular hyperplasia) (126-127), liver actinomycosis (128), postoperative intraabdominal abscesses (129-131), Crohn's disease (132), active ulcerative colitis (133), peritonitis (134), other GI inflammatory foci (135), osteomylitis (136), cellulitis (136), cerebral infarctions, myocardial infractions, fractures, Paget's disease, pyelonephritis, pneumonia, active tuberculosis, active sarcoidosis, sialoadenitis, gastritis, surgical wounds, rheumatoid arthritis, lactating breast, gynecomastic, and other sites of bacterial or mycotic infection or inflammation. (138)

^{67}Ga-citrate does not accumulate in the following benign processes: benign neoplasms, cystic disease of breast, liver, or

thyroid, cirrhosis, hemangioma, inactive tuberculosis reactive lymphadenopathy, cerebrovascular accident and encephalitis. (138)

^{67}Ga-citrate is greatest value in detecting bronchogenic carcinomas irrespective of cell type. The sensitivity for detecting lung cancer in one study involving 489 studies was 93%. (137) ^{67}Ga scanning is useful in preventing unnecessary thoractomies and detecting disseminated forms which cannot be cured by surgery. A negative scan with negative radiological, clinical, and cytological examination rule out the possibility of a tumor.

^{67}Ga is useful in staging of Hodgkin's disease, especially in patients for whom lymphangiography is contradicted. The useful-ness for monitoring therapy is not known. The scan is of great value in following patients who are asymptomatic. Early studies indicated that the sensitivity for detecting Hodgkin's disease was 76%. (139) This was later confirmed by other studies, 90% (140), 88% (141), and 87% (142).

^{67}Ga is less sensitive in detecting non-Hodgkin's lymphomas than Hodgkin's disease. Sensitivity varies on the type of lymphoma and anatomical regions. In one study (142) with 167 cases of untreated lyphomas, 78% had one or more positive sites on the scan. Only 51% of the histologically proven sites were positive.

A negative scan does not rule out the disease. Sites were detected on the scan which were not detected by other methods. A positive scan indicates disease but a negative scan does not rule out the disease.

^{67}Ga is useful in detecting tumors more specifically than a routine brain scan. A ^{67}Ga brain scan should be done if: (143-147) Uptake on conventional scan is equivocal. Follow up scanning a patient recovering from craniotomy. Scanning patients with a primary neoplasm that metastasizes frequently to be brain. Helping in diagnositic defferentiation between cerebral vascular lesions and brain tumors. Uptake by infarcts lower than tumor uptake or not at all (143), but one study did get increased uptake. (144) This may have been due to carrier Ga in the preparation.

Scans are of no value in the initial diagnosis of acute leukemia but are helpful in following therapy and recurrences of focal involvement. (148)

In patients with breast carcinoma undergoing therapy the positive rate was 54% and 14 out of 21 (67%) in patients not undergoing therapy. (149) Routine liver and bone scans are more sensitive than ^{67}Ga scans in detecting secondary tumors. The scan may be of some value in detecting mediastinal involvement but the scan is not used routinely. (150)

The ^{67}Ga scan is very important in the staging of testicular
tumors. Testicular tumors are similar to lymphomas and
usually asymptomatic. Total bowel cleansing is important to
obtain good images. One study showed a 43/46 (94%) detection
rate with no false positives and 3/21 (14%) false negatives. (151)

^{67}Ga scans are of no value in detecting prostatic carcinomas,
prostatic bone metastases, bladder tumors or urethra tumors.
Kidney tumor detection rate was 32% with a very high incidence
false positives (77%). (152)

^{67}Ga scanning is useful for head and neck tumors with a detect-
ability rate of 87% and 7% false positive rate (squamous cell
carcinoma), however only 77% of secondary sites were detected
(80). Patients receiving radiation therapy produced a high level
of false negative scans. (153-154)

^{67}Ga usually detects primary and to a lesser extend, secondary
bone tumors, but the bone scan is much more sensitive. (155)

Carcinomas of the thyroid and subacute thyroiditis accumulate
^{67}Ga while benign tumors do not. Scanning is of little diagnostic
value. (156-157)

3 Radiolabeled Antitumor Agents

a) Bleomycin

Bleomycin is an oncostatic polypeptide produced by the
organism Streptomyces veriticillus. Normally copper is
bound to the alpha-amino group and the carbamoyl group of
the beta-amino-abanylamide residue. The copper ion can be
displaced by other metal ions. It had been labeled with
[57]Co (158-159) (162-164), [67]Cu (158,165-167), [62]Zn (184),
[111]In (158-159, 154, 168-169), [67]Ga (163), [99m]Tc (158-159, 162
168,170), [51]Cr (159,171), [239]Np (172), [237]U (172), [140]La (172),
[153]Sm (172), [195m]Pt (173) and [203]Pb. Divalent cations of Cu,
Ni, Co and Zn are most stable in vitro. However only Co is
stable in vivo. (158-161,174)

[57]Co-bleomycin was used to image tumors of the lung, brain,
stomach, oesophagus, and pancreas. (175-179) Gliomas were
also differentiated from other brain tumors using this agent.
This agent also localizes in abscesses and inflammatory lesions
like ^{67}Ga-citrate. Studies done using this agent and [57]Co in
experimental tumor models have showed no difference between the
two in tumor uptake. (43) However, subcellular distribution
studies indicated that [57]Co-chloride and [57]Co-bleomycin bound
to different particles while ^{111}In-chloride and ^{111}In-bleomycin
bound to the same particle. Bleomycin also bound to DNA (180)
causing strand scission uncoiling of the helix and decreasing

its melting point. (181-182)

^{99m}Tc-bleomycin was similar to ^{111}In and ^{57}Co-labeled bleomycin complexes. Adenocarcinomas were well imaged but malignant lymphomas were not, due to the high blood and abdominal activity. (183) This indicated that the ^{99m}Tc dissociated off the bleomycin.

^{111}In-bleomycin is the only commercially available labeled bleomycin. It is unstable in the body, Cu ions displace the ^{111}In ions from the molecule. (184) Free ^{111}In binds to plasma proteins. There was no advantage in using this agent or ^{67}Ga. Probably similar results will be obtained if ^{111}In was injected by itself. There was lower abdominal uptake with this agent that ^{67}Ga allowing easier detection of pelvic tumors.

Uptake studies using ^{123}I-bleomycin have shown that it has higher tumor/blood and tumor/liver ratios than ^{67}Ga or ^{57}Co-bleomycin in mice. (162)

4 Radioiodinated Agents

a) Chloroquine analogs

Chloroquine is a drug used to treat malaria. The radioiodinated analog of chloroquine (NM115) was found to concentrate in dermal (185-187) and ocular (188-189) melanotic melanoma. Clinical

use was limited by the high uptake in the lungs and excretion from liver via bile into the GI tract. One interesting use of this agent was in using ultrasound first to localize the tumor and measuring uptake with a detector to determine if the tumor was a melanoma. (190) A new analog may be used in the future because it is more specific. (191)

b)   Iodocholesterol

Radioiodinate cholesterol, an organ specific tumor scanning agent, concentrates in the adrenal gland. The agent was shown to be most helpful in:(192) Differentiating Cushing's syndrome from hyperfunctioning adrenal cortical adenoma, lateralizing aldosteronomas. Detecting post-adrenalectomy remnants in patients with persistent corisol excess, diagnosing androgen-secreting and cortisol excess syndromes before conventional methods and diagnosing cortical carcinomas in patients whose adrenal vein cannot be catheterized or are hypersensitive to contrast medium.

D   Porphyrin Nomenclature

Porphyrins are related to the fundamental structure of porphin, which consists of four pyrrole-like rings linked by four CH groups or methane bridges in a ring system, $C_{20}H_{14}N_4$ (Fig. 1). The porphyrin structure contains a central 16-membered ring formed from 12 carbon and 4 nitrogen atoms contributed by 4 pyrrol rings. The

positions assigned to the alternating double and single bonds of porphyrin are arbitary due to resonance structures. By the addition of various side groups different types of porphyrins can be obtained (Table I).

There are two systems of nomenclature, one the Fischer approach and a more updated approach from the Commission on Nomenclature of Biological Chemistry. (193) Only the latter approach will be discussed. The updated approach uses a new ring numbering scheme but retains the trival names of most porphyrins rather than the new chemical name. Trival names are still used for iron complexes or porphyrins. These are shown below:

Heme--An iron porphyrin complex

Ferroheme-An iron (II) porphyrin complex

Ferriheme--An iron (III) porphyrin complex

Hemochrome-A low-spin iron porphyrin complex with one or
    more strong field axial ligands (eg pyridine)

Hemin--A chloro(porphyrinato) iron (III) complex

Hematin-An hydroxo(porphyrinato) iron (III) complex
    (anhydro or u-oxo dimers)

E   Porphyrin Uptake by Tumors

The first reported uptake of porphyrins by tumors was in 1942. (194) This was later confirmed by other people studying the carcinogenic action of both porphyrins and methylcholanthrene in mice. (195)
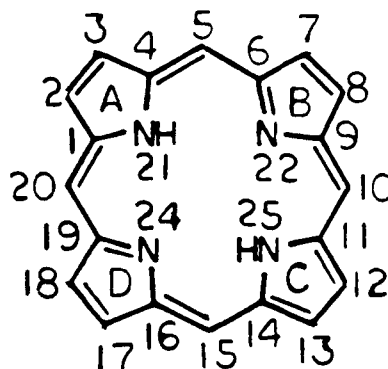
Fig. 1 Porphyrin Structure

TABLE 1
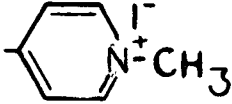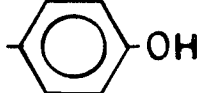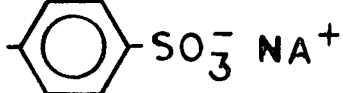
PORPHYRIN STRUCTURES

	Positions							
	2	3	7	8	12	13	17	18
Hematoporphyrin	M	HE	M	HE	M	P	P	M
Protoporphyrin	M	V	M	V	M	P	P	M
Photoprotoporphyrin	M	V	M OH	FE	M	P	P	M
	M OH	FE	M	V	M	P	P	M
2-Formyl-4-vinyl Deuteroporphyrin	M	F	M	V	M	P	P	M
2-Vinyl-4-formyl Deuteroporphyrin	M	V	M	F	M	P	P	M
2,4-Diformyl Deuteroporphyrin	M	F	M	F	M	P	P	M

	5	10	15	20
meso-tetra(4-N-methylpyridyl) porphine tetra I	MP	MP	MP	Mp
meso-tetra(4-car-oxyphenyl) porphine	CP	CP	CP	CP
tetra-Na-meso-tetra (4-sulfantophenyl) porphine	SP	SP	SP	SP

———————— cont.

TABLE 1 CONT.

Where:

M = –CH$_3$ (methyl)

F = –COH (formyl)

HE = –CHOHCH$_3$ (hydroxyethyl)

P = –CH$_2$CH$_2$COOH

V = –CH=CH$_2$

FE = =CHO (formylethylidine)

MP =

CP =

SP =

Hematoporphyrin injected IP concentrated in subcutaneous sarcomas causing the tumor to fluoresce a red colour under ultra-violet light. A further study done by the same group using normal and tumor bearing animals (including methylcholanthrene induced spindle cell fibrosarcomas and rhabdomyosarcomas; transplanted mammary adinocarcinomas, fibrosarcomas; and spontaneous mammary carcinomas) has shown that hematoporphyrin, protoporphyrin, mesoporphyrin, coproporphyrin, and zinc hematoporphyrin were all taken up by the tumors. (196) Also other nontumor sites including injury sites, placenta, developing embryos and lymph nodes (197) accumulated some porphyrins. Another more detailed study also showed that metallo-porphyrins were taken up by tumors. (198)

The first clinical study using hematoporphyrin in 1953 showed no tumor uptake. (199) Injected doses were kept low (less than 120mg/patient) due to the reported toxicity of hematoporphyrin. (200) The toxicity was due to the phenol in the product not the agent itself. Definite tumor uptake was reported using phenol-free hematoporphyrin at doses of 500-1000mg/patient with no toxicity. (201) The porphyrin was infused over a period of 3-12 hours. Squamous cell carcinoma of the tongue and penis; adenocarcinoma (signoid colon, rectum, ascending colon); olfactory-grove meningiona; and carcinoma of the breast all showed positive porphy-rin uptake.

Adenocarcinoma of the prostrate, ependynoma of the cervical cord,
and fibrotic abscesses of the breast did not take up the porphyrin.
They reported that this technique was very useful in detecting
tumors and visualizing them during removal surgery.

Quantitative studies using animals were done later using hemato-
porphyrin. (203) Porphyrins following injection were chemically
separated from the tumor and muscle tissue and assayed by both
fluorometric and spectrophotometric procedures. Only the tumor of
the rat (Walker carcinoma-sarcoma) and the Harderian gland of the
eye (203) showed positive uptake by fluorescence at autopsy. Total
uptake by muscle tissue was zero by fluorescence while hematopor-
phyrin uptake increased to 10μg/g at 24 hours and decreased again
to 2μg/g at 120 hours after injection. Increasing the injected
hematoporphyrin dose increased tumor uptake up to a maximum of 80 mg
hematoporphyrin per animal. Higher doses did not increase tumor
uptake. After hematoporphyrin administration both protoporphyrin
and deuteroporphyrin were found in the tumor tissue. It was assumed
that hematoporphyrin was converted to the other porphyrins in the
tumor rather than before it entered the tumor. This was suggested
because ^{14}C incorporated into the carbon of the hydroxymethyl group
of hematoporphyrin dimethyl ester incubated with bone marrow cells
only 5% was found in protoporphyrin and 15% in carbon dioxide. (204)

Another interesting theory to explain tumor uptake by porphyrins

was that only human tumor tissue contain a phospholipid material
called "malignolipin" which specifically bound the porphyrin. (205)

Due to the increasing use of hematoporphyrin its toxicity had to be
studied. The MLD_{100} for white mice was 0.3mg/g body weight for
crude hematoporphyrin and 0.15mg/g for the derivative (see below).
Also the derivative was shown to be a better photosensitizer than
the crude hematoporphyrin. Contrary to other people, other drugs
including protoporphyrin did not modify its photodynamic action.
(206)

Commercial hematoporphyrin was usually contaminated with other
porphyrins. (207) A hematoporphyrin derivative was prepared by
dissolving the crude mixture in glacial acetic acid: concentrated
sulfuric acid (1:15), filtering, and precipitating the derivative
by neutralization with 15 to 20 volums of 3% sodium acetate. The
derivative was a better tumor localizing agent than the crude mix-
ture with lower toxicity limits and patient doses. There was also
minimal accumulation in lymphatic tissue, benign fibroadenomas and
fresh woulds probably due to serum concentration in the area. The
derivative was not taken up by granulomatous lesions nor did it
pass through the placental barrier to the fetus. However, the
uterus and membrane did show fluorescence. (208) The true chemical
structure of the derivative is still not known today.

Lipson continued to do clinical studies with the hematoporphyrin derivative. (209) The dose was 2mg/kg of body weight. The derivative was injected into the rubber tubing used for intravenous infusion of 5% glucose because of the burning sensation when injected directly into the vein. Fifteen patients were used in the clinical trial. Tumors were observed by either bronchoscopy or esophagoscopy using ultra-violet light. If the light was of sufficient intensity to reach the tumor there were no false positives or false negatives. In three cases not enough light reached the tumor. Fluorescence was not influenced by the cell type of the malignant lesion. The only adverse side effect was a minor degree of photosensitivity exhibited by one patient who disregarded instructions against immediate exposure to direct sunlight. The photoreaction lasted a few days and caused only slight discomfort to the patient.

An unnatural porphyrin, tetraphenylporphine sulfonate (TPPS) was studied by Winkelman. (210) TPPS was found to be more highly concentrated in Walker carcinosarcoma than any other tissue of the rat; 10X more than hematoporphyrin. At autopsy there was brilliant red fluorescence in the tumor, bright red fluorescence distributed irregulary in the lung, and faint red fluorescence in the lymph nodes and pancreas. No fluorescence was apparent in the liver, kidney or spleen. Quantitative analysis using fluorescence and absorption spectrophotometry showed considerable amounts in the

liver, kidney, and spleen; followed by lung. However, small
amounts were present in all tissues assayed (total 18). Skin
and muscle always had the least amount. Maximum uptake occurred
at 24-48 hours and remained high until the third day. Organ uptake
at 6-120 hours for other tissues was the same but liver showed early
high accumulation. As the dose increased from 1 to 75mg/animal so
did the tumor and tissue uptake. The ratio of TPPS content of the
liver and kidney to tumor was highest in animals receiving the
largest doses and the lowest in those receiving less than 10mg/
animal. Animals receiving 75mg either died during injection or
developed profound muscular weakness and tachypaea and died 6-10
hours later. Serium electrophoresis of animals receiving TPPS
showed that TPPS migrated with the albumin fraction mainly and
some with the globulin fraction. TPPS behaved like bilirubin but
not like other porphyrins (uroporphyrin, protoporphyrin, or
hematoporphyrin). (211)

It was also shown that the Walker carcinosarcoma of the rat contains
some endogenous porphyrin. The highest concentration was in the
necrotic area of the tumor followed by the sub-capsular area, and
then the viable region. TPPS also accumulated highest in the
necrotic tissue followed by the viable area, and then the sub-
capsular area. It was assumed that the endogenous porphyrin was
removed from circulation rather than in situ breakdown of heme.
Visual observation of the tumor indicated brightest fluorescence

in the pearly white necrotic foci and no fluorescence in the central hemorrhagic necrotic area. Although liver, spleen, and kidney exhibited no red fluorescence sometimes they contained more TPPS than the tumor. (212)

The earlier clinical study by Lipson was expanded to include 35 more patients. (213) The dose of the hematoporphyrin derivative was reduced from 2 to 1.5mg/kg. Both bronchoscopy and esophagoscopy were very useful in detecting areas which were negative during X-ray, visual, and biopsy studies which then later developed into malignant tumors. The only problem was that fluorescence could not be observed if the light did not reach the tumor or if the tumor was obscured by blood. They recommended the procedure when the clinical picture suggests a malignant neoplasma but endoscopy failed to reveal it: where atypical or cancer cells were found in the sputum but the tumor could not be detected by roentgenograms; or in cases of inoperability because the lesion was near vital structures as demonstrated by other techniques.

The technique has been extended to other areas of the body including the cervix, vagina, tracheobroncial tree, esophagus, peritoneum, and rectum. (214) Thirty-three of 35 primary carcinomas of the cervix and vagina were detected by fluorescence with the hematoporphyrin derivative. Fluorescent endoscopy detected 32 malignant lesions out of 34 cases.

The hematoporphyrin derivative was used to detect neoplastic tissue in the mouth, pharynx, and larynx. (215) Twenty-nine of 40 patients had epidermoid carcinoma all of which were positive with hematoporphyrin derivative. Both benign neoplasms (3 cases) and chronic inflammation (4 cases) did not show any fluorescence with the agent. The technique was very useful in showing areas which were malignant when biopsied while previous biopsies were negative. They recommended that before the agent be used routinely that its side effects must be studied carefully.

Hematoporphyrin decreases platelet adhesiveness and aggregation causing cells to be incapable of supporting the clot reaction. (216) Patients should also receive careful fundoscopic examination before and after the study because of the high uptake of porphyrins by the eye and its photodynamic behavior. (217)

Sanderson reviews most of the development of using hematoporphyrin as a diagnostic tool to 1972. (218) They believed that the fluorescent technique was not the ultimate method for early localization of lung cancer but it had potential in localizing in situ and early invasive bronchogenic carcinoma.

The photodynamic action of hematoporphyrin has been used to destroy tumors both in vivo or in vitro although no clinical studies have been done. These photo-oxidiation reactions appear to involve the

the production of electronically excited metastable molecular oxygen (singlet oxygen) as a highly reactive and toxic substance. (129) Glioma cells in culture and subcutaneous tumors in rats were killed by hematoporphyrin and light. However in vivo tumor killing was not complete resulting in many smaller tumors due to the fact that not all cells were exposed to the light or took up the hematoporphyrin. (220) Over 300 tumors of various mouse or rat types were studied using photoradiation therapy and hematoporphyrin. (221) A dose of 2-5mg/kg for mice and 10-15mg/kg for rats was used. The highest tumor/liver ratio of 4 was obtained in 24 hours with a tumor concentration of 40μg/g. Fluorescence microscopy indicated discrete cytoplasmic uptake by tumor cells and not by the nucleus. The in vitro hematoporphyrin-light survival curve was similar to an X-ray survival curve but X-rays were at least a factor of 10,000 more effective. In vivo all tumors regressed to a nonpalpable mass within a few days after treatment but only 48% were cured (6 months without tumor recurrence). Lack of a cure was more a deficiency in the mechanism of the technique rather than treatment failure. This was due to inadequate light intensity and/or porphyrin concentration in all areas of the tumor. Complete destruction of 2-3 cm thick tumors was possible after three or four exposures to the light. The photodynamic destructive nature of hematoporphyrin was eliminated by a specific singlet oxygen trapping agent 1,2-diphenylisobenzofuran. (222)

There has been much interest in the use of hematoporphyrin in the photochemotherapy of brain tumors because it does not pass through the normal blood-brain barrier (223) and red light is able to pass through the skull of mammals. (224) Light and this agent were able to kill glioma cells in culture in less than 8 minutes and gliomas in rats in about 40 minutes. (225) A dose of 20mg/kg was used.

The exact nature of the photodynamic reaction of hematoporphyrin on the cell is not known but it may modify the DNA structure. (226) Hematoporphyrin (greater than 5×10^{-4}M) and light results in the selective degradation of the guanine moiety. DNA treated this way exhibited lowered sedimentation coefficients, lowered temperature helix-coil transitions and increased buoyant density values consistent with single-chain scissions and the generation of singly-stranded regions. Concentrations of hematoporphyrin less than 2.5×10^{-4}M resulted in a bipolymer exhibiting all the above physical properties except a higher sedimentation rate and the DNA was aggregated. Of the four deoxynucleosides only deoxyguanosine was destroyed.

Another interesting feature of porphyrins that has been shown was that they produced dose dependent modifications of radiation effects in mammalian tissue. This suggested that porphyrins may be useful as tumor selective radiation sensitizers in radiotherapy. Hemato-porphyrin was the first one tested and produced radiation sensiti-zation. (227-231) Other people described both a radioprotective and

radiosensitization action of hematoporphyrin. (232) The use of both
natural and synthetic porphyrins often gave contradictory results
probably due to the use of impure preparations. The Ni and Zn metal
chelate of meso-tetra(p-carboxyphenyl) porphine was effective as a
radiation sensitizer at concentrations as low as 10^{-9}M.

The Zn porphyrin was equally effective when added immediately after
irradiation or partially effective when added 90 minutes post
irradiation indicating possible interference on repair mechanisms.
(233) It was proposed that the difference in sensitivity of bio-
logically active NDA to gamma irradiation under aerobic oxygen and
anaerobic conditions was due to organometallic complexes. Metallo-
porphyrin mimic these organometallic compounds with regard to the
oxygen effect on DNA in vitro while normal porphyrins (protoporphyrin
and coproporphyrin) did not. The oxygen effect on DNA by hemin
could be eliminated by adding a high concentration of phosphate
or EDTA. (234)

The incorporation of a metal into the porphyrin did not destroy
its tumor seeking property. (235) This allowed one to use radio-
active metals and porphyrins as tumor imaging agents in nuclear
medicine. ^{64}Cu-protoporphyrin was shown to concentrate in mouse
tumors despite its lack of good tumor to liver, blood, or muscle
ratios. (236) However, human studies showed no tumor uptake of
this agent. (237) In the use of ^{57}Co-hematoporphyrin, tumor bearing

animals appeared to accumulate about half of the amount of radio-activity · in the liver, kidney, and spleen (liver/tumor ratio was 4.7). Twenty four hours after injection tumor concentration was higher than blood or muscle but only 1/5 of liver. High concentration in the liver and spleen was due to the metabolism of the agent. (239) ^{57}Co-hematoporphyrin was excreted mostly through urine while ^{64}Cu-protoporphyrin was eliminated mainly through feces. It was possible that the ^{57}Co compound was stable in vivo and that the ^{64}Cu compound was not resulting in colloidal particles. They concluded that ^{57}Co-hematoporphyrin may have a potential value for tumor detection but the tumors must not be located near the liver, spleen, and RE system.

F   Porphyrin Synthesis

In the past porphyrin synthesis and separation was very difficult because no standard methods were available and workers were reluctant to publish exact details. The work done by DiNello (240) and DiNello and Chang (241) has greatly eliminated the above problems.

Separation of natural porphyrins in the dicarboxylic acid form is not possible because they are too polar. They are soluble in pyridine, dimethyl sulfoxide, and potassium hydroxide (carboxylic acid groups go to carboxylate anions). Acid conditions make them soluble in methanol as diprotonated porphyrin dications. Separation

on silica gel (242) or cellulose (243) possible.

The standard method is to prepare the prophyrin ester from the free acid followed by chemical modifications and chromatography (silica gel or alumina). The purified porphyrin ester can either be metalated, purified, and hydrolyzed or hydrolyzed, metalated and purified. The former method is prefered because alumina or silica gel chromatography is easier than celite chromatography. The acid hydrolysis is a simple procedure and minimizes impurities but porphyrins with acid and base labile side chains may become hydrated (vinyl groups on protoporphyrin) (244). Conventional dimethyl esters must be deesterified using a hydration reaction which could modify the original porphyrin structure. Also hydrogenation reactions could modify the porphyrin sturcture. The tertiary butyl ester eliminates the above two problems because it can be deesterified via an elimination reaction with results in the production of isobutylene and water need not be present during the reaction.

Most natural porphyrins need not be synthesized from pyrroles but can be modified from an existing porphyrin structure. Hematoporphyrin is the usual starting material because it is the cheapest source of porphyrin. It can also be prepared by treating blood with sulfuric acid which removes the iron from the hemin and hydrates the vinyl side chains to hydroxyethyl groups. (246-247) The common

laboratory procedure is to treat hemin with HBr in acetic acid and decompose with water to get hematoporphyrin or methanol to get hematoporphyrin dimethyl ester. Commercial hematoporphyrin is relatively impure and contains substantial amounts of mono-hydroxyethyl monovinyl deuterporphyrin (two isomers) and small amounts of protoporphyrin. (246-247) Diazomethane can be used to esterify hematoporphyrin but not hematohemin and purified by the method of Caughey. (248)

Iron insertion is best done at a low temperature to prevent de-hydration of the a-hydroxyethyl groups using the ferrous sulfate-acetic acid method. (249-251)

Protoporphyrin is to be prepared by the removal of iron from protohemin. (244) Other methods involve the production of the dimethyl ester and chromatography. (248, 252) Both methods are tedious and result in low yields. However, protoporphyrin can be prepared from hematoporphyrin dihydrochloride by refluxing in DMF which results in instantaneous and quantitative dehydration. (240, 241, 253) The resulting protoporphyrin has a purity equal to or better than the best commercially available compound by the TLC method of Ellfolk and Sievers. (254) However, impure hematoporphyrin diHCl can produce contaminated protoporphyrin. (241)

Protohemin cannot be esterified with diazomethane. Protohemin or

its esters are not light sensitive but protoporphyrin and its derivatives are light sensitive. Protoporphyrin reacts with light and oxygen to give photoprotoporphyrin or 1(3)hydroxy-2(4)devinyl-2(4)formylethylidine protoporphyrin. (255-257)

The di tertiary butyl ester (DTBE) of protoporphyrin can be synthesized via the acid chloride method (240) modified from the method of Schwartz (259) and chromatographed on silica gel with chloroform: ether (100:1). Deesterification of protoporphyrin DTBE can be done by bubbling anhydrous HCl through a methylene chloride solution or by refluxing in the same solvent containing trifluoroacetic acid (240) (TFA). Refluxing in TFA results in the gross decomposition of hemins if they are used instead of porphyrins.

The spirographis porphyrin, 2-formyl-4-vinyl deuteroporphyrin and the isospirographis porphyrin, 2-vinyl-4-formyl deuteroporphyrin can be synthesized from protoporphyrin esters via the photoprotoporphyrin isomers (258) or directly from permanganate oxidation of protoporphyrin esters. (260) The Inhoffen (258) method involved the conversion of protoporphyrin di methyl ester to the two photoprotoporphyrin di methyl esters. These two esters were then easily separated by column chromatography on silica gel. The isospirographis porphyrin related chlorin comes off first, followed by the spirographis (natural) porphyrin related chlorin. Isomeric chlorins are frequently more easily separated than isomer porphyrins because

the deviation from planarity induced by chlorin formation magnified the differences in the interaction between the isomers and chromatographic adsorbents. (240) The pure isomers of photoprotoporphyrin esters were reduced with borohydride and treated with acid followed by hydration to give cis-diol porphyrin esters. The cis-diol porphyrin esters were cleaved when treated with periodate to give the spirographis and isospirographis porphyrin esters. Many workers had problems with the periodate cleavage because of incorrect reaction conditions and benzene as a solvent, dioxane is a better solvent. (261-262)

The method of Asakura and Sona (261) using permanganate oxidation of protoporphyrin ester resulted in the direct production of mixed spirographis and isopirographis porphrin esters and difcrmyl deuteroporphyrin ester. The porphyrin esters were separated from the deuteroporphyrin ester by column chromatography. The spirographis and isospirographis porphyrin ester must be separated by thick layer chromatography. The modification of Inhoffen's procedure was both more convenient on a large scale and gave superior yields (and can be used with protoporphyrin DTBE). (239-240)

Diformyldeuteroporphyrin can be prepared from the protoporphyrin ester by permanganate oxidation and alumina chromatography with 1,2-dichloroethane:chloroform (2:1) as an eluent. (248). The

addition of magnesium sulfate during oxidation prevented the diformyl compound from being further oxidized to the dicarboxyl compound. Instead of alumina, silica gel with chloroform: ether (100:1) until the protoporphyrin ester is eluted followed by 50:1 of the same solvent system could be used to separate the DTBE's. (240-241) However, the monoformyl monovinyl and diformyl compounds will have to be rechromatographed. The two formyl groups on di-formyldeuterohemin are very strong electron withdrawing groups.

G   Radioiron Production

Of all the radisotopes of iron only ^{52}Fe is suitable to be used in nuclear medicine based on half-life and gamma photon energy emission. (Table II) ^{52}Fe decays by positron emission yielding annihilation radiation of 511 KeV suitable for imaging with the newer positron cameras or ECAT scanners. Both methods of decay result in the production of ^{52m}Mn (T$\frac{1}{2}$ = 21m) and a gamma ray of 165KeV. ^{52m}Mn decays directly to stable ^{52}Cr (98%) or via ^{52}Mn (T$\frac{1}{2}$ = 5.7d) (2%). (Fig. 2)

^{52}Fe due to its short half-life (T$\frac{1}{2}$ =8.2h) must be made locally when required, only ^{55}Fe and ^{59}Fe are available commercially. In vivo hematological studies were done with 5-10 µCi/patient or bone marrow imaging with 100µCi/patient of ^{52}Fe. (265) The radiation dose to bone marrow was 2.5 rads for ^{52}Fe compared to 50 rads with ^{59}Fe. (266)

TABLE II

RADIONUCLIDES OF IRON

Nuclide	$T\frac{1}{2}$	Decay	Gamma Energy
^{49}Fe	0.08 s	B^+, EC	
^{52}Fe	8.2 h	B^+, EC	169 KeV
^{53}Fe	2.53 m		701
			1328
^{53m}Fe	8.53 m	B^-, EC	378
^{55}Fe	2.7 y	EC	No gamma
^{59}Fe	44.6 d	B^-	1099
			1292
^{60}Fe	10^5 y	B^-	58.6
			27
^{61}Fe	6.1 m	B^-	1200
			1020
			300
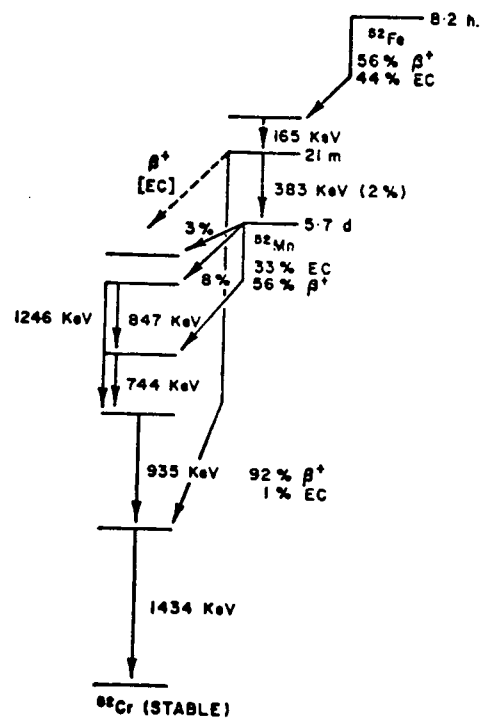
Fig. 2. Decay Scheme of ^{52}Fe (From Ref. 273)

Several methods could be used to produce ^{52}Fe. These include the
following: ^{50}Cr$(\alpha,2n)^{52}$Fe, ^{52}Cr$(^{3}$He,3n$)^{52}$Fe, ^{53}Mn$(p,4n)^{52}$Fe and
spallation reactions.

1) $\underline{^{50}Cr(\alpha,2n)^{52}Fe}$

^{52}Fe was first produced by bombarding natural chromium with 30 MeV
alpha particles via the ^{50}Cr$(\alpha,2n)^{52}$Fe nuclear reaction. (266)
High yields were reported but no numbers were stated. Also ^{55}Fe
was produced by the ^{53}Cr$(\alpha,2n)^{55}$Fe and ^{52}Cr$(\alpha,n)^{55}$Fe nuclear re-
actions depending on the particle energy and target thickness used.
Simple dose calculations were also done. Three μCi of ^{52}Fe would
give a radiation dose to the blood of 15 mr. Contamination of ^{52}Fe
with ^{55}Fe (600 d effective T½) would increase this value from 15 to
200 mr. The radiation dose from commercially available ^{59}Fe was
300 mr. Therefore, in order to keep the radiation dose down ^{52}Fe
must not be contaminated with ^{55}Fe.

Excitation function studies have shown that the threshold for the
^{50}Cr$(\alpha,2n)^{52}$Fe nuclear reaction was near 24 MeV and the peak above
70 MeV for thick (20 MeV) targets. (267) A high purity natural
chromium target (^{50}Cr 4.3%, ^{52}Cr(83.8%), ^{53}Cr 9.6%, ^{54}Cr 2.7%, less
than 100 ppm Fe) compressed out of powder was used. Improved heat
conductivity allowed higher beam currents to be used. Chromium
electroplated copper foil was not used due to the thiness of the
layer and increased radioactivity from the copper. A three hour

bombardment of 65 MeV alpha particles at 12 uA beam current produced about 100-200 μCi of ^{52}Fe. A yield of 150 μCi of ^{52}Fe at the end of chemical separation required a beam current of 40 μA/hr. The production rate was 8.5 μCi/μAhr/g of Cr target with a specific activity of 0.5 μCi ^{52}Fe/μg Fe. About 5-6% of ^{55}Fe was produced via ^{52}Cr(α,n)^{55}Fe reaction and 0.05% ^{52}Mn. The yield could have been improved by using enriched ^{50}Cr target material instead of natural chromium. The final product contained 1.0 μg of Cr, 300 μg of Fe, and 1.0 μg of Mn. The target and holder 3 hours after EOB had a radiation field of 5 R/hr at 12 in. All chemical operations were done remotely and behind 2 inches of lead. The target was dissolved in concentrated HCl for 1 hour and refluxed for another hour to reduce the hydrochloric acid (HCl) from 12N to 7N. Carrier Fe^{++} (2 μg) and Mn^{++} (4 μg) were then added and the mixture oxidized by nitric acid. The mixture was then cooled to 10° before extraction. The ^{52}Fe was extracted into pre-cooled di-isopropyl ether two times. The ether layer was washed six times with 8N HCl. The iron was back extracted three times into water. The ^{52}FeCl$_3$ was then converted to the citrate form by evaporating to near dryness under nitrogen and adding oxygen free distilled water, ascorbic acid (reducing agent 10^{-2} mM) and sodium citrate. The solution was made neutral, isotonic, and sterile before being used. Total processing time was 6-7 hours.

Process time was reduced to 3-4 hours by an automated system. (268)

An infinitly thick chromium plated target was bombarded by 30 MeV alpha particles with beam currents up to 300 uA and a production rate of 50 μCi ^{52}Fe/100 uAh at EOB. Using a proportioning pump the dissolved target was mixed in a spiral glass tube (phase mixer) and extracted in an U-tube (phase separator). Overall extraction efficiency dropped from 99% to 85% with this system. Large amounts of ^{55}Fe were also produced limiting the time after EOB when it could be used. This was the first time carrier free ^{52}Fe was produced.

In another experiment a copper target plated with nickel and then plated with high purity chromium was bombarded with 30 MeV alpha particles at 500 uA. (269) The yield of ^{52}Fe was 3.3 μCi/uAhr however, large amount of ^{55}Fe (14%) was produced at EOB. The final product contained 5 μg of Cr and Ni and 20 μg of Fe. The chromium layer was dissolved electrolytically (0.003 A/cm) in HCl in less that 20 minutes. The solution was then boiled. Unheated solution only had an extraction efficiency of less than 25%. Addition of hydrogen peroxide increased this to about 80%. Heating the solution and extracting it while still hot increased this to greater than 80% to 98%. Cooling the boiled solution decreased the extraction efficiency to 70-80%. Boiling caused the iron to be oxidized from Fe^{++} to Fe^{+++} and changed the concentration of several chromium (III) chloride isomers known to exist in acid media. The extraction with di-isprophy ether was done in a special swan-

necked vessel. The back extraction (98-100% efficiency) was done in a centrifuge tube. The aqueous layer was boiled to dryness and reconsituted with isotonic (3.8%) sodium citrate. The entire process time was about 1.5 hours.

Enriched ^{50}Cr targets were used at BNL but found to be impractical due to the high cost of the isotope. Reprocessing was time consuming and involved losses of the very expensive isotope. The production rate was 10.5 µCi/uAh with a 39 MeV alpha beam only 35% of the theoretical production rate. The $^{50}Cr(\alpha,2n)^{52}Fe$ reaction required alpha particles with energies greater than 65 MeV to increase the yield and decrease ^{55}Fe production. The problem with the reaction was that very few particle accelerators could attain this high energy and natural chromium contains less than 4.3% ^{50}Cr.

2) $\underline{^{52}Cr(^{3}He,3n)^{52}Fe}$

The $^{52}Cr(^{3}He,3n)^{52}Fe$ reaction was first used at BNL. (270) The excitation function for ^{52}Fe production peaked at about 30-40 MeV with a width of about 15 MeV and a cross-section of 5-10 millibarns (mb). The excitation curve for direct ^{52m}Mn and ^{52}Mn production had similar shapes with cross-sections of 70 mb and 200 mb respectively. Natural chromium (83.7% ^{52}Cr) was bomabrded with 45.5 MeV ^{3}He particles with an average yield of 50 µCi/uAh (thin target-- 0.56 mm). Only 0.001% ^{55}Fe was produced compared to 5-15% with the $^{52}Cr(\alpha,3n)^{52}Fe$ reaction. The ^{52}Fe was separated from the target

by solvent extraction with di-isopropyl ether (1-5 µg) Fe and Mn carrier added.

Similar studies at a lower beam energy were done later. (271) Natural chromium was electroplated onto copper plates. The target was bombarded with ^{3}He particles at 23 MeV. The yield was 0.7 µCi/uAh and 0.3% ^{55}Fe. The copper backing was removed with 10 M nitric acid and the chromium target dissolved in HCl. The ^{52}Fe was separated from the chromium target by either di-isopropyl ether solvent extraction or ion exchange chromatography. The 12 M HCl solution was passed through a 150 mm x 13 mm diameter column of Bio-Rad AG1x8 Cl$^-$ form 100-200 mesh anion exchange resin. Washing the column with 12 M HCl (125 mls) removed all the impurities. Fifty mls of 1 M HCl were used to elute the ^{52}Fe from the column.

Similar experiments at 35 MeV ^{3}He, 80 uA beam on 0.01 in thick natural chromium target produced 15 µCi of ^{52}Fe/uAhr. (272) The target had a radiation level of 50 R/hr at 4 in after several hours bombardment. The target was dissolved in 9 M HCl. Concentrated nitric acid and 20 µgs of Fe^{+++} were added to oxidize the ^{52}Fe. The solution was passed through a Dowex A-1 resin column (1 cm x 10 cm) at a flow rate of 3 ml/min. Washing with 50 ml of 9 M HCl removed the chromium and manganese, while 27 ml of 2 M HCl removed any residual galium. The ^{52}Fe was then eluted with 0.1 M HCl.

The solution was evaporated four times to dryness and a solution of 10 mg ascorbic acid and 6% soidum citrate was added. Process time of 1.5-2 hours with a chemical yield of 85-95% was obtained.

The $^{52}Cr(^{3}He,3n)^{52}Fe$ reaction takes advantage that ^{52}Cr is 84% of natural chromium so enriched targets did not have to be used. However, it has the same problem as the first reaction that few machines can accelerate ^{3}He particles to 45-50 MeV.

3) $^{55}Mn(p,4n)^{52}Fe$

Manganese dioxide of high purity grade was bombarded with 65 MeV protons at 0.5 uA for 1 hour. The target less holder had a radiation reading of 500 mR/hr at 1 ft 1 hr after EOB. The production rate was 160 µCi/uAh (specific activity 1.2-1.3 µCi/µg Fe). The ^{55}Fe level was not measured but calculated to be less than 3%. The iron was purified by ion exchange chromatography (Dowex 1x8 100-200 mesh 1 cm x 12 cm long). The solution with 5 µg iron carrier was loaded in 6 N HCl. Washing with 6 N HCl removed the Mn, Na, Cr and Al. The iron was eluted with 0.5 N HCl. Chromatography was repeated a second time. The processing time was 2 hours and 70-80% efficient. The final product contained 60-65 µg of iron due to the impurity in manganese dioxide target material. (272)

Both previous nuclear reactions require high energies and have low cross sections due to the crossing of a doublely charged particle

across the Coloumb barrier of the target nucleus. The $^{55}Mn(p,4n)$ ^{52}Fe reaction does not have this problem This is an ideal reaction because the only stable isotope of manganese is ^{55}Mn (100% abundant). Again the 55 MeV proton beam energy is too high for nearly all medical cyclotrons. An excitation function measuring both ^{52}Fe and ^{55}Fe cross sections and production rates must be done from 0-100 MeV before this nuclear reaction can be used to produce ^{52}Fe routinely.

4) Spallation Reactions

Bombardment of targets with high energy proton beams of 100 MeV or greater cause fragmentation of the primary target nuclei resulting in the production of new nuclei. One to two protons or neutrons are knocked out, the remaining nucleus boils off further neutrons resulting in proton-rich isotopes. Unlike low energy nuclear reactions, spallation reactions are very nonspecific. The desired final product (10-15 mass units lower) must be separated chemically from other radioelements. Another problem is that neighboring radioisotopes may interfere with the desired one.

High energy proton (588 MeV) spallation of Mn, Co, Ni and Cu

targets has been studied. (274) The cross sections for ^{52}Fe
production are Mn 0.066 mb, Co 0.152 mb, Ni 1.35 mb, and Cu 0.148
mb. Other cross sections have been reported in the literature--
Co 0.76 mb (277); Cu 0.70 mb (275) and 0.25 mb (276). The nickel
target was used for all further experiments. The irradiated target
contained the following radionuclides ^{48}Cr, ^{57}Co, ^{56}Ni, ^{57}Ni, ^{52}Mn,
^{56}Co, ^{55}Co, ^{48}V, ^{44}Sc, ^{52m}Mn and ^{52}Fe. The target was dissolved in
hot concentrated nitric acid, taken to dryness, redissolved in 6 N
HCl and extracted with di-isopropyl ether. The resulting ether
solution contained only ^{52}Fe and its daughter ^{52m}Mn. After 8.4 day
decay of this solution ^{44}Sc, ^{44m}Sc, ^{47}Sc, ^{48}V, ^{55}Fe and ^{59}Fe were
detected. The % activity at EOB was ^{44}Sc 0.02%, ^{44m}Sc 0.11%,
^{47}Sc 0.01%, ^{48}V 0.14%, ^{55}Fe 3.3% and ^{59}Fe 0.16%. Stable Ni had a
low distribution coefficient of less than 4×10^{-4} so only 0.04%
stable Ni was in the final product. A 4 g/cm^2 target at 600 MeV
and 500 uA of proton beam current would yield 350 mCi of ^{52}Fe/h. Up
to 95% of the ^{52}Fe could be separated with contaminants less than
0.5% total and 3.3% ^{55}Fe. If this 64 g target was used for 100
patient doses 0.4 mg of stable nickel would be administered per
patient. Another extraction would reduce this to 0.2 ng.

H   Chemistry and Separation Methods of Iron
Iron dissolves in HCl, sulfuric acid and dilute phosphoric acid to
form ferrous salts. Nitric, perchloric, bromic, and iodic also
yield ferrous salts if the acids are dilute and the reaction occurs

at room temperature. Concentrated acid or heating gives ferric
salts. Insoluble oxide films are formed with concentrated nitric,
iodic and perchloric acids and slow down the reaction. Ferrous
iron is quantitatively oxidized to ferric iron by strong oxidiz-
ing agents-nitric acid, hydrogen peroxide, dichromate, and per-
manganate. Ferric iron is quantitatively reduced by stannous
chloride, hydroxylamine HCl, hydroquinine, and iron and H_2S.

Ferric iron can be extracted from HCl by many organic solvents.
Extraction with ethyl ether is well suited for ferric iron
concentrations from 10^{-4} to 10^{-1}M. (278-279) The higher the ferric
ion concentration the greater is the distribution coefficient, the
maximum is at 6N HCl. Isopropyl ether provides a more quantit-
ative extraction with less sensitivity to acid concentration at its
maximum (7.5-8.0N HCl) (280). Isopropyl ether has a greater than
96% extraction efficiency with 1 mg of iron as compared with 80%
for ether. Ferrous iron is not extracted while feric iron is
extracted as the solvated molecule $(H^+FeCl_4^-)_{2-4}$ (281-282).
Isopropyl ether or ethyl ether can be used to separate Fe from
Cu, Co, Mn, Ni, Al, Cr, Zn, V(IV), Ti and sulfate but not from V(V),
Sb(V), Ga(III), Te(III), Mo or phosphate. Using hydrobromic or
nitric acid instead of hydrochloric acid greatly reduces extraction
efficiency. (283-284)

Amyl acetate has been used to separate ferric iron from Mo and Sn

but not from V. (285) Ketones have been studied and were more
efficient than ethers or esters. The distribution coefficient
between iron (ferric) and isobutyl methyl ketone and 5.5-7N HCl
is at least 1000 and may allow better separation from V. (286)

Extraction with diketones such as acetylacetone in xylene, carbon
tetrachloride or chloroform; or 2-thenoyltrifluoroacetone (TTA) in
benzene has been used to separate ferric iron from other elements.
(287-290) Other elements (Cu, Mn, Mo, Ti, V, Zr, Be, Ga) which co-
extract with iron; the amount depends on the pH of extraction. TTA
permits extraction at a lower pH than acetylacetone but equilibrium
is attained very slowly. The advantage of TTA is that the organic
residue can be easily removed by heating.

Cupferron in chloroform, ether, ether and benzene, or ethyl acetate
is ideal to separate iron from solutions containing large amounts
of Ca and phosphate but Ga, Sb(III), Ti(IV), Sn(IV), Zr, V(V), U(IV),
Mo(VI) and Cu may coextract with 1N HCl or sulfuric acid. (291-292)

Very little work has been done in the extraction of ferrous iron.
The follwing compounds have been studied: (293) Ferrous iron can
be extracted with bathophenanthroline in isoamyl alcohol or n-hexyl
alcohol at pH 4; phenyl-2-pyridyl ketone in isoamyl alcohol or
chloroform from 1M NaOH; tripyridyl-s-triazine in nitrobenzene at
pH 4 with perchlorate or iodide; isonitrosacetophenone in chloroform

at pH 8-9 (294); polyethers (295); or tri-n-butyl phosphate. (296)

Ferric iron is strongly adsorbed onto anion exchange resins from concentrated HCl acid solutions. (297) Other elements are not adsorbed strongly on the resin and these elements can be removed with decreasing HCl concentrations. Iron is eluted off the column with dilute HCl less than 1N or water.

Ferrous and ferric iron can be separated by paper chromatography as chloride or tartrate complexes, (298) chloride complexes in ether-methanol-HCl-water solvent (299) or butanol-12N HCl (85:15) (300); or acetate complexes in n-butanol-ethanol-acetic acid-water (40:25:25:35) (301) as a solvent.

I   Metalloporphyrin Synthesis

There are three general methods for labeling porphyrins:

1)   Acetate method--It has been used for V, Mn, Fe, Co
     and Ni. Thr protons of the porphyrin to be metalated
     ate transfered to the acetate. It can be used for all
     divalent metal ions except those unstable in acetic
     acid and some trivalent ions.

2)   Pyridine method--It can be used for metalloporphyrins
     very labile toweard acid. This reaction cannot be
     used with metal ions with high charge because pyridine
     forms complexes with the metal carrier.

3)   Dimethylformamide method--Dimethylformamide (weakly
     coordinating high-boiling oxygen-donor solvent) has
     been used to do 68 different metalations however,
     anhydrous metal halides may be required. (302)

In the past, the concentration of the metal has been much larger than that of the porphyrin. This was not possible if carrier-free radionuclides were used to label the porphyrin. Either carrier had to be added decreasing specific activity or a new metalation procedure had to be developed.

Porphyrins have been labeled with ^{111}In by the acetic acid method in 2 hours. However, Cl ions strongly interfere while other metals in the radionuclide also interfere. (303)

III Material and Methods

A Chemicals

1) ### Porphyrins

Hematoporphyrin dihdrochloride was obtained from ICN
Pharmaceuticals, Cleveland, Ohio or Sigma Chemical Co.,
St. Louis, Mo. Meso-tetra(4-carboxyphenyl) porphine, meso-
tetra(4-N-methylpyridyl) porphine tetraiodide, and tetra-
Na-meso-tetra(4-sulfantophenyl) porphine (12 hydrate) were
obtained from Strem Chemicals Inc., Newburyport, Ma.

2) ### Chromatography

Silica gel for column chromatography (Woelm activity I, 70-
150 mesh, catalog number 402747) was obtained from ICN Pharm-
aceuticals, Cleveland, Ohio. Polyamide for thin layer and
column chromatography was obtained from Brinkmann Instruments
Westbury, N.Y. Dowex AG 1-X8 anion exchange resin and basic
alumina AG10 were obtained from Bio-Rad Laboratories, Richmond
Ca.

3) ### Radionuclides

^{59}Fe-ferric chloride was obtained from Amersham Corp.,
Arlington Heights, Ill. ^{67}Ga-citrate was obtained from New
England Nuclear, Boston Ma.

4) Reagents

All other chemicals were of reagent grade or better. Di-chloromethane, methanol, and t-butanol were dried using either calcium hydride or sodium metal.

B   Instrumentation

1) Radioactivity Measurements

a) Gamma Spectrometry

For single radionuclide measurements the AECL Canberra Series 30 Multichannel Analyzer with a 2 in x 2 in high resolution NaI(Ti) detector (Canberra Industries, Meriden, Ca) was used. For final ^{52}Fe product activity determination, a radioisotope dose calibrator (Capintec Inc., Montvale, NJ) was used.

Gamma spectroscopy was done either on the TRIM system, Safety system, AECL/TRIUMF Ortec 7044 Minicomputer Based Data Aquisition and Analysis system (EG & G Ortec Inc., Oak Ridge, TN), Novatrack Ortec 7044 Minicomputer Based Data Aquisition and Analysis system or AECL Nuclear Data ND660 Multichannel Analyzer System (Nuclear Data Inc., Schaumburg, Ill). Both the Ortec or Nuclear Data systems were equipped with a 99.5 cc Ge(Li) coaxial detector (efficiency 18.2%) (EG & G Ortec, Oak Ridge, TN) or a 50 cc Ge Phyge planar detector (Aptec Nuclear Inc., Lewiston, NY).

The system was calibrated using liquid standards in a 1.0 ml standard AECL spectrum vial using ^{137}Cs, ^{57}Co, ^{60}Co, ^{133}Ba, ^{54}Mn, and ^{22}Na (New England Nuclear, Boston, Ma.) The system was also calibrated using Amersham (Amersham Corp., Arlington Heights, Ill.) or NEN point sources. All standards were traceable to NBS.

b) Radionuclide Imaging or Scanning

Animal scans were done at the Vancouver General Hospital using either the Searle Pho/Con tomographic scanner with a high energy collimator or Searle LFOV standard gamma gamera with a medium energy collimator (Searle Radiographics, Des Plaines, Ill.). The Pho/Con was set on both the gamma ray and on the 511 KeV peak and summed together.

c) Distribution Studies

An automated gamma counter with a 3 inch well type sodium iodide TI(activated) detector was used to count the animal tissue (Nuclear Chicago, Des Plaines) Radioactive samples were placed in counting tubes (15.6 x 125 mm) (Amersham Searle, Des Plaines) and counted in 4 pi detection geometry.

The gamma counter was calibrated using a ^{137}Cs source (Amersham-Searle, Des Plaines) Using the photopeak of 662 KeV, the fine and high voltage controls were adjusted until the photopeak

fell in the 662nd division. The attenuator was set at 16,
high voltage at 800, fine voltage at 8 for a range for 0-2
MeV.

d) Excretion Studies

For whole-body excretion studies, animals were counted in
a gamma counter equipped with two three inch NaI crystals
(Tubor, Nuclear Chicago, Des Plaines). The machine was
calibrated with a ^{137}Cs source. The course high voltage
was set at 1000, fine high voltage at 37 and the attenuator
at 8 for 0-2 MeV range.

2) Absorption Spectrophotometry

Absorption spectrophotometry was done on the Beckman Model 25
recording spectrophotometer with a solvent blank (Beckman
Instruments Inc., Irvine, Ca.)

C Porphyrin Synthesis

1) Protoporphyrin

Commercially available hematoporphyrin di-HCl was checked for
purity by silica gel thin layer chromatography (tlc) with
benzene: methanol: formic acid (BMF) (110:30:1) and visible
spectrophotometry. Five hundred and sixty ml of DMF were
brought to a boil with stirring and a vigorous stream of nitrogen.

With vigorous stirring, 6.2 g of hematoporphyrin dihydrochloride
in a small beaker was lowered into the flask containing the DMF.
After 30 seconds to allow for the hematoporphyrin to dissolve
and dehydrate, the solution was quickly cooled to 40-50° in a
hot water bath, then a tap water bath and finally an ice bath.
The solution was placed in a 1 lRB flask and the DMF removed
by rotary evaporation at 40-50° and a vacuum pump. The tary
residue was dissolved in minimal 90-100% formic acid. The
protoporphyrin was precipitated with diethyl ether. The
precipitate was filtered, washed with ether until the filtrate
was slightly colored, sucked dry, washed with water, sucked dry,
washed with ether, and dried to constant weight over KOH.

The protoporphyrin was checked for purity by visible spectro-
photometry and silica gel tlc with BMF (110:30:1). The proto-
porphyrin was stored in the dark and in a tightly closed
container to prevent reaction with light and oxygen to form
photoprotoporhyrin. Because protoporphyrin and its esters were
extremely light sensitive all subsequent experiments with this
compound were done under subdued light.

2) Protoporphyrin Di-Tertiary Butyl Ester (DTBE)

Five hundred mg of protoporphyrin were dissolved in 50 ml of
dry dichloromethane, heated to reflux in an oil bath with stir-
ring and under nitrogen. Two and a half ml of oxayl chloride

were added very carefully with a dropping funnel. The reaction was not overly vigorous if the dichloromethane was dry. Refluxing for 15 minutes allowed the complete formation of the acid chloride. The excess oxayl chloride and dichloromethane were removed by distillation and vacuum distillation to remove the last few milliliters of solution, both at less than 60° to obtain maximum yields. The residue acid chloride was dissolved in minimal dichloromethane and again removed by distillation. This was done to remove any residual oxayl chloride after the first distillation. The dry acid chloride was redissolved in 30 ml of dry dichloromethane and heated to reflux with a condenser fitted with a drying tube. Three and three tenths ml of dry tertiary butyl alcohol were added, refluxed for 45 minutes, followed by another 3.3 ml of dry tertiary butyl alcohol. After 45 minutes of additional refluxing excess tertiary butyl alcohol and dichloromethane was removed by rotary evaporation. The residue was dissolved in 66 ml of chloroform. Saturated sodium bicarbonate solution was added with vigorous stirring until carbon dioxide evolution stopped. Thirty-three ml of water were added to the chloroform solution and the layers separated in a separatory funnel. The organic layer was washed with water three times and dried over sodium sulfate. Solvent was then removed by rotary evaporation in vacuo.

The crude protoporphyrin DTBE was purified by column chromato-graphy on silica gel grade IV. The residue was dissolved in minimal chloroform and added to a 150 g column (2 cm diameter x 50 cm long) of silica gel. The column was eluted with chloroform: ether (100:1). The first band, a brown color, eluted was some unknown compound. The second band (red color) was the protoporphyrin DTBE. The red band was evaporated to dryness in vacuo, and was crystallized from benzene (1ml/100mg). The mother liquors were concentrated and a second crop of crystals was obtained.

The purity of the protoporphyrin DTBE was checked by visible spectrophotometry, tlc using chloroform, and melting point determination.

3) Photoprotoporphyrin DTBE

Isomer 1: 1-hydroxy-2-desvinyl-2-formylethylidine protoporphyrin DTBE (B ring reacted)

Isomer 2: 3-hydroxy-4-desvinyl-4-formylethalidine protoporphyrin DTBE (A ring reacted)

Five hundred mg of protoporphyrin DTBE were dissolved in 250 ml of dichloromethane containing 10% pyridine. The solution was exposed to direct sunlight for 1-3 days or mercury vapor lamp for 3-4 hours until the amount of unreacted protoporphyrin DTBE

remained constant by tlc analysis using chloroform. The

mixture was reduced to 100 ml, washed with water, 1N HCl

twice, 5% sodium bicarbonate solution, and water again. The

solution was dried over sodium sulfate and taken to dryness by

rotary evaporation in vacuo.

The crude photoprotoporphyrin DTBE was redissolved in minimal

dichloromethane and chromatographed on 100 g of silica gel

grade IV (2 cm x 50 cm column), equilibrated and eluted with

dichloromethane: ether (20:1). The first band (red) was the

unreacted protoporphyrin DTBE. The second band (green) was

the B ring reacted photoprotoporphyrin DTBE isomer (Isomer 2).

The third band (green) was a mixture of both isomers and was

rechromatographed on 70 g silica gel to separate the isomers.

The fourth band (green) was the A ring reacted photoproto-

porphyrin DTBE isomer (Isomer 1.) Each isomer fraction was

combined and taken to dryness and crystallized from chloroform-

methanol. Purity was checked by absorbtion spectrophotometry

and melting point analysis.

4) 2-Formyl-4-vinyl deuteroporphyrin DTBE
Spirographis (natural porphyrin DTBE

Fifty mg of the A ring reacted photoprotoporphyrin DTBE

(Isomer 2) were dissolved in 25 ml of dry dichloromethane.

A solution consisting of 50 mg of sodium borohydride in 2 ml of dry methanol was added and the reaction mixture stirred for 1 hour at room temperature. The color of the solution changed from green to red-brown. After 1 hour tlc with dichloromethane-ether (20:1) as a solvent was done to check for reaction completeness. The green photoprotoporphyrin band was completely replaced by the gray alcohol band. The red band near the solvent front also appeared (unknown compound). Acetic acid was then added dropwise until hydrogen evolution ceased and excess sodium borohydride was destroyed. The mixture was poured into 100 ml of water. The solution was extracted with 100 ml of chloroform and the organic layer washed with 5% sodium bicarbonate water, and dried over sodium sulfate and taken to dryness by rotary evaporation. The brown-green residue was dissolved in 50 ml of dioxane. A solution consisting of 100 mg of sodium iodate in 1 ml of water was added followed rapidly by 0.2 ml of concentrated sulfuric acid. The reaction was allowed to go to completion for 4 hours at room temperature with continous stirring, after which it was poured into 150 ml of 5% sodium chloride solution and extracted with 50 ml of dichloro-methane or chloroform. The organic layer was washed with 5% sodium bicarbonate solution, water, and dried over sodium sulfate and taken to dryness by rotary evaporation. The red-purple residue was dissolved in minimal chloroform and chromato-graphed on 20 g silica gel grave IV with chloroform: methanol

(20:1) or chloroform: ether (20:1) as the eluent. The first
red band to come off was the spirographis porphyrin DTBE. The
second band which came off much later could be the mono tertiary
butyl ester. The monoformyl monovinyl deuteroporphyrin fraction
was taken to dryness by rotary evaporation and crystallized from
chloroform-petroleum ether (30-60°). Purity was checked by
absorption spectrophotometry in chloroform.

5) 2-Vinyl-4-formyl deuteroporphyrin DTBE
   Isospirographis porphyrin DTBE

This procedure was similar to 2-Formyl-4-vinyl deuteroporphyrin
DTBE except that the B ring reacted photoprotoporphyrin DTBE
(Isomer 1) was used instead of the A ring reacted photoproto-
porphyrin DTBE (Isomer 2).

6) 2-Formyl-4-vinyl deuteroporphyrin free acid
   Twenty-five mg of the 2-formyl-4-vinyl deuteroporphyrin DTBE
   was dissolved in 10 ml of dry dichloromethane containing 10%
   trifluoroacetic acid. The solution was refluxed for 4 hours
   in an inert atmosphere (nitrogen). The progress of the reaction
   was monitored by two tlc systems: 1) benzene-methanol (110:17)
   DTBE R_f = 0.7, monoester R_f = 0.5 and free acid R_f = 0; and
   2) BMF (110:17:1) DTBE R_f = 0.8, monoester R_f = 0.7 and free
   acid R_f = 0.5. When the reaction was complete the dichloro-

methane. The porphyrin free acid was precipitated by adding
1 drop of triethylamine to the solution. The precipitate was
filtered, air dried, washed with dichloromethane, and dried to
constant weight. Purity was checked by tlc analysis using the
same two solvent systems and by absorption spectrophotometry.

7) 2-Vinyl-4-formyl deuteroporphyrin free acid

A similar procedure to the 2-Formyl-4-vinyl deuteroporphyrin
free acid except 2-vinyl-4-formyl deuteroporphyrin DTBE was
used instead of 2-formyl-4-vinyl deuteroporphyrin DTBE.

8) 2,4-diformyl deuteroporphyrin DTBE

One hundred mg of protoporphyrin DTBE were dissolved in 10 ml
of acetone and heated to reflux. A solution containing 200 mg
of magnesium sulfate and 100 mg of potassium permanganate in
50 ml of water was added dropwise to the DTBE solution for 45
minutes. The reaction mixture was cooled to room temperature
and filtered. The filtrate was poured into 1 l of water and
extracted with chloroform--100 ml twich, 50 ml and them 30 ml.
The chloroform from each extraction was combined, dried over
sodium sulfate, and taken to dryness by rotary evaporation.
The residue was dissolved in minimal chloroform and chromato-
graphed on 20 g of silica gel grade IV equilibrated in chloro-
form: ether (100:1). The column was eluted with chloroform:
ether (100:1) until the first band (red) came off. When all

the unreacted protoporphyrin DTBE was off the column the eluting
solvent system was changed to chloroform: ether (50:1). The
next red band to come off was the monoformyl monovinyl deutero-
porphyrin DTBE mixed isomer fraction. This was followed by a
mixed fraction of the monovinyl monoformyl deuteroporphyrin DTBE
mixed isomers and the diformyldeuteroporphyrin DTBE. The last
band to come off was the desired product diformyl deuteropor-
phyrin DTBE. The mixed fraction was rechromatographed on 15 g
of silica gel grade IV with chloroform: ether (50:1) as the
solvent. The pure fractions of diformyl deuteroporphyrin were
combined , taken to dryness and crystallized from chloroform-
methanol. Purity was checked by melting point analysis and
absorption spectrophotometry.

9) Diformyl deuteroporphyrin free acid
   Ten mg of diformyl deuteroporphyrin DTBE were dissolved in 5 ml
   of dry dichloromethane. Anhydrous HCl gas was bubbled through
   the solution for about 6-10 hours. The progress of the reaction
   was monitored by the same two tlc systems used in the deesteri-
   fication of monoformyl monovinyl deuteroporphyrin DTBE. After
   completion of the reaction the solution was evaporated to dry-
   ness. The free acid residue was dissolved in 3 mls of pyridine.
   Addition of 5 ml of hot acetic acid resulted in the immediate
   crystallization of the diformyl deuteroporphyrin. Purity was
   checked by tlc analysis and absorption spectrophotometry.

10) Photoprotoporphyrin free acid

One hundred mg of protoporphyrin were dissolved in 100 ml of pyridine. The solution was exposed to light as described for photoprotoporphyrin DTBE. The pyridine was removed by rotary evaporation. The residue was dissolved in 90-100% formic acid and an equal volume of pyridine was added. The crude photo-protoporphyrin was precipitated by adding ether to the solution. The precipitate was filtered and washed. Tlc analysis using BMF (110:17:1) was done on the crude product.

D ^{52}Fe Production

1) Target Irradiations

The TRIUMF cyclotron at the University of British Columbia was used to irradiate 0.625 in diameter, 4.5 g nickel targets for the production of ^{52}Fe. The TRIUMF cyclotron is unique because its specially shaped magnet accelerates a constant stream of proton particles and the use of H^{-} ion allows multiple beams of different energies and currents to be extracted. There are three possible isotope production facilities at TRIUMF (Fig.3).

The beam line 4A open-air multisample irradiation station (Fig.4) was used to irradiate nickel targets for low level tracer and safety evaluation studies. The irradiation facility consisted of three stringers which moved targets in and out of an open air

BEAM LINES AND EXPERIMENTAL FACILITIES
——— EXISTING   -------- PROPOSED

L-101/F 30/12/79
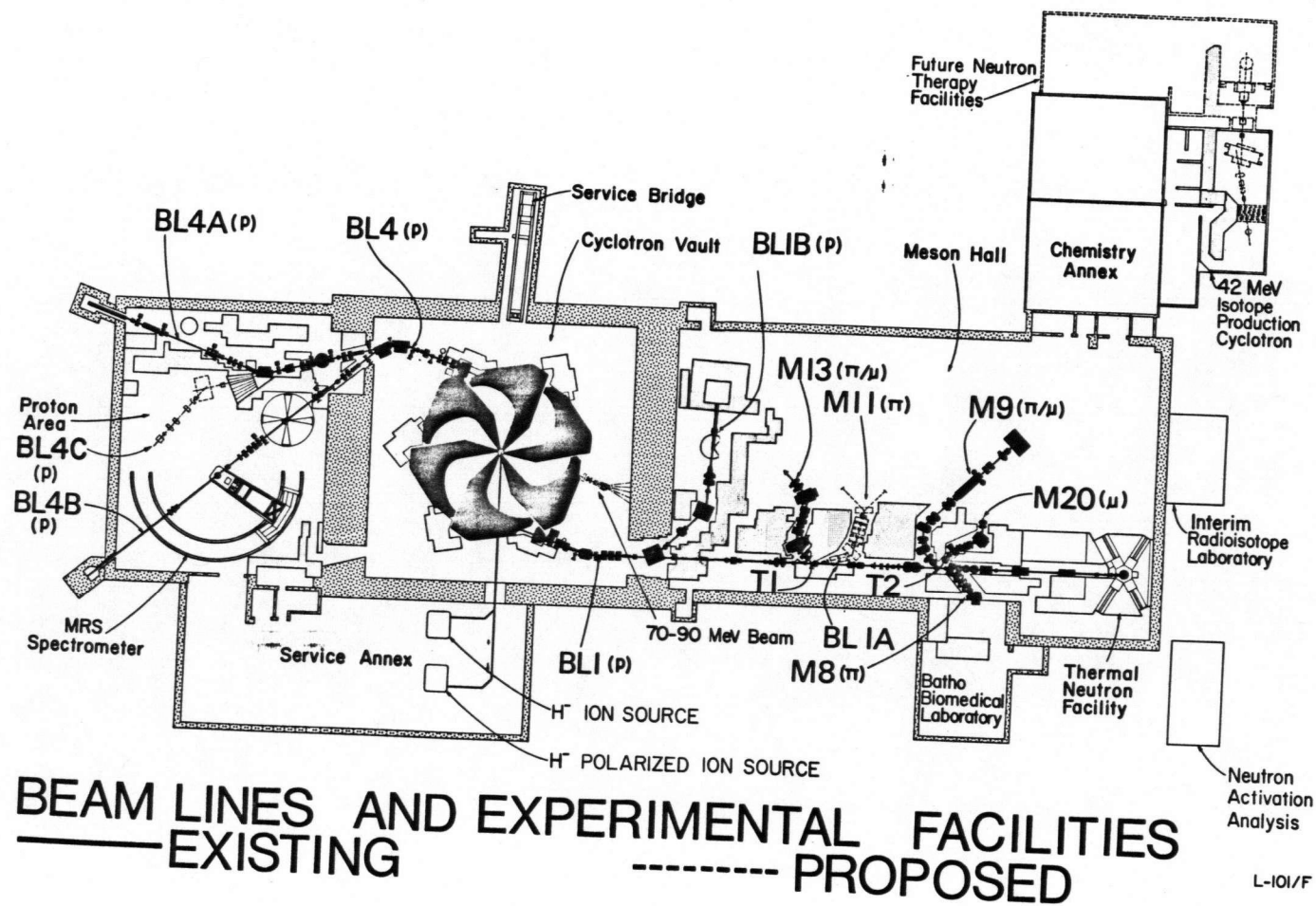
Fig 3. Possible Isotope Production Sites
at TRIUMF.
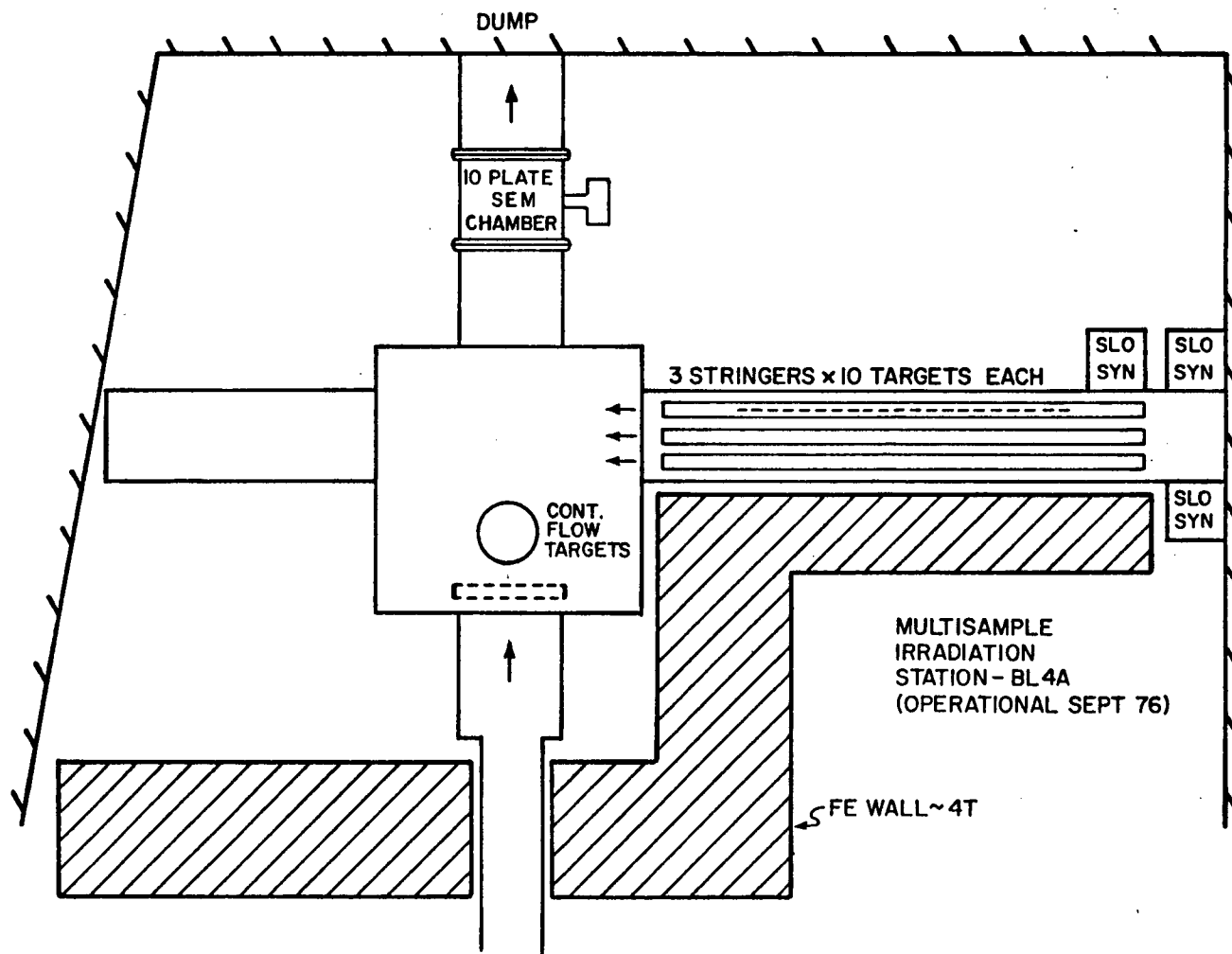
Fig. 4. BL4A Multisample irradiation station.

chamber where the proton beam passed through. Nickel targets were glued onto an aluminium foil backing supported in an aluminium target holder.

For higher level production of ^{52}Fe a new target system upstread from the 4A multisample irradiation facility was desigend, built, and installed (Fig.5). The target had beam windows on both sides of the target holder to provide complete containment of the target. For high level production of .Fe targets were irradiated in the 500 MeV isotope production facility by the Applied Program Group at TRIUMF (Fig.6).

2) Safety Evaluation and AECB License Application

Before targets could be irradiated a detailed safety evaluation regarding types of radioelements produced, activity levels, radiation levels, etc. had to be done. Also, before targets could be chemically separated, detailed calculation showing expected radiation fields, radiation exposure, amount of lead shielding required, etc. had to be done. All facilities and procedures had to be approved by the TRIUMF Safety Group (TSG), TRIUMF Safety Advisory Committee (TSAC) and Atomic Energy of Canada Control Board (AECB).

The Simon Fraser University Dose program and initial low level experiments were used for these calculations (304). The Dose
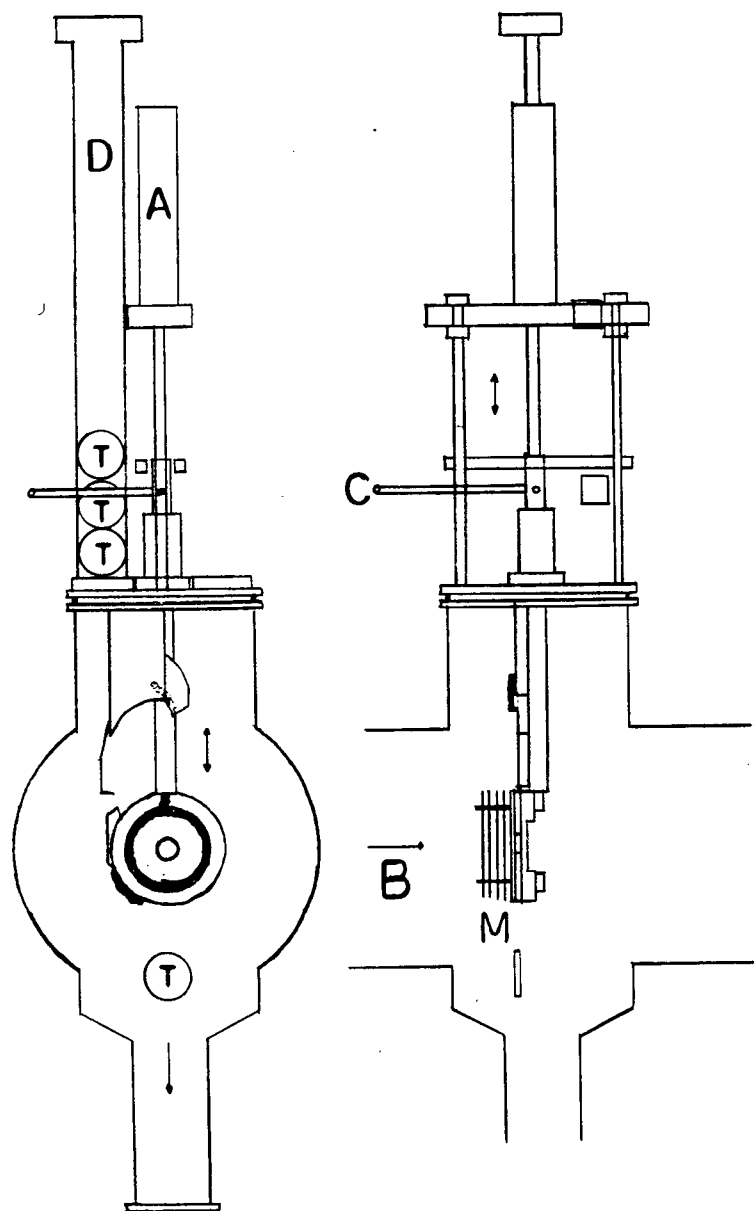
Fig 5. BL4A ^{52}Fe Production Facility.
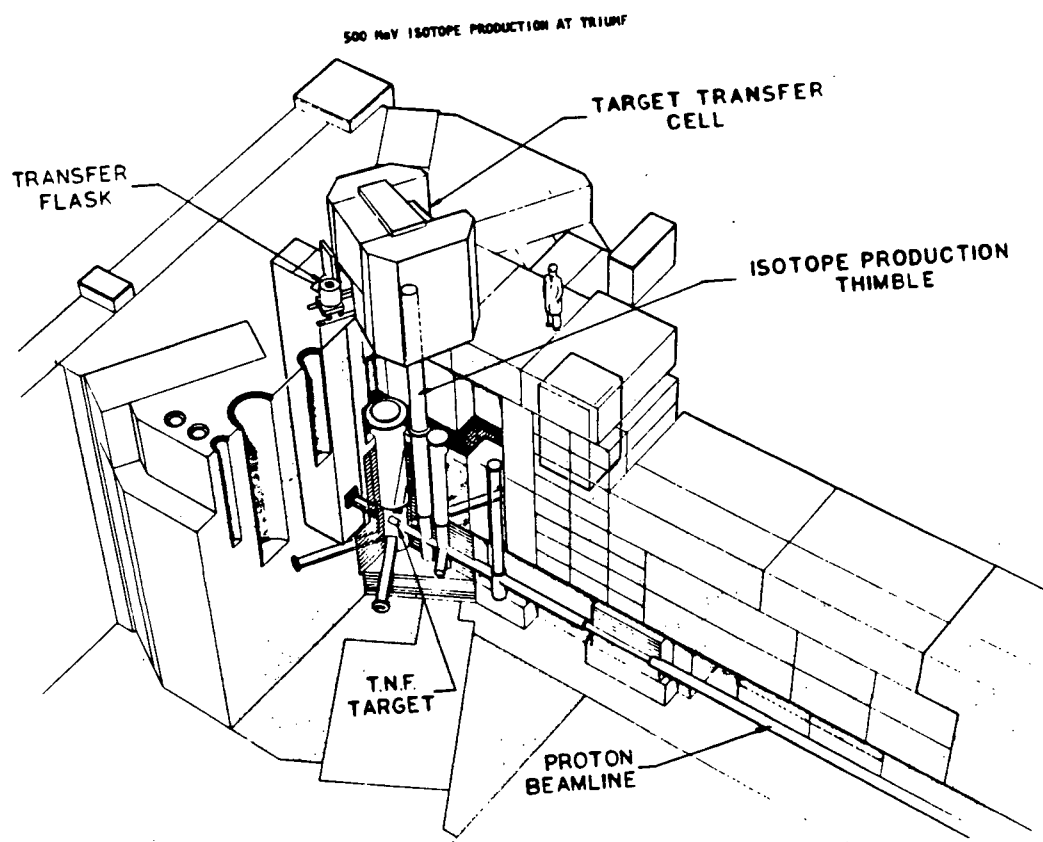
Fig 6. BL1A 500 MeV irradiation facility

program calculated cross sections in millibarns (mb) for the
various radioelements produced via the Rudstam (305) or
Silberberg-Taso (306) formulae and determined yields for a
given proton current assuming one gram of target material and
one uA of beam current. The program allowed one to use
experimental cross section values if they were known instead
calculating them. In addition the following were calcualted:
the contribution to the gamma dose rate in mrad, source
strength in mCi, the contribution to the beta dose rate, the
contribution to the danger parameter, and the contribution to
the gamma spectrum. The output contained the following: the
target date; total cross section for each isotope; and for each
combination of irradiation and cooling times the following were
calculated: total number of gammas, total number of betas, the
gamma dose in mrad/hr at 1 m, the beta dose rate, the danger
parameter and gamma spectrum; list of stable nuclei produced
and a list of alpha emitters.

In the initial experiments used for the safety evaluation,
nickel targets were irradiated in the 4A open-air multisample
irradiation facility. Irradiated targets were dissolved in
concentrated nitric acid, evaporated to dryness and redissolved
in 8N HCl. The ^{52}Fe was extracted from the hydrochloric acid
solution into di-isopropyl ether and back extracted into water.
Aliquots were taken before and after solvent extraction and

counted for radioactivity using a Ge(Li) detector as described previously. Based on the efficiency curve of the detector, cpms were converted to μCi values. The specific gamma ray constant for each radionuclide was calculated with no lead shielding and various thicknesses of shielding. (307)

3) Hot Cell Design and Construction

A hot cell was designed and built in the Interm Radioisotope Laboratory at TRIUMF to permit the safe handling of irradiated nickel targets and to allow the ^{52}Fe to be separated from the target. (308-310) The hot cell consisted of a stainless-steel fume hood (liner) (30 in X 60 in working surface) surrounded by 4 inches of lead on all sides and bottom, and 2 inches of lead on top. Over 1200 2 inch X 4.5 inch X 16 (22 lbs) lead bricks were used for shielding. A 16 inch X 16 inch X 2 inch lead glass window (density 6.2 g/cc) allowed observation of the fume hood contents. The window actually consisted of 8 shigle 8 inch X 8 inch X 2 inch pieces of lead glass. The hot cell was equipped with two Tru-Motion Mini-Manip Master Slave manipulators (PaR Programmed and Remote Systems Corporation, St. Paul, Minn).

Access for two 9 inch diameter lead pigs containing the irradiated target was provided by two entry/exit ports with raised lips on the bottom of the hot cell. When the hot cell was in use, these ports were sealed but unshielded. Lead pigs were

raised or lowered by two 12 volt electric hoists mounted on top and outside of the fume hood and hot cell.

Routine chemical equipment was placed in or removed from the hot cell through the lead shielded "Pass-Thru" on the left hand side of the hot cell. Larger items were either loaded or removed from the hot cell through the two bottom entry/exit ports or the removable lead glass window.

4) Selection of ^{52}Fe Process Chemistry using ^{59}Fe

a) Recovery Tests

A column (15 mm diameter X 12 cm) of Dowex 1-X8 100-200 mesh ion exchange resin was prepared and washed with 20 ml of 8N HCl. A 25 ml solution containing 10 g of nickel acetate, 30 drops of 30% hydrogen peroxide and 0.1 ml of ^{59}Fe citrate (0.6 µCi) was added to the column. The column was washed with 3 bed volumes of 8N HCl. The ^{59}Fe was eluted off with 2 X 15 ml fractions of 0.5N HCl. Aliquots of the starting solution, washing solution, and final product were counted for radioactivity. The above procedure was repeated using different HCl concentrations during the loading of the column (0, 2, 4, 8, 10, and 12N HCl).

The same 25 ml solution as above was prepared. The solution was extracted with 20 ml of di-isopropyl ether. The ether was

washed with 20 ml of 8N HCl and the iron back extracted into 10 ml of water. Each fraction was counted for radioactivity. The above experiment was repeated using various HCl concentrations (0, 2, 4, 6, 8, 10, 12N HCl). The above experiment was also repeated using methyl isobutyl ketone instead of di-isopropyl ether.

b) Radionuclide Impurity Determination

An irradiated nickel target was dissolved in 30 ml of hot concentrated nitric acid and the nitric acid was evaporated to dryness. The residue was redissolved in 25 ml of 8N HCl. A five ml fraction was assayed for radioactivity. Another 5 ml fraction was extracted with 5 ml of di-isopropyl ether, washed with 5 ml of 8N HCl, and back extracted into 5 ml of water. Each fraction was assayed for radioactivity. Another 5 ml fraction was extracted with methyl isobutyl ketone instead of di-isopropyl ether. Another 15 ml fraction was passed through a Dowex 1-X8 ion exchange resin column (15 mm diameter X 12 cm). The column was washed with 3 bed volumes of 8N HCl. The iron was eluted off with 0.5N HCl made up to 15 ml again with concentrated HCl and water to make a 8N HCl solution. Five ml of the 15 ml solution was counted for radioactivity. Another 5 ml fraction was extracted with di-isopropyl ether and another 5 ml fraction with methyl isobutyl ketone as described above. Each fraction was decayed and counted for radioactivity.

5) <u>High Level ^{52}Fe Production</u>

A bread-board set up containing the glassware for the necessary

chemical operations for use in the hot cell was designed (Fig.7)

The irradiated nickel target was dissolved in a mixture of 30 ml

of concentrated nitric acid and 30 ml of concentrated HCl with

heat. After dissolution the solution was evaporated to dryness

and redissolved in 20 ml of 8N HCl. Twenty ml of methyl

isobutyl ketone were added HCl target solution and mixed. After

phase separation, the bottom inorganic layer was discarded. Ten

ml of distilled water were added and mixed. The bottom layer

containing the ^{52}Fe product was dispensed into bottles. The

product was swipe tested and removed from the hot cell to a

fume hood. It was heated to boiling to drive off any residual

solvent, cooled and adjusted to pH 7-8 with either HCl or NaOH.

An aliquot was removed to be checked for purity using a Ge(Li)

detector. Total activity was determined by a dose calibrator.

After each separation of ^{52}Fe the glassware was rinsed with

distilled water.

E   Metalloporphyrin Synthesis

1) <u>^{59}Fe-Hematohemin</u>

The ferrous sulfate or chloride method was used (244). Ten

mg of hematoporphyrin were dissolved in a solution containing

0.5 ml of pyridine, 10 ml of glacial acetic acid and 10 mg of
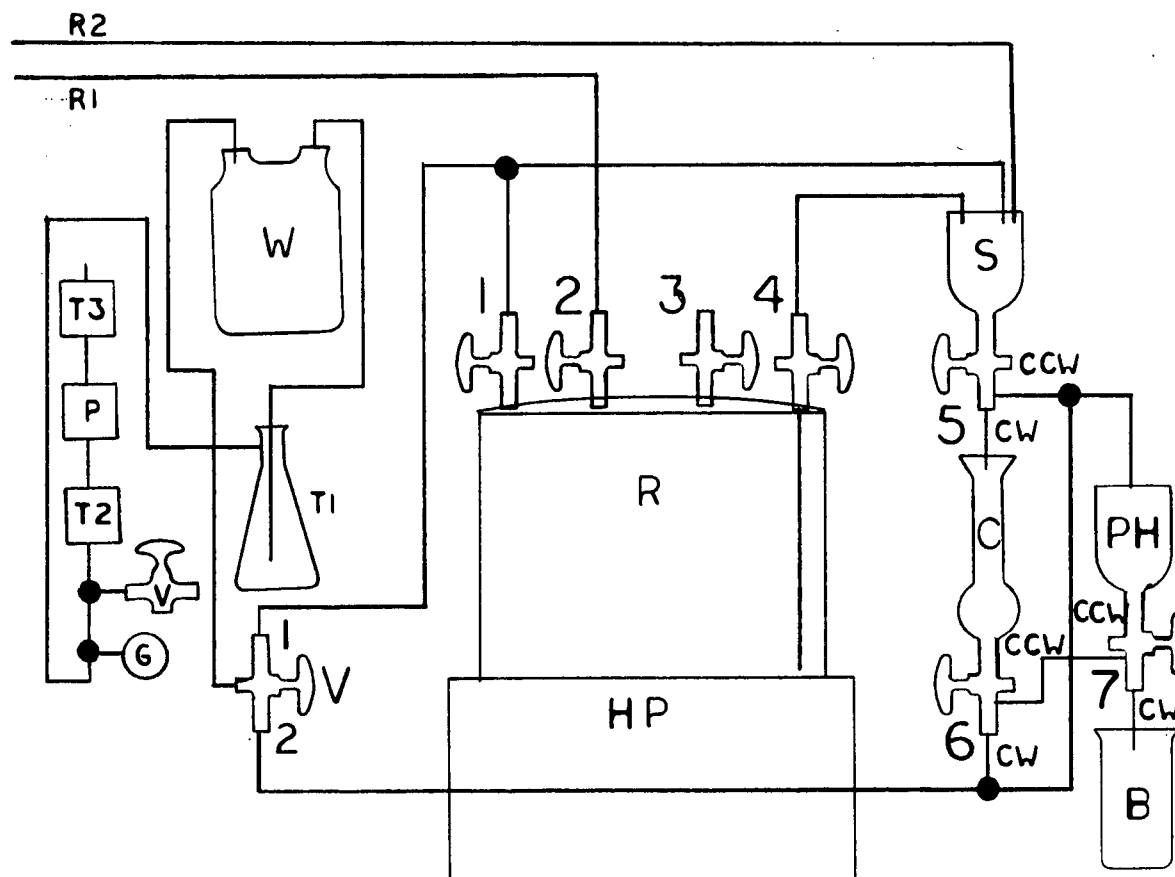
Fig⁹7.   Fe Production Hot cell Breadboard.

ascorbic acid in a pear-shaped or long necked flask. Nitrogen
was bubbled through the solution with the aid of a gas inlet
tube. The solution was heated in an oil bath to 80°. The
^{59}Fe (100 µCi) as the ferric chloride or citrate was added to
the mixture and the temperature raised to 90°. After 5 minutes,
1.0 ml of saturated ferrous chloride or sulfate was added.
After an additional 5 minutes at 90°, the nitrogen was turned
off and the solution allowed to cool to room temperature. Air
was then passed through the solution for 30 seconds. This
solution was then added to 10 ml of distilled water and 20 ml
of chloroform. After extraction the organic layer was washed
with 0.2M HCl and then with distilled water several times. The
hemin was extracted out of the organic layer into 5 ml of 1.0N
NaOH. The solution was adjusted to pH 7-8 with about 5 ml of
1.0N HCl. The progress of the reaction was checked by paper
chromatography with ethanol (Hemin $R_f=0$, ^{59}Fe $R_f=1$) and
absorption spectrophotometry. Each fraction was also counted
for radioactivity to determine reaction yields. The final
product was checked by absorption spectrophotometry, paper
chromatography as above and tlc using n-butanol-water-acetic
acid (50:1.5:1.4) (protohemin $R_f=0.47$, hematohemin $R_f=0.40$) and
hexane-n-propanol-acetic acid (10:5:1.5) (hematohemin $R_f=0.13$
protohemin $R_f=0.28$) and polyamide chromatography using methanol-
acetic acid (100:2) (hematohemin $R_f=0.69$, protohemin $R_f-0.34$).

2) ^{59}Fe-Protohemin

This procedure was similar to hematohemin except that proto-porphyrin was used instead of hematoporphyrin. The product was then crystallized from chloroform/methanol. The same quality control procedures were done on protohemin as hemato-hemin (see above).

3) ^{59}Fe-Photoprotohemin

Seventy-five mg of photoprotoporphyrin were dissolved in 10 ml of DMF. The solution was heated to 100° under a nitrogen atmosphere. Fe in the form of ferric chloride or citrate (100 μCi) was added. After 15 minutes of constant stirring, 20 gm of ferric chloride were added. After an additional 30 minutes of heating and stirring the solution was cooled to room temperature and the DMF removed by rotary evaporation. The hemin residue was dissolved in minimal pyridine and an equal amount of 90-100% formic acid was added. The hemin was precipit-ated by the addition of ether. The precipitate was filtered and washed with ether, air dried, washed with water, air dried, washed with ether again, and then dried to constant weight.

The crude photohemin was purified by both thick layer and thin layer chromatography. Fifty mg of crude photohemin were dissolved in minimal pyridine containing 5% of 90-100% formic acid. This solution was applied to a 30 cm X 30 cm thick silica gel plate.

The plate was developed on BMF (110:30:1). The green photo-
protohemin band (middle band) was scraped off, pulverized, and
the hemin eluted with methanol. The solution was reduced to
2 ml and 25 ml of petroleum ether were added. The hemin was
precipitated, filtered, and washed as for the crude photo-
protohemin as above. It was again purified on silica tlc
plate as above except after chromatography, the methanol solution
was taken to dryness. The pruified photoprotohemin was dis-
solved in 5 mls of 1.0N NaOH and the pH adjusted to pH 7-8
with about 5 mls of 1.0N HCl. The progress of the reaction
and purification, and purity of the final product was monitored
by paper chromatography with ethanol, absorption spectrophoto-
metry, tlc using BMF (110:30:1) and polyamide tlc using BMF
and methanol-acetic acid (100:2).

4) ^{59}Fe-2-formyl-4-vinyl deuterohemin

Thirty mg of 2-formyl-4-vinyl deteroporphyrin were added to
10 ml of DMF at relux under nitrogen. ^{559}Fe as the ferric
chloride or citrate was added followed by 15 mg of ferric
chloride 15 minutes later. The progress of the reaction was
followed by paper chromatography as previously described and
absorption spectrophotometry. When the reaction was complete
(45-47min) the mixture was taken to dryness by rotary evapora-
tion. The crude hemin was precipitated by ether, washed and
purified by thick layer silica gel chromatography as previously

described for ^{59}Fe-Photoprotohemin.

The purified hemin was extracted from the silica gel by BMF (110:30:1). The solvent mixture was slowly removed by rotary evaporation until the product precipitated. The precipitate was washed with benzene and air dried. The purified hemin was crystallized by dissolving it in 1.5 ml of pyridine and 3 ml of chloroform added. The solution was filtered through glass wool and the wool washed with two 1.35 ml aliquots of pyridine-chloroform (35:100). The filtrate and washings were combined, heated to boiling and 25 ml of boiling acetic acid were added. Then 0.35 ml of concentrated HCl were added and the mixture heated to boiling again. The solution was allowed to stand for 24-48 hours to complete crystallization. The hemin was re-covered by suction filtration. The 2-formyl-4-vinyl deutero-hemin was dissolved in 5 ml of 1.0N NaOH and the pH adjusted to pH 7-8 with about 5 ml of 1.0N HCl. The purity was checked by absorption sepctrophotometry and silica gel and polymide tlc as described previously for ^{59}Fe-photoprotohemin.

5) ^{59}Fe-2-vinyl-4-formyl deuterohemin

This procedure was similar to 2-formyl-4-vinyl deuterohemin except that 2-vinyl-4-formyl deuteroporphyrin was used instead of 2-formyl-4-vinyl deuteroporphyrin.

6) ^{59}Fe-2,4-diformyl deuterohemin

Thirty mg of diformyl deuteroporphyrin were metalated using the ferric chloride method (refluxing in DMF) as previously described. The resulting residue was dissolved in minimal methanol. The addition of water caused the crude product to precipitate. The precipitate was air dried, washed with ether, and air dried again. The crude hemin was dissolved in 5 ml of pyridine containing 10% acetic acid. This solution was streaked out on a thick layer silica gel plate and dried. The preloaded silica gel was scraped off, pulverized, and suspended in BMF (110:30:1). The slurry was poured onto a 25 g polyamide column equilibrated with the same solvent system. The column was eluted with BMF (110:30:1) until the minor band was eluted. The hemin eas eluted off the column with BMF (110:70:1). The band was taken to dryness and crystallized and prepared as described for 2-formy-4-vinyl deuterohemin.

7) ^{59}Fe-meso-tetra(4-carboxyphenyl) hemin (TCP)

Ten mg of meso-tetra(4-carboxyphenyl) porphine were dissolved in 10 ml of glacial acetic acid containing 10 mg ascorbic acid and 10 mg of sodium acetate. The solution was heated to reflux under nitrogen. ^{59}Fe in the form of ferric chloride was added and refluxed for 30 minutes. Then, 1 ml of saturated ferrous chloride solution was added and refluxed for an additional 30 minutes. The nitrogen was turned off and the solution cooled to

room temperature. Air was passed through the solution for 1-2 minutes. Finally, the solution was adjusted to pH 7-8 with sodium bicarbonate. The % tag was determined using paper chromatography as described previously.

8) ^{59}Fe-meso-tetra(4-N-methylpyridyl) hemin tetraiodide

This procedure was similar to ^{59}Fe-meso-tetra(4-carboxyphenyl) hemin except that meso-tetra(4-N-methylpyridyl) porphine tetraiodide was used instead of meso-tetra(4-carboxyphenyl) porphine.

9) ^{59}Fe-tetra-Na-meso-tetra(4-sulfonatophenyl) hemin (TPPS)

This procedure was similar to ^{59}Fe-meso-tetra(4-carboxyphenyl) hemin except that tetra-Na-meso-tetra(4-sulfonatophenyl) porphine (12 hydrate) was used instead of meso-tetra(4-carboxyphenyl) porphine.

10) Nickel spallation product labeled meso-tetra(4-N-methyl-pyridyl) porphyrin tetraiodide

The ferric chloride method (refluxing in DMF) was used as described previously except nickel spallation HCl solution after nitric evaporation was used instead of [59]Fe. After leabelling, the DMF solution was evaporated to dryness and resuspended in water or 1.0N NaOH. The pH was adjusted to pH 7-8 using either HCl or NaOH.

11) ^{52}Fe-Protohemin

This procedure was similar to ^{59}Fe-protohemin except that ^{52}Fe ferric chloride was used instead of ^{59}Fe ferric chloride.

12) ^{52}Fe-meso-tetra(4-carboxyphenyl) hemin

This procedure was similar to ^{59}Fe-meso-tetra(4-carboxyphenyl) hemin except that ^{52}Fe ferric chloride was used instead of ^{59}Fe ferric chloride. A simpler procedure was also used where the solution was heated to boiling not under nitrogen and the ascorbic acid and ferrous chloride were not added.

13) ^{52}Fe-meso-tetra(4-N-methylpyridyl) hemin tetraiodide

This procedure was similar to ^{52}Fe-meso-tetra(4-carboxyphenyl) hemin except meso-tetra(4-N-methylpyridyl) porphine tetraiodide was used instead of meso-tetra(4-carboxyphenyl) porphine.

F. Tumor Tissue Culture Uptake Studies

P815 tumor cells were grown for several days before use in RMPI 1640 tissue culture medium. A 1/10 dilution of cells in RMPI 1640 tissue culture medium was done before uptake studies were done. Five ml of this solution were dispensed into 60 mm x 15 mm tissue culture dishes. After 1 hour of incubation, 0.5 ml of ^{59}Fe labeled hemin (specific activity 10 µCi/mg hemin; hemin concentration 0.5mg hemin/dish) or radionuclide were added to all but two petri

dishes. A 0.5 ml sample of cell suspension at the start and end of the experiment was taken and counted for activity. At selected time intervals (0, 1, 3, 6, 12, 24, 48, 72 hours) a 0.5 ml sample was taken from each dish and filtered through a millipore filter. The cells were washed with 5 ml of PBS and counted for radio-activity. Also at selected time intervals as stated above, a 0.5 ml sample was taken from the two non-radioactive tissue culture dishes and counted for cell number using a coulter counter. All results of uptake were corrected for varying amounts of radio-activity and cell numbers during the course of uptake. Each time point per hemin or radionuclide was done in duplicate and the whole experiment was repeated five times. All hemins and radionuclides were tested together per experiment to rule out any differences between individual hemins or radionuclides.

G Animal Studies

1) Distribution Studies

Male CDI Swiss mice weighing 30-40 g were injected IV (tail vein) either with $^{59}FeCl_3$ or ^{59}Fe-TMPI at less than 0.1 mg porphyrin/animal in 0.1 ml. At selected time intervals (0, 0.5, 1, 3, 6, 12, 24, and 48 hours) after injection, animals were placed in ether until comatose and decapitated. The following organs were counted for radioactivity: blood, liver, spleen, kidney, bone, eyes and lung. At least five animals

were used per time point. Animals were given food and water
ad libium.

2) Scintigraphy

^{52}Fe-TMPI at a dose of 10 mg porphyrin/animal in less than 0.5
ml was injected LV (ear vein) into normal New Zealand male white
rabbits weighing 2-2.5 kg. Animals were scanned several hours
after injection as previously described.

Tumor bearing rats with breast carcinoma on neck or side regions
and some with prostate carcinoma were injected with ^{52}Fe-chloride
(III), ^{52}Fe-protohemin, ^{52}Fe-TMPI or ^{52}Fe-TCP (IV tail vein
<5 mg porphyrin/animal, <0.5 ml). The animals were scanned
three hours and 24 hours after injection.

3) Excretion Studies

Male CDI Swiss mice weighing 25-25 g were injected IV (tail vein)
with 0.1 mg porphyrin/animal in 0.1 ml. At selected time
intervals (1, 2, 3, 6, 7, 8, 9, 10, 20 days) after injection
animals were counted for radioactivity as previously described.
(whole body counter).

IV RESULTS AND DISCUSSION

A. Porphyrin Synthesis

1) Hematoporphyrin

The absorption spectrum in pyridine indicated that the hematoporphyrin was pure.

Absorption Spectrum:

Pyridine						
λmax(obs)	402	500	–	570	596	–
λmax(lit)	402	499.5	532	569.2	596	623

Thin layer chromatography showed that a very small amount of protoporphyrin was present which chromatographed far ahead of the hematoporphyrin. A spot between hematoporphyrin and protoporphyrin which was monohydroxyethyl monovinyl deuteroporphyrin was also present.

Note: All literature valves for absorption spectrophotometry and melting points here from references 240 or 241.

2) Protoporphyrin

The yield of the reaction was 80-90%. This could have been improved if a better method was available to scrape off all the precipitate and not lose it because of its solubility in ether. The saturated protoporphyrin ether solution was saved and used when the reaction was repeated.

The visible absorption spectrum in pyridine and tlc analysis indicated that the protoporphyrin was not contaminated with hematoporphyrin.

Absorption Spectrum:

Pyridine	λmax(obs)	409	506	541	576	–	631
	λmax(lit)	409	506	541	576	605	631

3) <u>Protoporphyrin DTBE</u>

All three analytical techniques indicated that the proto-porphyrin DTBE was pure.

Absorption Spectrum:

Chloroform	λmax(obs)	406	506	541	576	–	631
	λmax(lit)	406.5	506	540.5	575.5	603	630

Melting Point:

Obs 229–230°

Lit 228–229° (dec)

Thin layer chromatography in chloroform (protoporphyrin R_f=0, protoporphyrin DTBE R_f=1) showed no detectable amounts of protoporphyrin free acid.

If the silica gel column was overloaded or too small, the brown band tended to run into the protoporphyrin DTBE band and a clean separation could not be obtained. The result

of this was that the yeild was much higher than the true

actual yield.   The yield of the reaction was 65%.

4)   Photoprotoporphyrin DTBE Isomer 1 (A ring reacted)

The yield of the reaction was 18%.   The isomer was pure

as determined by absorption spectrophotometry and melting

point analysis.

Absorption Spectrum:

Chloroform	λmax(obs)	387	436	500	565	613	671
	λmax(lit)	−	436	500	565	613	671

Melting Point:

   Obs 226-228°

   Lit 227-229°

5)   Photoprotoporphyrin DTBE Isomer 2 (B ring reacted)

The yield of the reaction was 20%.   The compound was pure.

Absorption Spectrum:

Chloroform	λmax(obs)	422	−	567	609	669
	λmax(lit)	422	500	565	608	668

Melting Point:

   Obs 226-228°

   Lit 226-228°

6) <u>2-Formyl-4-vinyl deuteroporphyrin DTBE</u>

The yield of the reaction was 55%. Absorption spectro-
photometry indicated that the compound was pure.

Absorption Spectrum:

Chloroform	λmax(obs)	420	519	558	583	641
	λmax(obs)	420	518.5	559	584	642

7) <u>2-Vinyl-4-formyl deuteroporphyrin DTBE</u>

The yield was 60% and the porphyrin was pure.

Absorption Spectrum:

Chloroform	λmax(obs)	420	519	558	583	641
	λmax(lit)	420	518.5	559	584	642

8) <u>2-Formyl-4-vinyl deuteroporphyrin free acid</u>

Thin layer chromatography analysis indicated that only
the free acid was present and none of the ether. Spectro-
photometry showed that the product did not change or was not
contaminated. The reaction yield was 98%.

Absorption Spectrum:

Chloroform	λmax(obs)	420	519	558	583	641
	λmax(lit)	420	518.5	559	584	642

9) 2-Vinyl-4-formyl deureroporphyrin free acid

   No esters were found in the free acid product by tlc analysis.
   The reaction yield was 85%.

   Absorption Spectrum:

   Chloroform λmax(obs)   420   519   558   583   641

                λmax(lit)   420   518.5   559   584   642

10) 2,4-Diformyl deuteroporphyrin DTBE

    The reaction yield was 10%. The product was pure by
    absorption spectrophotometry and melting point analysis.

    Absorption Spectrum:

    Chloroform λmax(obs)   437   527   563   595   650

                 λmax(lit)   436   526   562   595   650.5

    Melting Point:

           Obs 227-228°

           Lit 228-229° (dec)

11) **2,4-Diformyl deuteroporphyrin free acid**

Thin layer chromatography analysis of the product showed that it was free of the monoester and diester. The reaction yield was 98%. The absorption spectrum was normal.

Absorption Spectrum:

Pyridine	λmax(obs)	436	525	562	594	649
	λmax(lit)	436	525	561	593.5	649

12) **Photoprotoporphyrin free acid (mixed isomers)**

Thin layer chromatography analysis showed that the crude photoprotoporphyrin contained about 5% of unreacted protoporphyrin and other minor impurities.

B. ^{52}Fe Production

1) **Target Irradiations**

The open-air multisample irradiation facility in beam line 4A was limited to beam currents less than 250 nA and total activity/target to several hundred microcuries. There was no containment of radioactive material if a target was to delete or explode. Open-air operation also highly activated surrounding air in the beam line tunnel. The removal of a highly radioactive target from the facility had to be done by hand and placed into a lead transport pig. It was difficult to shield the above procedure and reduce radiation

exposure to the operator. The aluminium backing of the target holder was also very radioactive and greatly increased the radiation field.

The ^{52}Fe irradiation facility reduced the handling of the irradiated target, eliminated the air activation, and allowed higher beam currents to be run.

The use of beam line 4A had several problems. It was virtually impossible to run parasitic to another experiment. Other targets up stream from the irradiation facilities caused the beam spot size to be increased at the irradiation facilities. This resulted in running only 100-200 nA in order not to trip the beam. Another problem with running parasitic was that entry into the beam line to load or remove an irradiated target was controlled by the prime user of the beam line. Many times, access was delayed for many hours making it impossible to set up any type of schedule of when the final product would be ready. General radiation fields in the beam line area ranged from 50 mr/h to over 3 R/h near the irradiation facilities.

The use of the 500 MeV irradiation facility eliminated the above problems. Although the facility was running parasitic it was no problem to irradiate targets. The transport pig

used for the ^{52}Fe irradiation facility did not fit into the 500 MeV hot cell. Therefore a target transfer had to be done in the AECL hot cell.

2) Safety Evaluation

The cross sections for 500 MeV proton spallation calculated by the Dose program showed that the cross section for ^{52}Fe production was low compared to the other major contaminants (Table III). Also many radionuclides were produced ranging from Z=17 to Z=28 and A=34 to A=61. Changing the proton energy from 200 to 500 MeV did not change the cross section values. Production rates for various radionuclides for a 1 g Ni target were calculated for various irradiation times (Table IV). The shorter the irradiation time the lower the activity of the contaminants including ^{55}Fe and ^{59}Fe. The one hour irradiation time was impractical because not enough beam current was available on beam line 4A. It would be possible on the 500 MeV irradiation facility provided the target size was increased from 0.625 in to 4 in. in diameter. This was not practical because the increased target size would not fit into the reaction vessel and large volumes of acids would be required to dissolve the target. Based on the radionuclide activity (Table V) and gamma dose rate at 1 m (Table VI) both values could be reduced by one-half if a 1 h decay period followed 12 h of irradiation. Routinely

TABLE III

DOSE PROGRAM CALCULATED CROSS SECTIONS

Radionuclide	X-section (mb)	Radionuclide	X-section (mb)
^{61}Co	37.1	^{52}Fe	2.35
^{60}Co	39.3	^{51}Cr	27.8
^{59}Fe	0.681	^{51}Mn	8.52
^{58}Co	43.0	^{50}V	7.89
^{57}Mn	0.421	^{49}Sc	0.0174
^{57}Co	38.1	^{49}V	19.7
^{57}Ni	62.4	^{49}Cr	6.7
^{56}Mn	1.34	^{48}Sc	0.0842
^{56}Co	34.1	^{48}V	15.9
^{56}Ni	25.2	^{48}Cr	2.0
^{55}Cr	0.168	^{47}Ti	6.54
^{55}Fe	60.8	^{46}Sc	1.43
^{55}Co	18.2	^{46}Ti	1.23
^{54}Mn	24.2	^{45}Ti	5.04
^{54}Co	1.73	^{44}Sc	5.57
^{53}Mn	46.5	^{43}Sc	2.84
^{53}Fe	8.56	^{42}Sc	5.76
^{52}Mn	23.9	^{41}Cl	0.573

TABLE IV

DOSE PROGRAM PRODUCTION RATES FOR DIFFERENT IRRADIATION TIMES

| Irradiation time (hr) | 1 | 12 | 24 |
| Cooling time (hr) | 1 | 0 | 1 |
Radionuclide	Activity (mCi)		
^{61}Co	0.674	2.99	1.96
^{60}Co	0.0371	2.02	0.0384
^{59}Fe	0.00024	0.003	0.0057
^{58}Co	0.818	7.20	9.45
^{57}Co	0.00735	0.099	0.228
^{57}Ni	2.04	22.3	39.3
^{56}Mn	0.432	2.3	1.83
^{56}Co	0.0222	0.271	0.555
^{56}Ni	0.206	2.41	4.66
^{55}Fe	0.00317	0.041	0.087
^{55}Co	1.83	1.86	2.91
^{53}Fe	0.141	15.37	0.115
^{52}Mn	2.93	24.56	8.77
^{52}Fe	0.308	2.65	3.33
^{51}Cr	0.0618	0.773	1.56
^{51}Mn	3.66	15.21	6.14
^{49}Sc	0.00755	0.0303	-
^{49}V	0.0038	0.0475	0.0146
^{49}Cr	2.84	12.2	0.0968
^{48}Sc	0.00227	0.025	4.52
^{48}V	0.049	0.597	0.0438
^{48}Cr	0.102	1.07	1.20
^{44}Sc	0.719	4.83	5.20
^{43}Sc	0.711	4.61	4.32

TABLE V

DOSE PROGRAM ACTIVITIES FOR VARIOUS COOLING TIMES

Irradiation Time 12 hrs

Cooling Time (hrs)	0	1	12	84
Radionuclide		Activity (mCi)		
^{61}Co	2.99	1.97	0.0191	–
^{60}Co	2.02	0.0387	0.00036	0.00036
^{59}Fe	0.003	0.003	0.00283	0.00264
^{58}Co	7.20	6.68	2.98	0.109
^{57}Co	0.099	0.102	0.125	0.215
^{57}Ni	22.3	21.9	17.7	0.873
^{56}Mn	2.30	1.86	0.0917	–
^{56}Co	0.271	0.271	0.280	0.355
^{56}Ni	2.41	2.40	2.78	1.08
^{55}Fe	0.041	0.041	0.0458	0.544
^{55}Co	18.6	17.9	11.7	0.0288
^{53}Fe	15.37	0.115	–	–
^{52}Mn	24.6	6.68	1.34	0.635
^{52}Fe	2.65	2.44	0.971	–
^{51}Cr	0.773	0.784	0.781	0.633
^{51}Mn	15.21	6.14	0.00029	–
^{49}Sc	0.0303	0.0147	–	–
^{49}V	0.0475	0.481	0.0486	–
^{49}Cr	12.2	4.52	–	0.0478
^{48}Sc	0.025	0.0249	0.0201	0.00176
^{48}V	0.597	0.599	0.603	0.492
^{48}Cr	1.07	1.04	0.745	0.00670
^{44}Sc	4.83	4.23	1.13	–
^{43}Sc	4.61	3.86	0.551	–

TABLE VI

GAMMA DOSE RATES (MRAD/HR AT 1M)

Irradiation time (hrs)	1	12	12
Cooling time (hrs)	1	0	1
Gamma dose rate	14.5	131	67
Irradiation time (hrs)	12	12	12
Cooling time (hrs)	3	12	24
Gamma dose rate	50.6	32.9	24.8
Irradiation time (hrs)	12	12	24
Cooling time (hrs)	48	84	1
Gamma dose rate	8.26	4.26	99.8
Irradiation time (hrs)	24	24	
Cooling time (hrs)	12	24	
Gamma dose rate	57.6	44.4	

the target was allowed to decay at least 1 h in the beam line before being removed. The gamma dose rate dropped off fairly fast with time, thus greatly reducing radiation health physics problems with waste disposal (Fig. 8). The radioactive waste was allowed to decay 20-100 days before being removed from the hot cell.

Although the dose rate decreased very rapidly with time the number of gamma rays per energy did not (Fig.9, 10, 11). The computer calculated gamma spectrum for various cooling times showed that most of the gammas were of high energy and actually their numbers increased as the cooling period increased. The number of high energy gammas was a problem in shielding the hot cell and transport flask.

Based on initial experiments, high energy proton spallation of nickel produced a large number of radionuclides from Z=21 to Z=28 and A=43 to A=61 (Table VII). Most of the radionuclides produced emitted high energy gamma rays from 800 KeV to 1.5 MeV. The $T_{\frac{1}{2}}$ ranged from 3.76 min to 48 yr with the average around a few days. The following radionuclides were always detected ^{44}Sc, ^{48}V, ^{48}Cr, ^{52m}Mn, ^{52}Mn, ^{52}Fe, ^{55}Co, ^{57}Co, ^{56}Ni and ^{57}Ni.

Specific gamma ray constants for the radionuclides and
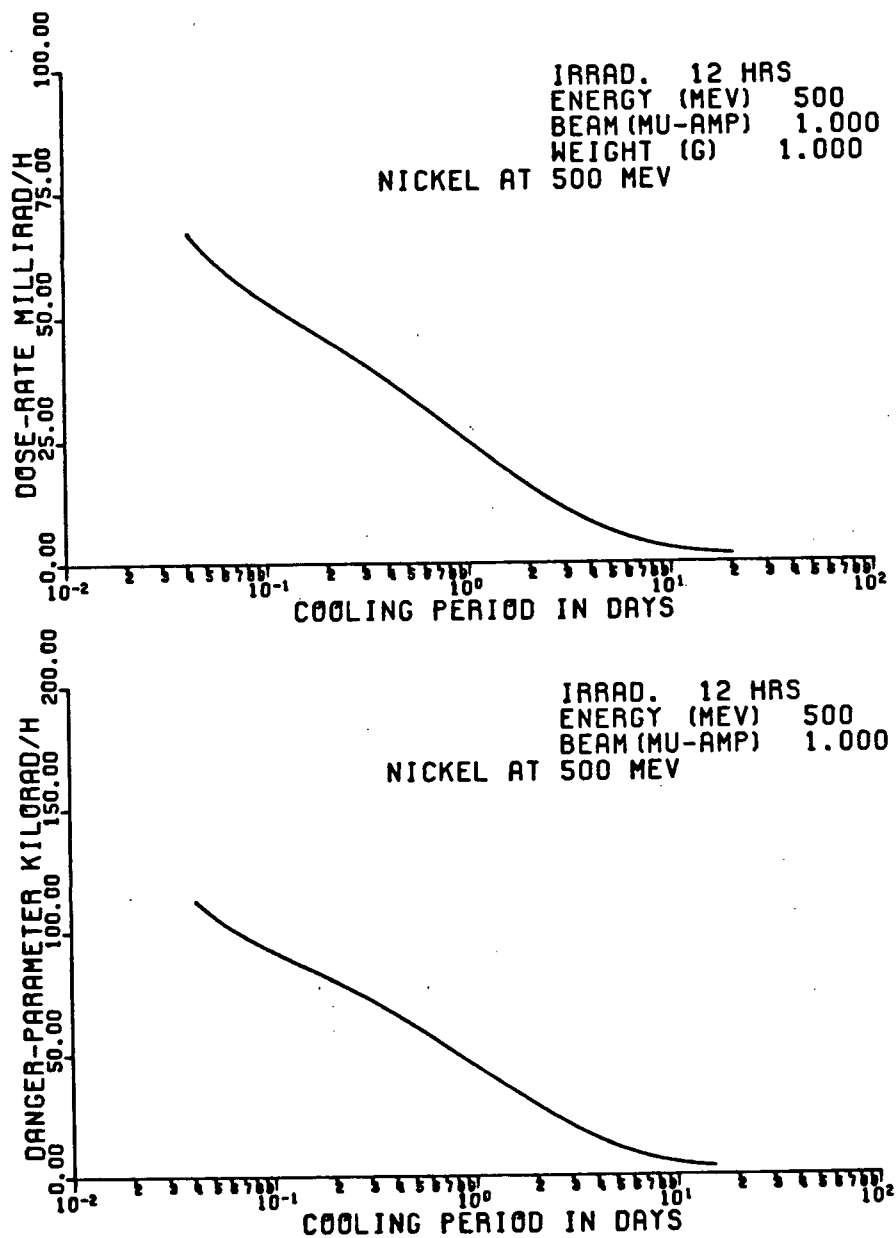
Fig 8. Dose rate vs. cooling period.
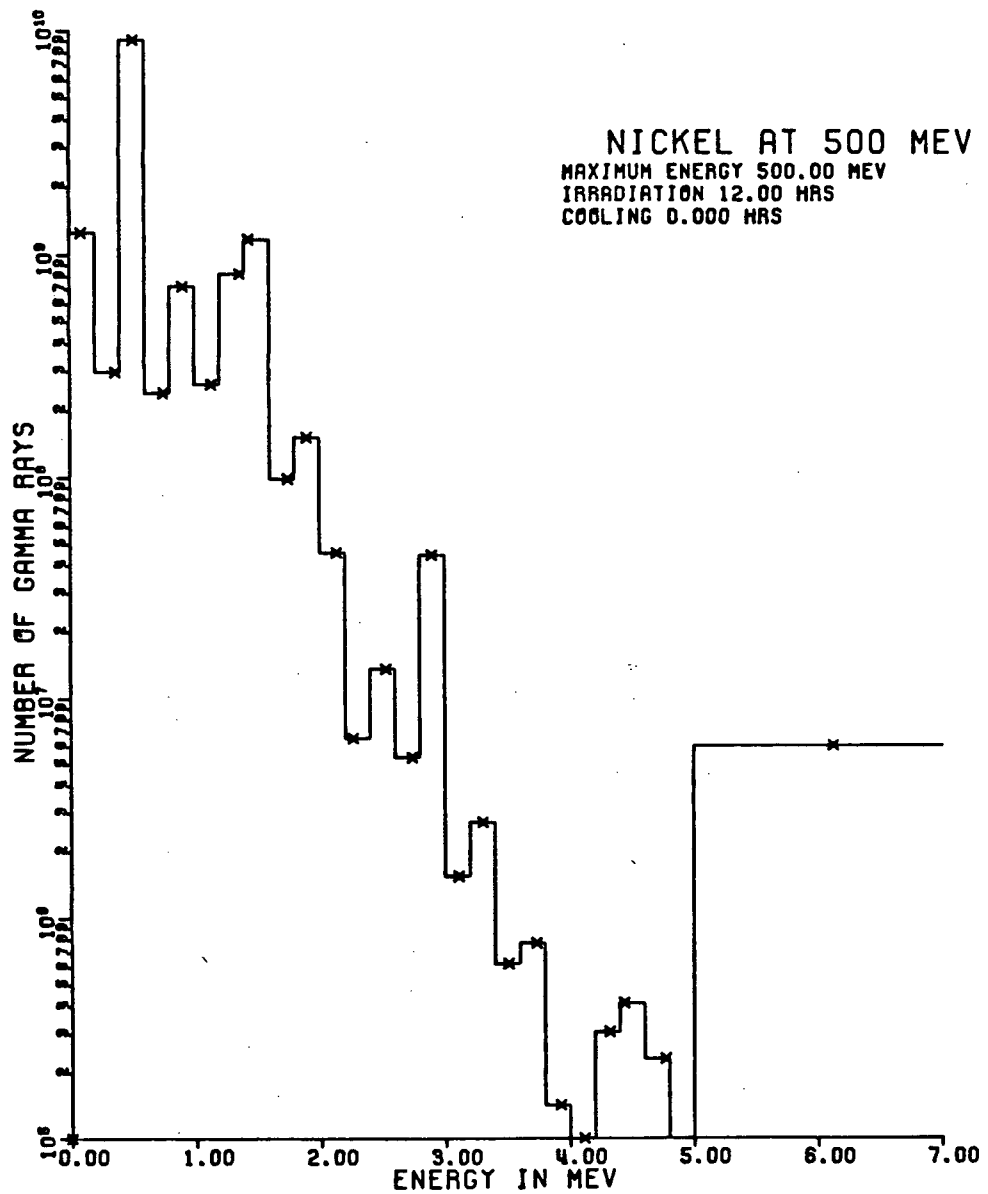
Fig 9. Computer calculated gamma spectrum I

Fig 10. Computer calculated gamma spectrum II

NICKEL AT 500 MEV
MAXIMUM ENERGY 500.00 MEV
IRRADIATION 0.50 DAYS
COOLING 7.000 DAYS
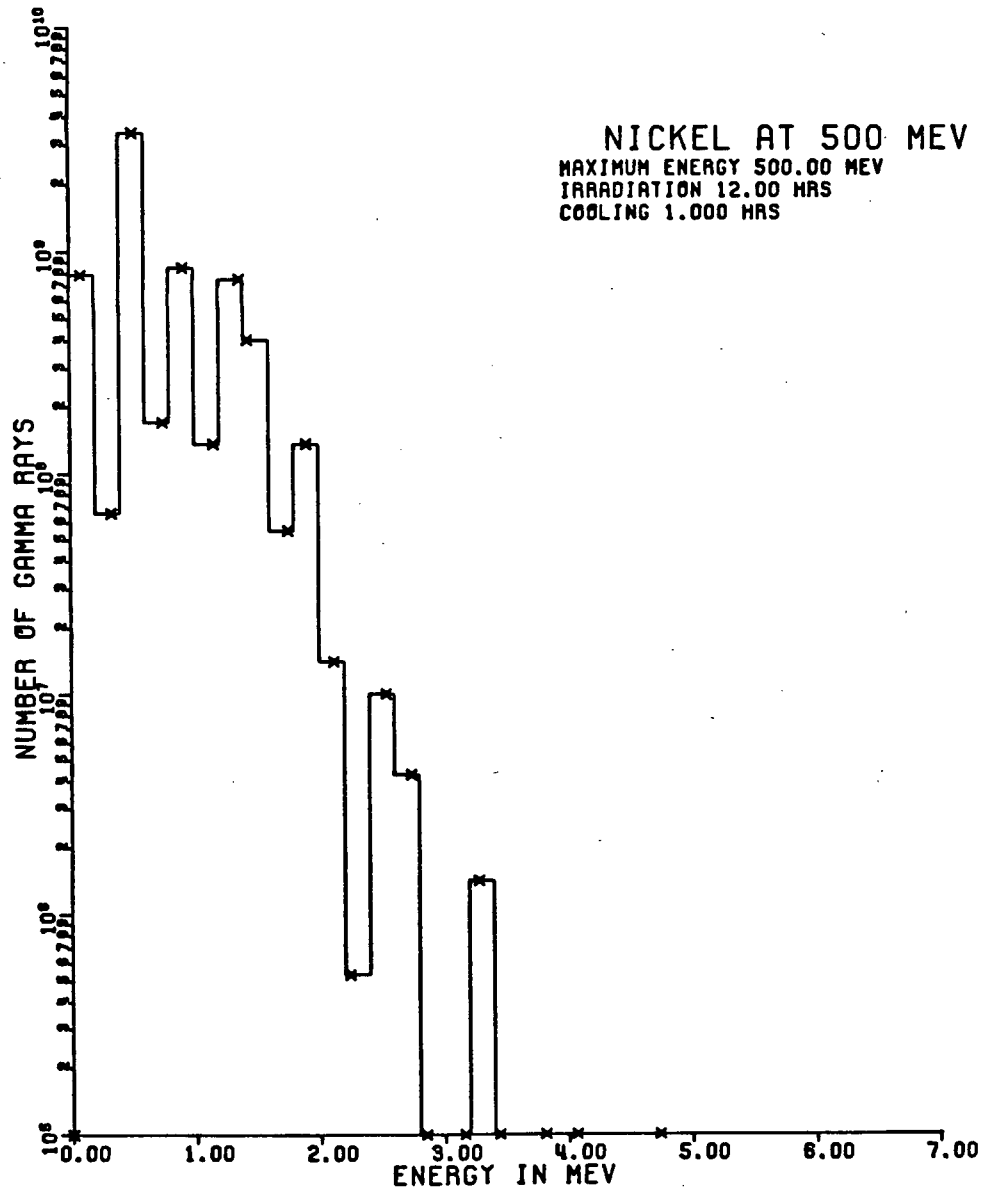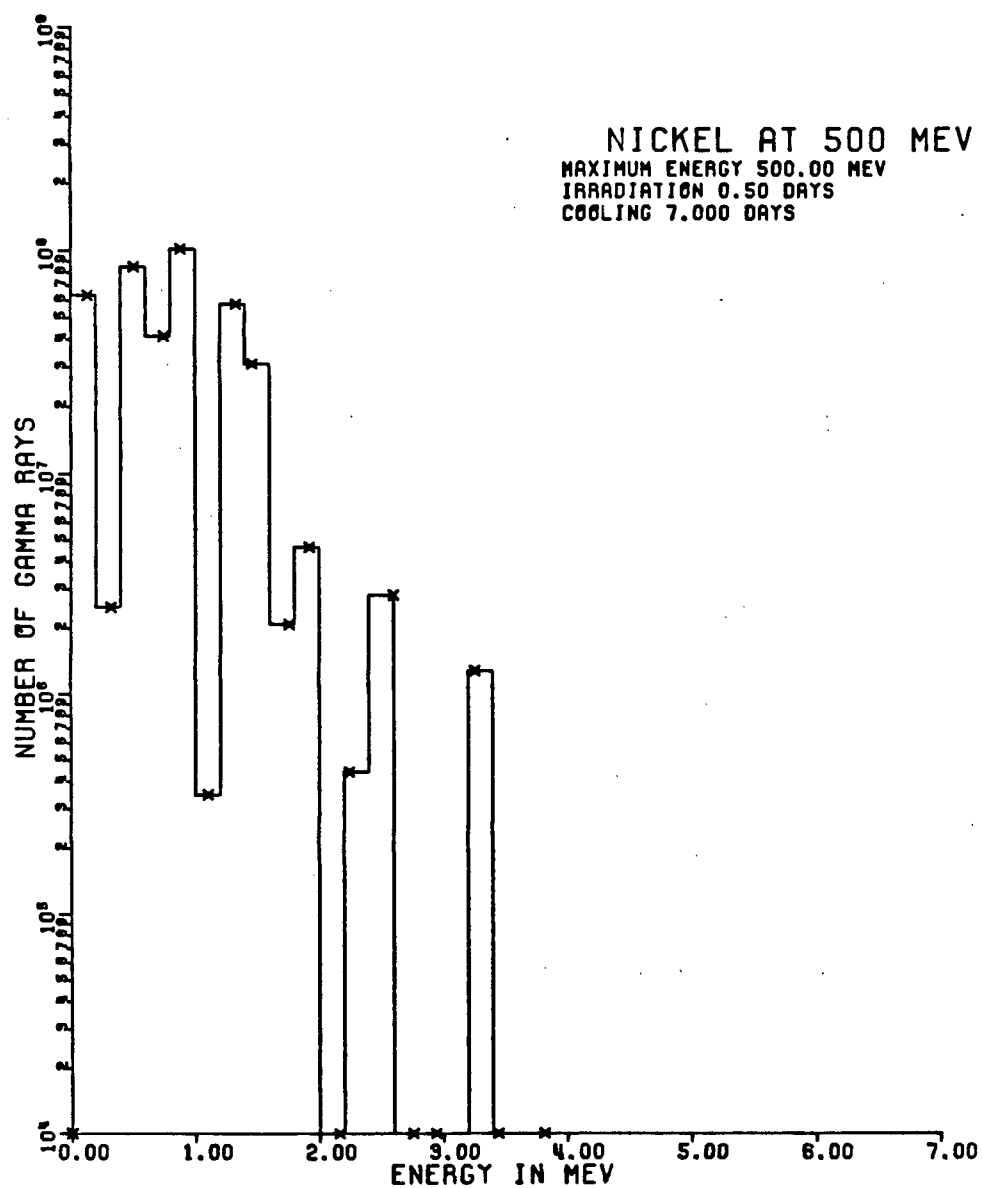
Fig 11. Computer calculated gamma spectrum III

TABLE VII

NI SPALLATION PRODUCTS

Radionuclide	Decay Mode	$T\frac{1}{2}$	Gamma Ray Energy (KeV)
^{43}Sc	B^+, EC	3.9 h	220, 370
^{44m}Sc	IT, EC	2.4 d	271
^{44}Sc	$B^{\pm}$	3.9 h	1157
^{47}Sc	B^-	3.4 d	159
^{48}Sc	B^-	1.8 d	1312
^{44}Ti	EC	48 y	66, 78
^{48}V	B^+, EC	16 d	983, 1312
^{52}V	B^-	3.8 m	1433, 1331
^{48}Cr	EC	23 h	310, 116
^{49}Cr	B^-	42 m	90.7
^{51}Cr	EC	28 d	320
^{52m}Mn	B^+, IT, EC	21 m	1437
^{52}Mn	B^+, EC	5.7 d	744, 847, 938, 1434
^{52}Fe	B^+, EC	8.2 h	165
^{55}Fe	EC	2.6 y	MN X-rays
^{59}Fe	B^-	45.1 d	1292, 1099
^{55}Co	B^+, EC	18 h	930, 1410
^{56}Co	B^+, EC	77 d	847, 1238
^{57}Co	EC	270 d	122, 136
^{61}Co	B^-	1.7 h	67.4
^{56}Ni	EC	6.1 d	163, 812
^{57}Ni	B^+, EC	36 h	1377, 129

modified gamma ray constants for various thicknesses of
lead shielding were calculated (Table VIII). Some radio-
nuclides had very high gamma ray constants which were not
reduced significantly by the lead shielding due to high
energy gamma rays.

Based on 10-12 hrs irradiation and 1 hr of cooling, 30 times
more spallation products than ^{52}Fe were produced (Table IX).
The major products were ^{57}Ni (14X), ^{52m}Mn (4X), ^{44}Sc (3.5X),
^{52}Mn (1.7X) and ^{56}Ni (1.2X). To produce one mCi of ^{52}Fe
(30 mCi spallation products) the target had a radiation
field of 27 mR/h at 1 m. Five cm of lead would reduce this
to 1.41 mR/h at 1m, 7.5 cm of lead to 0.229 mR/h at 1m,
and 10 cm of lead to 0.0709 mR/h at 1m (Table IX). The
majority of radiation came from ^{57}Ni, ^{52m}Mn, ^{56}Ni, ^{44}Sc,
^{52}Mn, ^{56}Co and ^{48}Sc.

Comparison of the initial experiments to the Dose program
showed both calculated similar gamma dose rates but differ-
ent activities for the different radionuclides(Table X).
This was due to the difference on how the Dose program
calculated cross sections from actual experimental cross
sections and the gamma ray constants used.

TABLE VIII

MODIFIED GAMMA RAY CONSTANTS

Gamma Ray Constants (R/hr/Ci)

Radionuclide	0	cm Lead		
		5cm	7.5cm	10cm
^{44}Sc	0.578	2.60×10^{-2}	4.18×10^{-3}	6.35×10^{-4}
^{47}Sc	0.0556	0	0	0
^{48}Sc	1.67	2.01×10^{-2}	2.67×10^{-3}	2.52×10^{-4}
^{48}V	1.56	5.90×10^{-2}	8.90×10^{-3}	1.84×10^{-3}
^{48}Cr	1.77	5.91×10^{-2}	8.91×10^{-3}	1.85×10^{-3}
^{52m}Mn	0.734	3.27×10^{-2}	5.21×10^{-3}	8.10×10^{-4}
^{52}Mn	0.799	2.20×10^{-2}	9.91×10^{-4}	1.07×10^{-4}
^{52}Fe	0.818	3.28×10^{-2}	5.22×10^{-3}	8.13×10^{-4}
^{55}Co	0.586	1.47×10^{-2}	2.32×10^{-3}	6.17×10^{-4}
^{56}Co	1.76	1.34×10^{-1}	3.76×10^{-2}	1.17×10^{-2}
^{57}Co	0.09	0	0	0
^{56}Ni	2.26	1.55×10^{-1}	4.24×10^{-2}	1.29×10^{-2}
^{57}Ni	0.83	4.99×10^{-2}	1.10×10^{-2}	2.50×10^{-3}

TABLE IX

EXPECTED RADIATION LEVEL FROM PRODUCTION OF 1 MCI OF ^{52}Fe

Z	Activity	mR/hr at 1 m cm lead			
		0	5cm	7.5cm	10cm
^{52}Fe	1 mCi	0.818	3.28×10^{-2}	5.22×10^{-3}	8.13×10^{-4}
^{44}Sc	3.49	2.02	9.07×10^{-2}	1.46×10^{-2}	2.28×10^{-3}
^{47}Sc	0.170	0.0095	0	0	0
^{48}Sc	0.750	1.25	1.51×10^{-2}	2.00×10^{-3}	1.89×10^{-4}
^{48}V	0.524	0.817	3.09×10^{-2}	4.66×10^{-3}	9.64×10^{-4}
^{48}Cr	0.330	0.584	1.95×10^{-2}	2.94×10^{-3}	6.11×10^{-4}
^{52m}Mn	4.06	2.98	1.33×10^{-1}	2.12×10^{-2}	3.29×10^{-3}
^{52}Mn	1.74	1.39	3.83×10^{-2}	1.72×10^{-3}	1.86×10^{-4}
^{55}Co	1.00	0.586	1.47×10^{-2}	2.32×10^{-3}	6.17×10^{-4}
^{56}Co	0.780	1.37	1.05×10^{-1}	2.93×10^{-2}	9.13×10^{-3}
^{57}Co	0.135	0.0122	0	0	0
^{56}Ni	1.24	2.80	1.92×10^{-1}	5.26×10^{-2}	1.60×10^{-2}
^{57}Ni	14.7	12.2	7.34×10^{-1}	1.62×10^{-1}	3.68×10^{-2}
Sum	30.1	26.8	1.41	2.29×10^{-1}	7.09×10^{-2}

TABLE X

COMPARISON OF DOSE PROGRAM TO INITIAL EXPERIMENTS

Radionuclide	Dose Program	Initial Experiments
	Activity	
^{52}Fe	1 mCi	1 mCi
^{44}Sc	1.82	3.49
^{47}Sc	-	0.70
^{48}Sc	0.0094	0.750
^{48}V	0.225	0.525
^{48}Cr	0.404	0.330
^{52m}Mn	3.00	4.06
^{52}Mn	9.27	1.74
^{55}Co	7.02	1.00
^{56}Co	0.102	0.78
^{57}Co	0.0374	0.135
^{56}Ni	0.102	1.24
^{57}Ni	8.42	14.7
Sum	31.4	30.1
	Gamma Dose Rate	
Gamma dose rate (mR/hr at 1 m)	25.3	26.8

3) <u>Selection of ^{52}Fe Process Chemistry using ^{59}Fe</u>

a) Recovery Tests

When the ^{59}Fe was passed through the column 99.4% of the activity stuck to the resin. Some of the Ni also stuck to the resin. No ^{59}Fe was detected in the column washes. The Ni zone slowly moved down the column but also broadened to several cm. With 0.5 N HCl elution, the Ni band started to move down the column with the solvent front. After the major Ni band was eluted off the column, 79% of the activity was in 1-2 ml of solution. One hundred per cent of the activity was in 7.5 ml of solution.

Repeating of this procedure at different HCl concentrations showed that most of the iron III stuck to the column between 8 M and 12 M HCl with the peak around 9.5 M (Fig.12). The distribution coefficient was 10^5. Removal of the iron from the column was possible with any HCl concentration less than 1 M of HCl down to ordinary distilled water.

The di-isopropyl ether extraction efficiency (overall) was 97.5% with 8 N HCl. The forward extraction efficiency was 99.4% while the back extraction efficiency was 98.1%. The maximum distribution coefficient of 100 occurred between 5.5 and 7 M HCl concentration (Fig. 12).
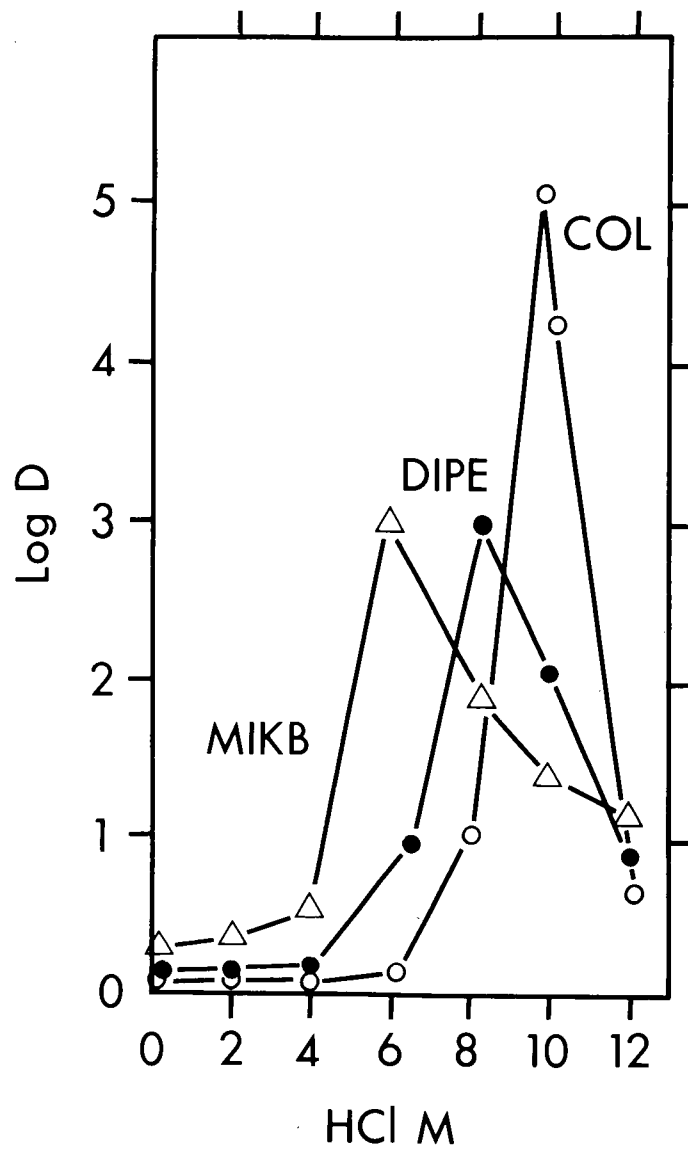
Fig 12. Distribution coefficients vs HCℓ conc
for various Fe separation methods

b) <u>Radionuclide Impurity Determination</u>

In general the extraction method with di-isopropyl ether or methyl isobutyl ketone was better than the ion exchange column (Table XI). Valves in the table were expressed as purification ratios. A solution of Ni spallation products would have a value of 10,000. All radionuclides regardless of activity were normalized to this valve. The problem with the column was that other radionuclides (^{46}Sc, ^{51}Cr, ^{54}Mn, and especially ^{56}Co) came off the column very close to the ^{52}Fe and it was not always possible to keep them separate during elution. However it was possible to eliminate all the ^{48}V and ^{56}Ni by either solvent extraction or ion exchange chromatography. Although the ^{56}Ni eluted very close to the ^{52}Fe it could be separated from the ^{52}Fe due to its intense green color. There was no difference in separating ^{46}Sc using methyl isobutyl ketone or di-isopropyl ether extraction. However both ion exchange chromatography and solvent extraction were needed to completely eliminate all the ^{46}Sc in the final product.

Methyl isobutyl ketone extraction reduced the ^{51}Cr concentration by a factor of 2 as compared with di-isopropyl ether extraction. Again both solvent extraction and ion exchange chromatography were required to completely

TABLE XI

^{52}FE CONTAMINATION TESTS
Purification Factors*
Purification Method $(\text{X } 10^{-4})$

Radionuclide	MIKB	DIPE	Column	Column & MIKB	Column & DIPE
^{46}Sc	10.0	10.5	135	0	0
^{48}V	0	0	0	0	0
^{51}Cr	2.97	5.83	102	0	0
^{54}Mn	4.81	4.35	20.8	2.24	5.65
^{56}Co	3.84	2.22	5290	1.98	2.18
^{56}Ni	0	0	0	0	0

No Purification   10,000
(Ni spallation solution)

---

*Purification Factor--Ratio of Ni spallation solution to that of the purified solution of Fe-52. Value of unpurified Ni spallation solution = 10,000. All values normalized to this value.

eliminate all the ^{51}Cr in the final product. There was no difference in either methyl isobutyl ketone or di-isopropyl ether extraction in the level of ^{54}Mn. Column ion exchange chromatography and methyl isobutyl ketone extraction reduced this level by a factor of two. Di-isopropyl ether extraction was better than methyl isobutyl ketone in reducing the ^{56}Co level by a factor of two.

Based on this data it was decided to use solvent extraction with methyl isobutyl ketone first followed by ion exchange column chromatography and eluted with water when required to purify the ^{52}Fe. The solvent extraction step reduced many of the radionuclides which overloaded the ion exchange column. The ion exchange step allowed the final product to be concentrated in a very small volume.

4) High Level ^{52}Fe Production

The total processing time was from 3 to 4 hrs with the evaporation step and cooling steps taking the longest. The product was clean as determined by gamma spectrometry (Fig. 13). The radiation field for the processing of a Ni target resulting in 1.6 mCi of ^{52}Fe at the end of separation was 1.5 mR/h contact through the lead glass window. Only 0.1 mR/h contact was measured through 4 in of lead shielding.
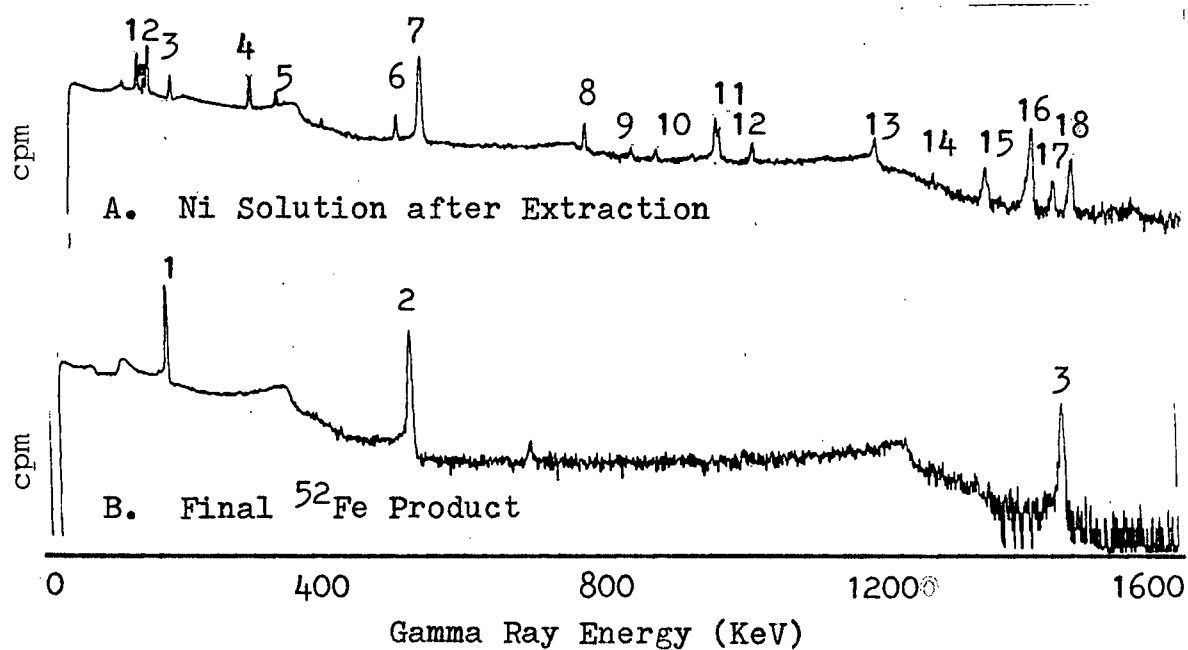
A	Energy	Radionuclide		A	Energy	Radionuclide
1	112	^{48}Cr		10	847	^{56}Co
2	126	^{57}Ni		11	932	^{55}Co
3	158	^{56}Ni		12	948	^{48}V
4	271	^{56}Ni		13	1157	^{44}Sc
5	308	^{48}Cr		14	1241	^{56}Co
6	477	^{56}Ni		15	1313	^{48}V
7	511	Positron		16	1376	^{57}Ni
8	745	^{52}Mn		17	1409	^{55}Co
9	812	^{56}Ni		18	1437	^{52m}Mn

| B	Energy	Radionuclide
1	169	^{52}Fe
2	511	Positron
3	1437	^{52m}Mn

Fig. 13 Ge(Li) Spectrum of Ni Solution and Product.

The radiation field at the operator position at window level was 0.25 mR/h. Ten mR/h contact on top and 20 mR/h contact on the sides of the lead transport pig were measured.

C. Metalloporphyrin Synthesis

1) ^{59}Fe-Hematohemin

After the reaction period, paper chromatography indicated that 45% of the ^{59}Fe went into the porphyrin. During the first extraction 55% of the activity went into the chloroform layer. This was due to incomplete extraction from the reaction mixture into the organic layer. Extraction could have been improved by using larger volumes of chloroform but it was not increased due to the problems associated with handling larger volumes of radioactive solutions. During the HCl wash and water wash 8% and 16% respectively unreacted ^{59}Fe was removed. The %tag determined by counting all fractions was 55%.

Paper chromatography of the final product indicated that the tag was greater than 99%. Any unreacted ^{59}Fe was removed in the extraction steps. Absorption spectrophotometry of the product in pyridine reduced with sodium dithionite showed that the product was pure.

Absorption Spectrum:

Pyridine λmax(obs) 410 519 550

λmax(lit) 409 519 549

Thin layer chromatography and polyamide chromatography indicated that the product was pure and did not decompose during metalation.

2) ^{59}Fe-Protohemin

The %tag as determined by paper chromatography was 60%. The %tag determined by counting all fractions was 65%. The above values refer to the metalation reaction only. After solvent extraction, paper chromatography indicated that the %tag was greater than 99%.

The hemochrome absorption spectrophotometry in 4 M pyridine and 0.2 N KOH also showed that the product was pure.

Absorption Spectrum:

Hemochrome λmax(obs) 420 526 557

λmax(lit) 419 526 557

3) ^{59}Fe-Photoprotohemin

First the ferrous sulfate or chloride method was used to metalate the porphyrin. Although paper chromatography indicated a good %tag several problems were encountered.

First, the photoprotohemin had a low solubility in chloro-
form. Increasing the volume of chloroform to 50 ml or
higher still resulted in a large loss of the product.
Second, during HCℓ extraction (wash) a heavy precipitate
formed at the solvent interface. Third, during the water
wash, a very heavy precipitate formed at the solvent inter-
face. During the extraction procedure 76% of the product
was lost.

Absorption spectrophotometry of the crude photoprotohemin
(and tlc) showed that it was contaminated with protohemin
resulting from the protoporphyrin in the photoprotoporphy-
rin and a decomposition product of photoprotohemin re-
sulting from the metalation reaction. The decomposition
could have been reduced by using the ferrous sulfate
method rather than the ferric chloride method but a new
purification procedure would have to be designed.

The first purification step was always required. The
second step was only required to remove the remaining
protohemin if it interfered in the uptake studies.

Absorption spectrophotometry (pyridine and 2% formic acid)
and tlc indicated that the product was pure. The %tag of
the final product was greater than 99%

Absorption Spectrum:

Hemochrome λmax(obs)   416   624

λmax(lit)   417   625

4) ^{59}Fe-2-formyl-4-vinyl deuterohemin

Again, during the metalation reaction, some of the product decomposed and the purification step was required to remove this contaminate. Absorption spectrophotometry (4 M pyridine 0.2 N KOH) indicated that the product was pure. The %tag of the final product was greater than 99%.

Absorption Spectrum:

Hemochrome λmax(obs)   434   538   582

λmax(lit)   434   538   582

5) ^{59}Fe-2-vinyl-4-formyl deuterohemin

Results similar to those for ^{59}Fe-formyl-4-vinyl deuterohemin were obtained.

6) ^{59}Fe-2, 4-Diformyl deuterohemin

Again the purification step was required to remove the metalation reaction decomposition products. The crystallization step was very important to remove acetal formation during column chromatography and/or solvent evaporation. Absorption spectrophotometry and tlc indicated that the

product was pure. The %tag was greater than 99%.

Absorption Spectrum:

Hemochrome				
	max(obs)	452	550	587
	max(lit)	452	550	587

7) ^{59}Fe or ^{52}Fe labelled

meso-tetra (4-carboxyphenyl) hemin,

meso-tetra (4-N-methylpyridyl) hemin tetraiodide or

tetra-Na-meso-tetra (4-sulfonatophenyl) hemin

The ferrous sulfate metalation procedure was tried.
The problem with it was that the hemins were so water
soluble that they could not be transferred into an organic
solvent. There was very little transfer into chloroform.
However there was more transfer into dichloromethane but
it would still have required a large volume of solvent for
complete transfer. There was no transfer into 4-methyl-2-
pentanone, ether, or di-isopropyl ether. Solvents where
the hemins were soluble, DMF or pyridine, however were
miscible with water.

The ferric chloride metalation procedure also worked but any
residual DMF could have caused problems in the uptake
studies. Therefore, the sodium acetate-acetic acid method
was used. The %tag determined by paper chromatography was
from 90-100%.

D. Tumor Tissue Culture Uptake Studies

The majority of hemins and some of the radionuclides
showed an initial uptake followed by a decline phase which
again was followed by an uptake phase usually higher than
the first uptake phase.

Of the two radioactive labelled porphyrins used before,
protohemin showed better uptake than hematohemin (Fig. 14).
Hematohemin uptake was 18.3% at 1 h, dropping to 10.6% at
24 h and slowly increasing to 12.4% at 72 h. Protohemin
had a very high initial uptake of 63.7% at 3 h followed by
a decline to 30% at 6 h followed by another rapid uptake
to 87% at 24 h.

Of the natural porphyrins tried the deuterohemin derivatives
showed the best early uptake (Fig. 15). The deuterohemin
derivatives showed rapid uptake of 69% at 10 h followed by
a slow increase in uptake to 100% at 72 h. The 2-formyl-
4-vinyl, 2-vinyl-4-formyl, and the 2,4-diformyl deuterohemins
had similar uptake and were shown as one curve. Photoproto-
hemin showed rapid increase to 37% at 3 h but was followed
by a decline phase, 20% at 10 h, and again followed by an
increase to 100% at 72 h.
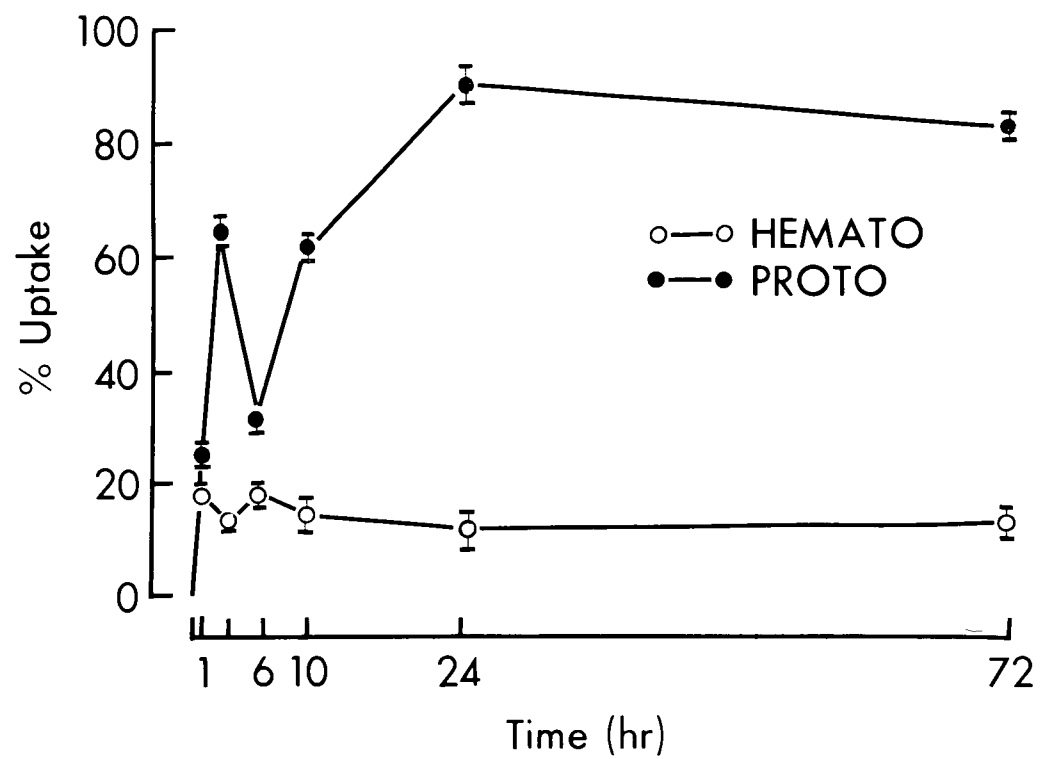
Fig 14. Tumor tissue culture uptake of previously
labelled natural porphyrins.
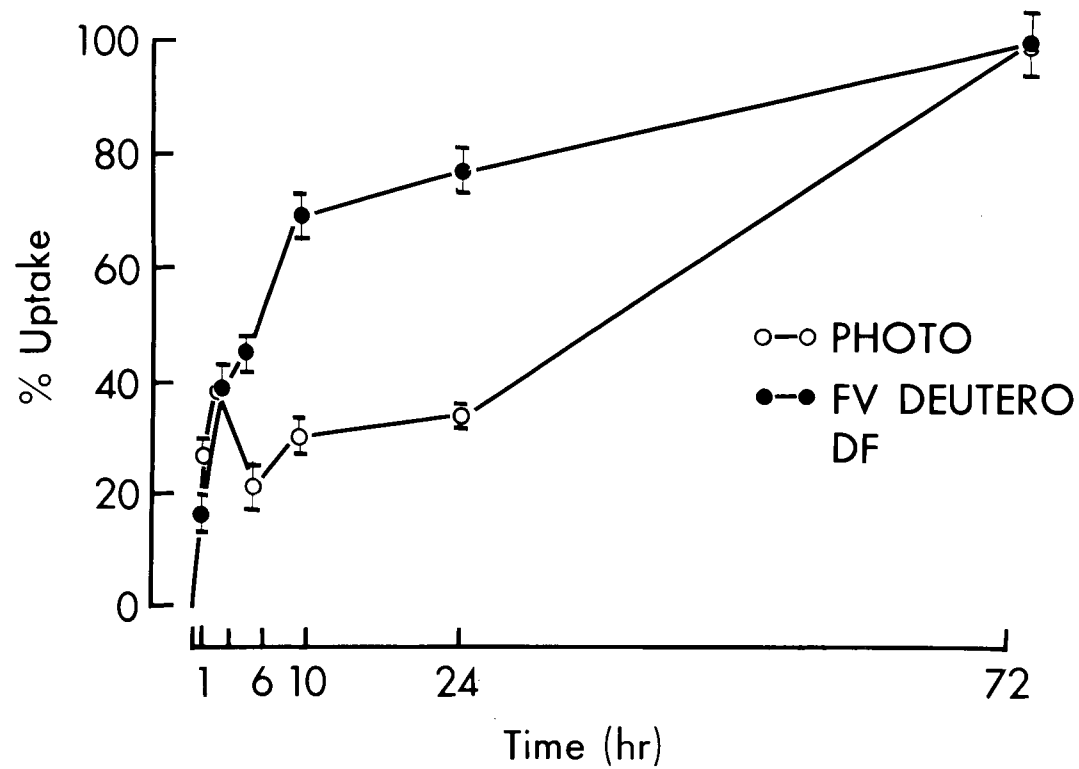
Fig 15. Tumor tissue culture uptake of natural hemins.

Of the artificial hemins tested, meso-tetra (4-carboxy-phenyl) hemin (CP) showed very rapid uptake to 60% at 3 h followed by a slow decline to 30% at 72 h (Fig.16). Tetra-na-meso-tetra (4 sulfonatophenyl) hemin (TPPS) had a similar low uptake curve as hematoporphyrin. Meso-tetra (4-N-methyl pyridyl) hemin tetraiodide (TMPI) also showed very rapid initial uptake at TPPS (60% at 1 h) but decreased to 42% at 10 h and then increased to 100% at 72 h (Fig 17).

Due to the short $T\frac{1}{2}$ of the ^{52}Fe, only hemins with rapid initial uptake were investigated further. These included the following : protohemin, TCP, and TMPI. Other hemins that showed good uptake at 24 to 72 h could not be used because a very large amount of ^{52}Fe would have to be given resulting in a very large radiation dose to the patient.

If other radionuclides were going to be used, TMPI would be the best choice because it shows very high initial uptake which was ideal for short-lived radionuclides and uptake continued up to 100% at 72 h which is ideal for longer-lived radionuclides. TMPI was labelled with ^{59}Fe (as described above), Co, Cr, and Mn. Of the four, Fe-TMPI was the best (Fig. 17). Co-TMPI showed no uptake until 3 hrs and was 21% at 6 h decreasing to 18% at 10 h. Both Cr-TMPI and Mn-TMPI showed no uptake at 10 h.
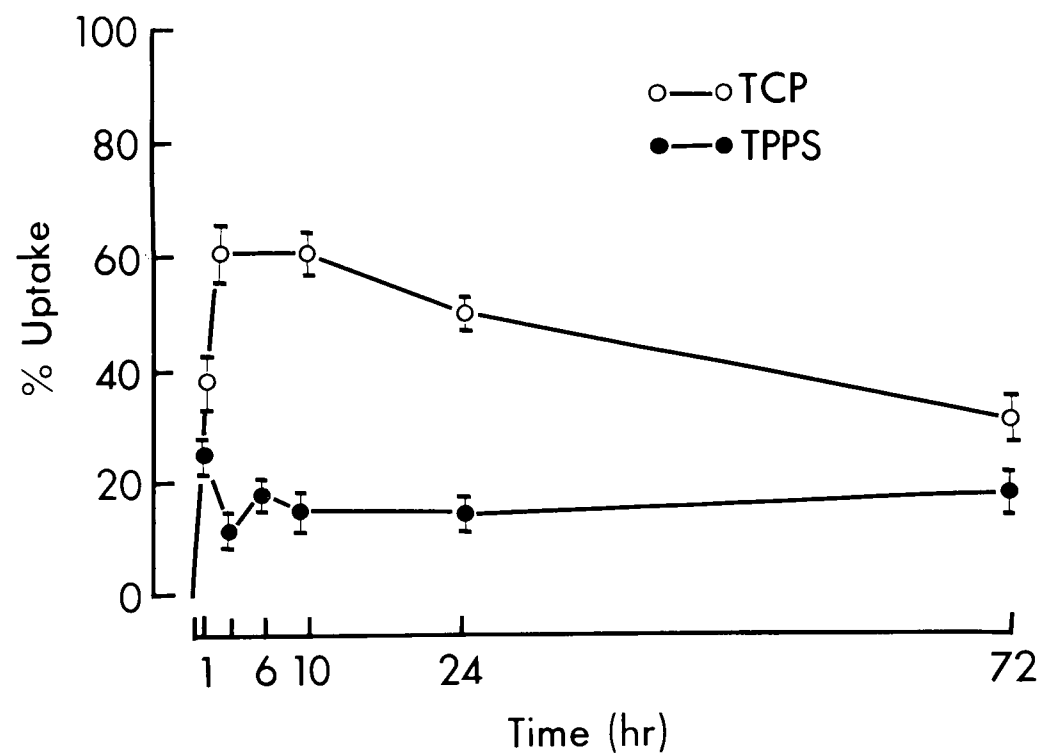
Fig 16. Tumor tissue culture uptake of artificial hemins.
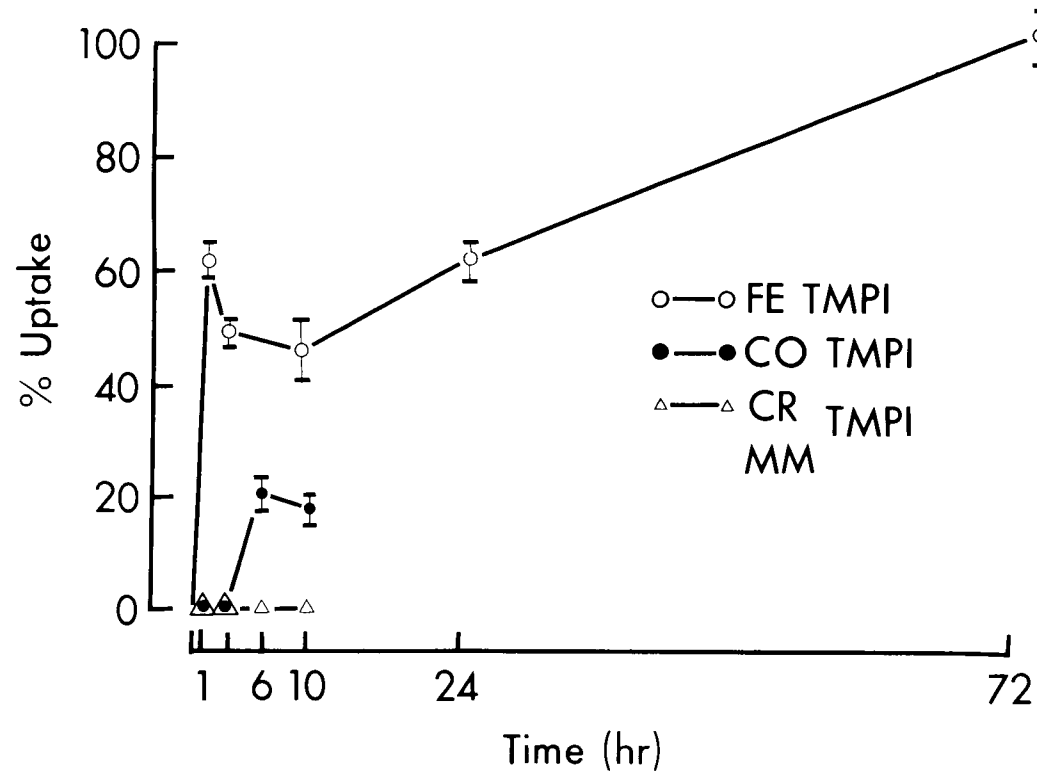
Fig 17. Tumor tissue culture uptake of TMPI labelled with different metals.

Uptake of the radionuclides by themselves was very different from that of the labelled porphyrin (Fig.18). Both ^{59}Fe and ^{67}Ga had similar uptake patterns. ^{67}Ga showed maximal uptake of 2% at 1 h followed by a decline to 0.3% at 3 h and a very slow uptake to 1.4% at 72 h. ^{59}Fe was taken up to 13% at 1 h, dropped to 2.1% at 3 h and showed slow uptake to 25% at 72 h. Both ^{46}Sc and ^{54}Mn showed no uptake until 3 h but ^{46}Sc was taken up to 49% and ^{54}Mn to 32% at 6 h. ^{48}V, ^{56}Co, and ^{51}Cr showed no uptake at 10 h.

E. Animal Studies

1) Distribution Studies

The target organs of the ^{59}Fe-labelled TMPI were the liver and spleen (Fig 19). The liver continued to take up the compound throughout the study. The % dose/g organ for the liver at 48 h was 28.6%. Uptake by the spleen increased dramatically and peaked at 12 h to 22.7% dose/g organ and slowly decreased to 10.6% dose/g organ at 48 h. Lung (Fig 20), kidney and eye (Table XII) remained relatively constant throughout the study - lung 2.5% dose/g organ; kidney 4.7% dose/g organ and eyes 0.5% dose/g organ. Blood was relatively constant at 2.8% dose/ml until 24 h but increased to 7.6% at 47 h. Bone slowly increased from 1.6%
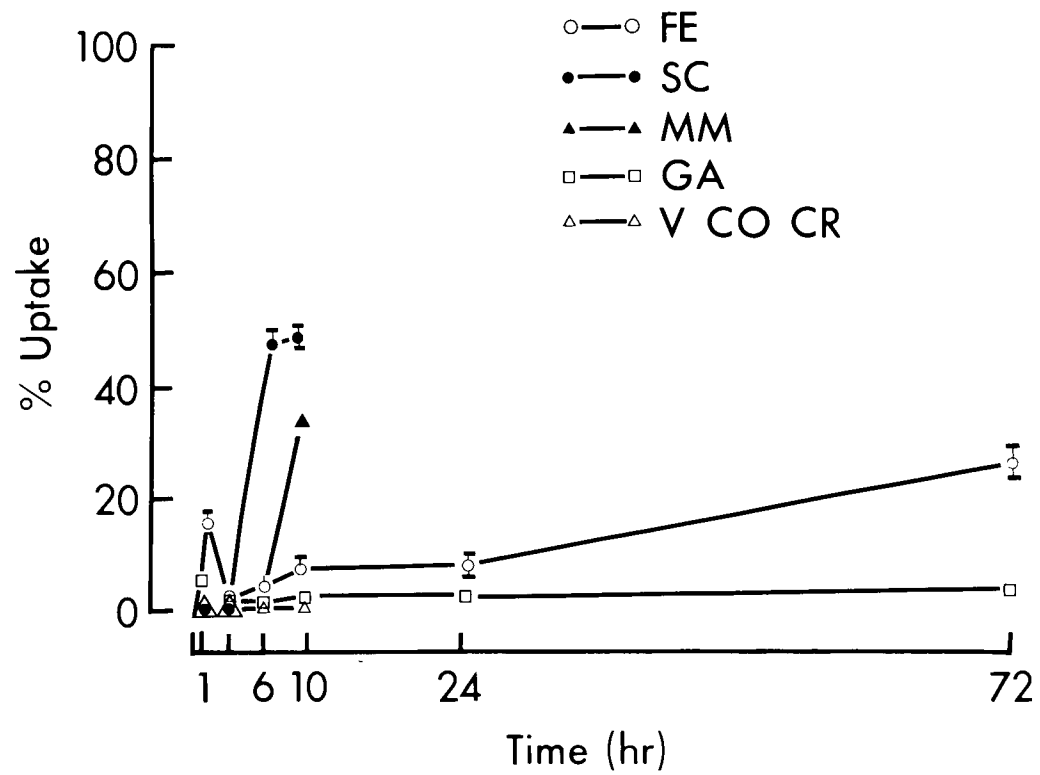
Fig 18. Tumor tissue culture uptake of various metals.
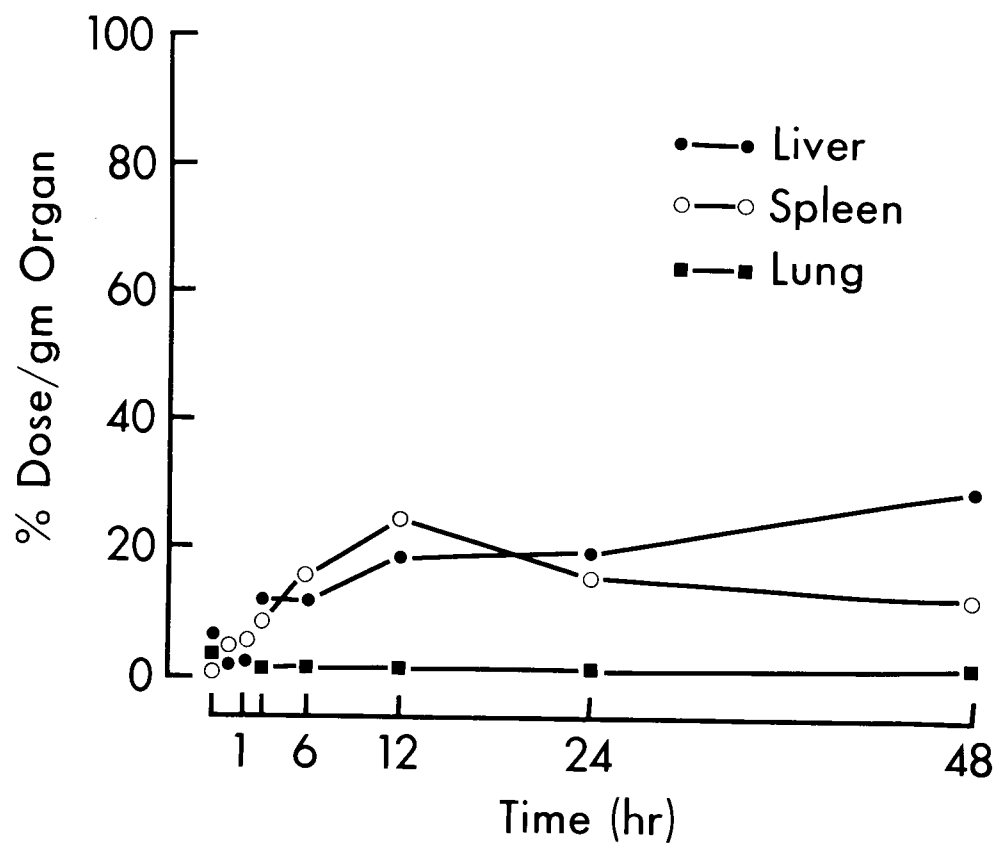
Fig 19. Animal distribution of ^{59}Fe TMPI

dose/g organ at 6 hr to 4.9% dose/g at 48 h.

Although no distribution studies have been done with this porphyrin or other Fe-labelled porphyrins, other porphyrins also showed high liver uptake. TPPS was found in considerable amounts in the liver, spleen, kidney and lung (210), although only the tumor exhibited red fluorescence. The liver, spleen and kidney contained more TPPS than the tumor (212) ^{64}Cu-protoporphyrin was shown to concentrate in mouse tumors with poor tumor to liver, blood and muscle ratios (236). Clinical studies show no tumor uptake at all (237). [57]Co-hematoporphyrin showed similar distribution in nromal and tumor-bearing animals although the tumor did show some accumulation (238). Most of the radioactivity was in the liver, kidney and spleen. Twenty four hours after injection tumor uptake was higher than blood or muscle, but only 1/5 of liver uptake. The liver was the target organ for these porphyrin because the liver is the natural site of normal porphyrin and bile acid metabolism. Porphyrins are broken down into bile acids in the liver.

The distribution of the ^{59}Fe cl$_3$ was completely different from that of the ^{59}Fe-labelled TMPI indicating that the ^{59}Fe was attached to the TMPI and not free (Fig. 20 Table

% Dose/gm Organ

Time (hr)

●—● Liver
○—○ Spleen
■—■ Lung
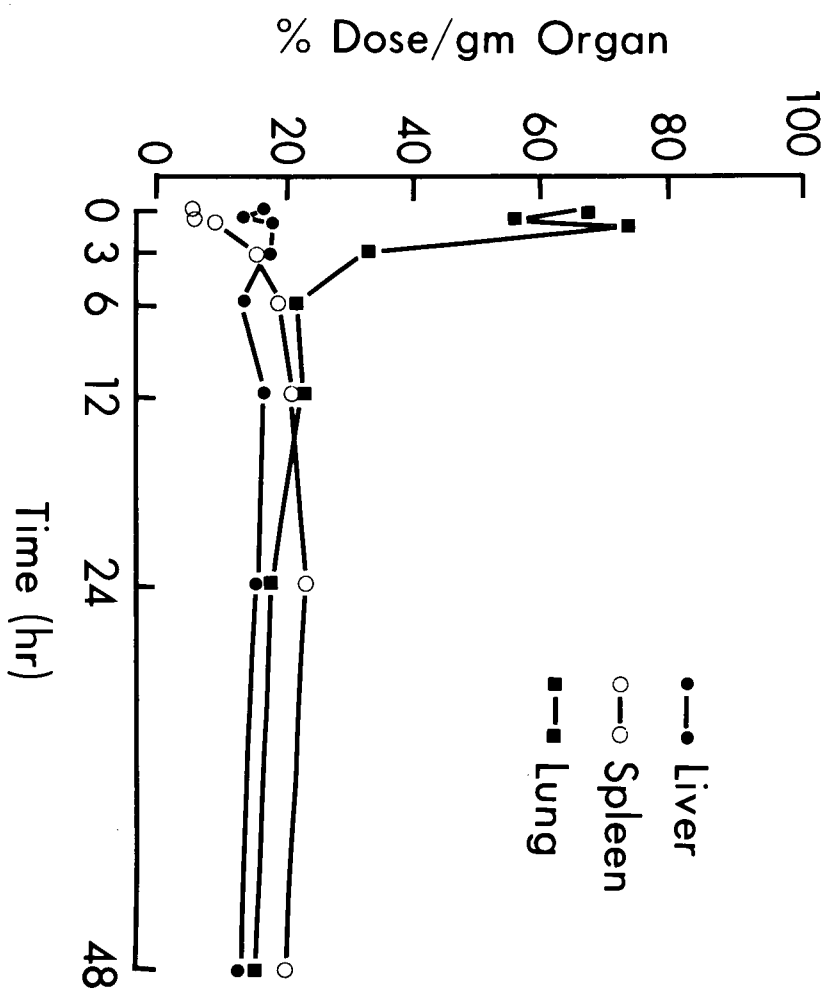
Fig 20. Animal distribution of $^{59}FeCl_3$

XIII). The ^{59}Fe-chloride was strongly taken up by the lung. The % dose/g organ was 67.3% at time 0; increased to 74.5% dose/g organ at 1 h and decreased dramatically to 22% dose/g organ at 6 h. Lung uptake remained relatively constant at 18% dose/g organ from 6 to 48 h. Spleen uptake increased to 19% dose/g organ at 6 h and remained relatively constant for the rest of the study.

Liver uptake remained relatively constant from 0 to 48 h at 15% dose/g organ. Bone increased to 3.4% dose/g organ at 12 h and remained constant thereafter. Both kidney (15% dose/g and eye (0.2% dose/g) remained constant throughout the study. Blood was slowly increasing from 1.4% dose/ml at 0.5 h to 11% dose/ml at 48 h..

No studies have been done with ^{59}Fe-chloride but with ^{59}Fe-citrate. The ^{59}Fe-citrate showed high uptake by the spleen, marrow and blood with low uptake by other soft tissues (311). Blood uptake was 19% dose/g at 72 h and spleen uptake was 117% dose/g at 7 h. Lung uptake was not tested for. ^{59}Fe-citrate showed no affinity for tumor tissue as ^{67}Ga-citrate did. During the distribution study 30%, (8/40) of the animals died during injection if the dose was given too fast. Reducing the dose by 1/2 or injecting very slowly prevented this. Animals went into muscular spasms and died within a few minutes. Animals who survived the injection were healthy and

TABLE XII

ANIMAL DISTRIBUTION OF ^{59}FE-TMPI

%Dose/Gm Organ (Mean ± SEM)

Time(h)	Blood	Kidneys	Bone	Eyes
0	6.57 ± 0.642	6.25 ± 1.95	0.730 ± 0.218	0.330 ± 0.115
0.5	1.65 ± 0.240	4.76 ± 1.47	1.91 ± 0.840	0.437 ± 0.289
1	1.76 ± 0.667	5.29 ± 1.36	1.01 ± 0.316	1.02 ± 0.408
3	2.73 ± 0.870	3.56 ± 0.632	0.331 ± 0.133	0.521 ± 0.409
6	2.63 ± 0.396	2.37 ± 0.480	1.57 ± 0.678	1.19 ± 0.639
12	2.75 ± 0.455	4.33 ± 0.565	1.92 ± 0.147	0.686 ± 0.247
24	2.72 ± 0.596	4.67 ± 0.450	2.75 ± 0.309	0.578 ± 0.209
48	7.61 ± 0.897	5.30 ± 1.60	4.90 ± 0.466	0.415 ± 0.298

TABLE XIII

ANIMAL DISTRIBUTION OF ^{59}FE-CHLORIDE

%Dose/Gm Organ (Mean ± SEM)

Time(h)	Blood	Kidneys	Bone	Eyes
0	3.56 ± 0.722	2.60 ± 0.574	0.570 ± 0.142	0.125 ± 0.0725
0.5	1.39 ± 0.194	0.86 ± 0.079	0.295 ± 0.039	0.109 ± 0.032
1	1.64 ± 0.146	1.53 ± 0.143	0.593 ± 0.121	0.115 ± 0.037
3	1.75 ± 0.407	1.59 ± 0.124	0.618 ± 0.201	0.132 ± 0.038
6	2.72 ± 0.404	1.62 ± 0.382	2.86 ± 0.431	0.289 ± 0.072
12	4.53 ± 0.696	1.50 ± 0.167	3.47 ± 0.786	0.128 ± 0.056
24	6.77 ± 0.687	1.56 ± 0.071	3.42 ± 0.374	0.280 ± 0.050
48	10.8 ± 0.694	1.76 ± 0.178	3.42 ± 0.405	0.162 ± 0.056

normal 48h after injection. Injecting the porphyrin too fast over loads the animal and was related to concentration. Patients given hematoporphyrin experienced severe burning, when injected directly into the vein (209). Infusion over a long period with glucose caused no discomfort to the patient.

2)   Scintigraphy

Studies in normal rabbits showed that all the ^{52}Fe-TMPI localized in the liver. Studies using ^{52}Fe-TMPI, ^{52}Fe-TCP, and ^{52}Fe-Protohemin with tumor bearing rats showed no tumor localization at 3 h and 24 h after injection (Fig.21). All of the activity went to the liver. ^{52}Fe-chloride III) did concentrate in the tumor and RE system.

3)   Excretion Study

The whole body excretion curve showed that the biological half-life of ^{59}Fe-TMPI was extremely long (Fig. 22)

The effective half life can be calculated from :

$$t \tfrac{1}{2} \text{ eff} = \frac{t\tfrac{1}{2}\text{bio} \times t\tfrac{1}{2}\text{phy}}{t\tfrac{1}{2}\text{bio} + t\tfrac{1}{2}\text{phys}}$$

where $t\tfrac{1}{2}$bio = 270d = 6480 h
        $t\tfrac{1}{2}$phy = 8.2h

therefore $t\tfrac{1}{2}$eff = $\sim$8.2h

1. PROTO
2. TCP
3. FE
4. TMPI
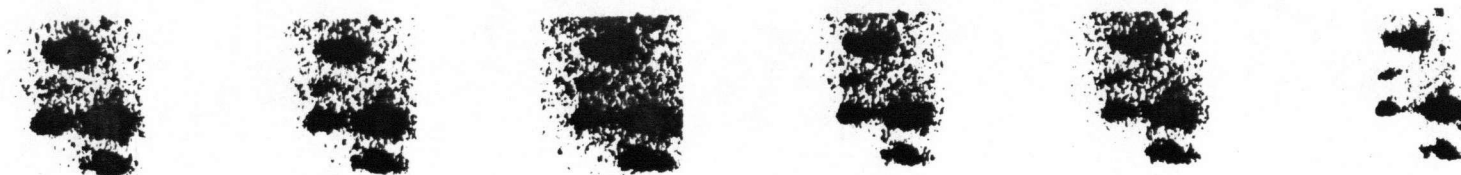
Fig 21. Tomographic scan of tumor bearing rats using ^{52}Fe hemins
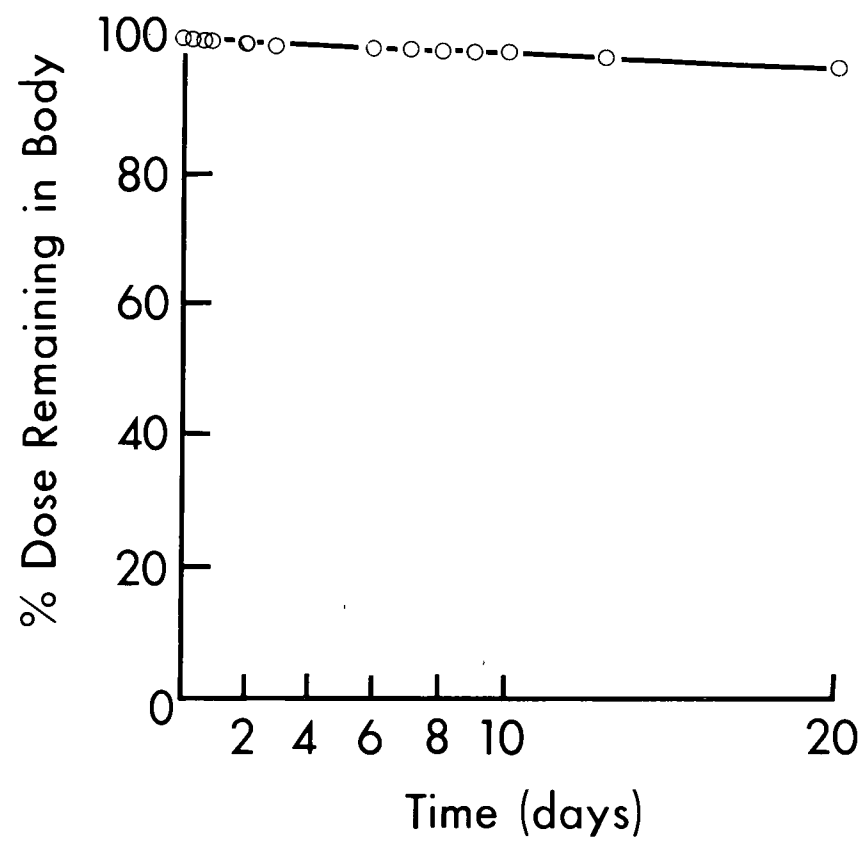
Fig 22. Excretion curve of ^{59}Fe-TMPI

It appears that the ^{59}Fe-TMPI was taken up by the liver but cannot be metabolized and thus cannot be excreted from the body too readily.

Again 30% (3/10) of the animals died during injection when given the dose too fast. Reducing the dose by 1/2 on injecting very slowly prevented this. Mice 1 week after injection showed some signs of muscular weakness and hair loss but were normal after 2 weeks.

F. Dosimetry

The radiation dose from 1 mCi of ^{52}Fe-TMPI to the whole body, liver, spleen, kidney and lung were calculated. The following assumptions were made for the dose calculations :

1) The distribution and excretion data determined in mice also applied to humans.

2) The distribution and biological half-life of ^{52}Fe-TMPI will be the same as ^{59}Fe-TMPI

3) The effective $t_{\frac{1}{2}}$ was 8.2 h

4) Since organ uptake was increasing or remained constant during the first $t_{\frac{1}{2}}$phy or 8.2 h of the distribution study, an effective $t_{\frac{1}{2}}$ of 8.2 h was used for every organ.

5) The maximum organ uptake in the first 8.2 h of the distribution study were :

Organ	Max % Dose/G Organ	Max % Dose
Liver	14.4	27
Spleen	18.6	2.32
Kidney	6.25	3.13
Lung	3.33	0.732

The absorbed doses were calculated using the following equation proposed by Loevinger (312) and modified by Snyder et al (313)

$$\bar{D}\,(r_1 \leftarrow r_2) = \frac{\tilde{A}_2}{m_1} \sum_i \Delta i \; \phi i \; (r_1 \leftarrow r_2) \text{ rads}$$

$$= \tilde{A}_2 \sum_i \Delta i \; \phi i (r_1 \leftarrow r_2) \text{ rads}$$

where:

$\bar{D}\,(r_1 \leftarrow r_2)$ = The mean absorbed dose to a target organ r_1 from a radionuclide uniformly in source organ r_2 (rads)

$\tilde{A}_2$ = The cumulated activity in source organ r_2 (νCi-h)

m_1 = The mass of target organ r_1 (g)

Δi = The equilibrium dose constant for radiation type i = 1,2,3.. with fractional frequency n_1 per disintegration and a mean energy $\bar{E}_i$ in MeV

= 2.13 $n_i \, E_i$ (g-rads)

$\phi i(r_1 \leftarrow r_2)$ = The absorbed dose fraction of energy for target organ r_1 for particles i emitted in source organ r_2

$\Phi i(r_1 \leftarrow r_2)$ = The specific absorbed fraction of energy for target organ r_1 for particles i emitted in source organ r_2

The above equation can be simplified:

$$\bar{D}(r_1 \leftarrow r_2) = \tilde{A}_2 S(r_1 \leftarrow r_2)$$

where $S(r_1 \leftarrow r_2) = \sum_i \Delta i \, \phi i(r_1 \leftarrow r_2)$

S values were obtained from Snyder et al (313) Table XIV) Since there are generally a number of source organs, the total average dose to target organ r_1 is

$$\bar{D}(r_1) = \sum_2 \bar{D}(r_1 \leftarrow r_2)$$
$$= \sum_2 \tilde{A}_2 S(r_1 \leftarrow r_2)$$

where:

$$\tilde{A}_2 = \int_{t_1}^{t_2} A_o e^{->t}$$

a) Whole Body

Assuming uniform distribution in the whole body and 69,880 g standard body weight the whole body dose was calculated as follows :

$$\tilde{A}_{WB} = A_o \sum 1.44 \; t_{½eff} \propto hj$$

where αhj = the initial value of ith exponential

component of radionuclide that appears

in the source.

$$= (1000) \ (1.44) \ (8.2)$$

$$= 11800 \ \mu Ci-h$$

$$\bar{D}_{TB} = \tilde{A}_{WB} \ S(TB \leftarrow TB)$$

$$= (11800) \ (1.4 \times 10^{-S})$$

$$0.1652 \ rad/mCi$$

where $S \ (TB \leftarrow TB) = 1.4 \times 10^{-S} \ rad/\mu Ci-h$

b) Cumulated Activity

The following values were calculated from the distri-

bution data and the effective $+\frac{1}{2}$:

$$\tilde{A}_{WB} = 11800 \ \mu Ci-h$$

$$\tilde{A}_{L} = A_0 \Sigma 1.44 \ t\frac{1}{2} \ eff \ \alpha hj$$

$$= (0.27) \ (1000) \ (1.44) \ (8.2)$$

$$\tilde{A}_{L} = 3188 \ \mu Ci-h$$

$$\tilde{A}_{S} = 274 \ \mu Ci-h$$

$$\tilde{A}_{k} = 370 \ \mu Ci-h$$

$$\tilde{A}_{Lu} = 86.4 \ \mu Ci-h$$

c) Mean dose

Liver $\quad \bar{D} = \Sigma \ \tilde{A}_{2} \ S(r_{1} \leftarrow r_{2})$

$$\bar{D}_L = \tilde{A}_{wb}\, S(L{\leftarrow}WB) + \tilde{A}_L\, S(L{\leftarrow}L) + \tilde{A}_S\, S(L{\leftarrow}S)$$
$$+ \tilde{A}_k\, S(L{\leftarrow}K) + \tilde{A}_L\, S(L{\leftarrow}Lu)$$
$$= 11{,}800(1.5{\times}10^{-S}) + 3188(3.8{\times}10^{-4})$$
$$+ 274(6{\times}10^{-6}) + 370(2.2{\times}10^{-5})$$
$$+ 86.4\,(3.8{\times}10^{-4})$$
$$= 1.43 \text{ rads/mCi}$$

Spleen
$$\bar{D}_S = \tilde{A}_{WB}\, S(S{\leftarrow}WB) + \tilde{A}_L\, S(S{\leftarrow}L) + \tilde{A}_S\, S(S{\leftarrow}S)$$
$$+ \tilde{A}_k S(S{\leftarrow}K) + \tilde{A}_{Lu} S(S{\leftarrow}Lu)$$
$$= 1.06 \text{ rads/mCi}$$

Kidney
$$\bar{D}_k = \tilde{A}_{WB}\, S(K{\leftarrow}WB) + \tilde{A}_L\, S(K{\leftarrow}L) + \tilde{A}_S\, S(K{\leftarrow}S)$$
$$+ \tilde{A}_k\, S(K{\leftarrow}K) + \tilde{A}_{Lu} S(K{\leftarrow}Lu)$$
$$= 0.924 \text{ rads/mCi}$$

Lung
$$\bar{D}_L = \tilde{A}_{WB}\, S(Lu{\leftarrow}WB) + \tilde{A}_L\, S(Lu{\leftarrow}L) + \tilde{A}_S\, S(Lu{\leftarrow}S)$$
$$+ \tilde{A}_k\, S(Lu{\leftarrow}K) + \tilde{A}_{Lu}\, S(Lu{\leftarrow}Lu)$$
$$= 0.271 \text{ rads/mCi}$$

Table XV summarizes the dose values calculated.

TABLE XIV

S VALUES FOR ^{52}FE (RAD/UCI-H)

Source Organ

Target Organ	Whole Body	Liver	Spleen	Kidney	Lung
Liver	1.6×10^{-5}	3.8×10^{-4}	6.0×10^{-6}	2.2×10^{-5}	1.4×10^{-5}
Spleen	1.6×10^{-5}	5.6×10^{-6}	3.1×10^{-3}	4.7×10^{-5}	1.2×10^{-5}
Kidney	1.6×10^{-5}	2.1×10^{-5}	4.8×10^{-5}	1.8×10^{-3}	5.7×10^{-6}
Lung	1.5×10^{-5}	1.4×10^{-5}	1.2×10^{-5}	5.2×10^{-6}	5.1×10^{-4}

From Ref. 313

TABLE XV

DOSE CALCULATIONS FOR ^{52}FE-TMPI

Organ	Dose (rad/mCi)
Whole Body	0.165
Liver	1.43
Spleen	1.06
Kidney	0.924
Lung	0.271

V   CONCLUSIONS

No problems were encountered in the synthesis of the various porphyrins. The only disadvantage being that some reaction yields were low, resulting in the use of large quantities of starting materials. Quality control of the desired product was very simple because absorption spectrophotometry and/or thin layer chromatography was used.

The 500 MeV irradiation facility was the best facility to irradiate targets because entry into the beamline was not required. Also targets could be irradiated at any time without requesting beam time.

^{52}Fe produced by high energy proton spallation and separation by methyl isobutyl ketone was pure as determined by Ge(Li) spectroscopy. The amounts of ^{55}Fe and ^{59}Fe in the ^{52}Fe limited the clinical use of the ^{52}Fe but the radiation dose to the patient from ^{55}Fe contaminated ^{52}Fe was still lower than the ^{59}Fe. The dissolving of the target and evaporation of the nitric acid were the most time consuming steps.

Metalloporphyrin synthesis procedures had to be modified when carrier-free radionuclides were used to label the porphyrins. Most procedures did remove any unreacted

porphyrin and radionuclide. However, this was not possible with the artificial hemins. These were so water soluble that they were impossible to transfer into an organic solvent. If these porphyrins are going to be used in the future, better separation techniques must be developed.

TMPI, TCP and protohemin showed high initial uptake using tissue culture techniques with mouse tumor cells (P815). Both porphyrins used in detecting tumors showed poor uptake. TMPI labelled with other radionuclides also showed poor uptake along with the radionuclides by themselves.

Normal mice distribution studies using ^{59}Fe-TMPI showed that the target organ for this agent was the liver and spleen. Initial animal scans using ^{52}Fe-TMPI and normal rabbits showed that it all localized in the liver studies using ^{52}Fe-TMPI, ^{52}Fe-TCP and ^{52}Fe-protohemin with tumor bearing rats showed no localization at all. All of the above agents went to the liver. However ^{52}Fe-chloride did concentrate in the tumor and RE system.

It appears from this study, the more unnatural the porphyrin structure the better the tumor and liver uptake. If liver uptake in the animal could be reduced, the porphyrin may go to the tumor. It was assumed that the very un-

natural structure of TMPI would show high tumor uptake and low liver uptake. Based on this study, all porphyrins tested were not suitable to be used as a tumor scanning agent in nuclear medicine.

More work has to be done on the mechanism of porphyrin uptake and metabolism in both tumor and liver tissue. A large number of ^{52}Fe labelled porphyrin may have to be screened to find one which has high tumor and low liver uptake.

VI BIBLIOGRAPHY

1.   Anderson   W.A.D. and Scotti   T.M., Synopsis of Pathology, Saint Louis, C.V. Mosby Company, 1976 p.345.

2.   McCready   V.T. and Trott   N.G., in Tumor Localization with Radioactive Agents 1974 (Proc. Symp. Vienna 1974) 1, IAEA, Vienna: 63-66, 1976.

3.   Hubner   K.F., Gould   A.A., Washburn   L., Wieland   B.W., J. Nucl. Med. 18: 1215, 1977.

4.   Welch M.J., Coleman   R.E., Straatmann   M.G., Asberry B.E., Primeau   J.L., Fair   W.R., Ter-Pogossian   M.M., J. Nucl. Med. 18: 718, 1977.

5.   Fowler   J.S., J. Nucl. Med. 14: 63, 1973.

6.   Wolf   W. and Berman   J.A., J. Nucl. Med. 16: 502, 1975.

7.   Gelbard   A.S., Christie   T.R., Clarke   L.P., Laughlin J.S., J. Nucl. Med. 18: 718, 1977.

8.   Thomas   C.G., Ann. Surg. 170:396, 1969.

9.   Lembares   N., J. Nucl. Med. 14: 630, 1973.

10.   Spolter   L., J. Nucl. Med. 14: 456, 1973.

11.   Sterberg   J. and Imbach   A., Int. J. Appl. Radiat. Isot. 18: 557, 1967.

12.   Quastel   J.H. and Brickis   I.J., Nature 183: 281, 1959.

13.   Spencer   R.P., J. Nucl. Med. 8: 197, 1967.

14.   Pateson   A.H.G. and McGready   V.R., in Tumor Localization with Radioactive Agents 1974 (Proc. Symp. Vienna 1974) 1, IAEA, Vienna: 63, 1976.

15.   Honda   T., Heindel   N.D., Risch   V.R., Burns   H.D., Micalizzi   M., Brady   L., Appl. Rad./N.M. nov./dec.:169, 1975.

16.   Blau   M., in Medical Radioisotope scanning (Proc. Symp. Vienna 1964) 2, IAEA, Vienna: 275, 1964.

17.   Sodee   D.B., in Medical Radioisotope scanning 1964 (Proc. Symp. Vienna 1964) 2, IAEA, Vienna: 289, 1964.

18.   Potcher   E.J., Radiol. Clin. North Am. 5(A):267, 1967.

19.   D'Angio   G.T., Rad. 93: 615, 1969.

20.   Stolzenberg   J., J. Nucl. Med. 13: 565, 1972.

21.   Ferrucci   J.T.,Am. J. Roentgenol Rad. Ther. Nucl.
Med. 109: 793, 1970.

22.   Herrera   N.E., J. Nucl. Med. 6: 792, 1966.

23.   Toole   J.F. and Witcofski   R., JAMA 198:   1219, 1966.

24.   Thomas   C.G., Ann. Surg. 170: 396, 1969.

25.   Eddleston   A.L.F., Gut 12: 245, 1971.

26.   Thomas   R.L., Am. J. Roentgen. Rad. Ther. Nucl. Med.
104:646, 1968.

27.   Jacobstein   J.D. and Quinn   J.L., Rad 107: 677, 1973.

28.   Mathews C.M.E. and Molinaro G., Br. J. Exp. Pathol.
44: 200, 1963.

29.   Van der Werff   J.T., ACTA Radiol. suppl: 243, 1965.

30.   Larson S.M., Milder   M.S., Johnston   G.S., in Radiophar-
maceuticals, Subramania   G., Rhodes   B.A., Copper   J.F., Sodd
V.J., Eds. New York: Society of Nuclear Medicine 1975 p.413.

31.   Raynaud   E., J. Nucl. Med. 14: 947, 1973.

32.   Wrenn   F.R., Science 113: 525, 1951.

33.   Baker   W.H., N. Engl. J. Med. 252: 612, 1955.

34.   Zipper   A. and Freedberg A.S., Cancer Res. 12: 867, 1952.

35.   Charkes   N.D., Skarooff   D.M., Cantor   R.E., Recent
Advances in Nuclear Medicine, New York, Appleton-Century-Crofts,
1966 p.235.

36.   Baker, W.H., N. Engl. J. Med. 252: 612, 1955.

37.   Carr   E.A. Jr., Radioactive Pharmaceuticals (Andrews
G.A., Kinsely   R.M., Wagner H.N. Jr Eds.) AEC Symp. Series
6, April 1966, p.619.

38.   Ferguson D.J. and Harper P.V., Ann. Surg. <u>174</u>: 419, 1971.

39.   DeLong R.P., Cancer <u>3</u>: 718, 1950.

40.   Uchiyama G. in Nuclear Medicine, Crall M.N., Brady L.W. Eds. New York, Appleton-Century-Crofts, 1969, p.235.

41.   Murray I.P., Br. Med. J. <u>2</u>:653, 1970.

42.   Nishiyama H., Sodd V.J., Schreiber T.J., Lovdon R.G., Saenger E.L. in Radiopharmaceuticals, Subramania G., Rhodes B.A., Copper J.F., Sodd V.J. Eds., New York Society of Nuclear Medicine, 1975, p.482.

43.   Hayes R.L. in Tumor localization with Radioactive Agents 1974 (Proc.Symp. Vienna 1974) 1, IAEA Vienna: 29, 1976.

44.   Hisada K. in Tumor localization with Radioactive Agents 1974 (Proc. Symp. Vienna 1974) 1 IAEA Vienna: 113, 1976)

45.   Hayes R.L. and Edwards C.L. in Medical Radioisotope Scinitigraphy 1973 (Proc. Symp. Vienna 1973) 2, IAEA Vienna: 531, 1973

46.   Goodwin D.A., in Radiological and Other Biophysical Methods in Tumor Diagnosis, Chicago, Year Book Medical Publishers Inc., 1975, p.57.

47.   Saha G.B., and Farrer P.A. in Radiopharmaceuticals, Subramania G., Rhodes B.A., Copper J.F., Sodd V.J. Eds., New York Society of Nuclear Medicine, 1975, p.435.

48.   Hunter W.W. Jr. and Riccobono X.J., J. Nucl. Med. <u>11</u>:328, 1970.

49.   Goodwin D.A. et al. Radiol. <u>100</u>: 175, 1971.

50.   Konikowski T. et al., J. Nucl. Med. <u>15</u>:508, 1974.

51.   Farrer P.A. et al., J. Nucl. Med. <u>13</u>:429, 1972.

52.   DeLucas S. et al., Clin. Nucl. Med. <u>2</u>:179, 1977.

53.   Goodwin D.A. et al., J. Nucl. Med. <u>12</u>:434, 1971.

54.   Merrick M.V. et al. in Medical Radiosotope Scintigraphy 1972 (Proc. Symp. Monte Carlo, 1972) 2, IAEA Vienna: 721, 1973.

55.   Wolf R. and Fischer J. in 45th Dtsch. Rontgen-
kongress, Wesbaden 1964, G. Thieme, Stuttgart:57, 1965.

56.   Gardel J. et al., Ann. Otto-Laryngo 84:633, 1967.

57.   Isaac R. et al., Nucl. Medizin 7:97, 1968.

58.   Buchwald W. et al., Radioisotope in der Lokal-
isationsdiagnostil, Schattaure-Verlag Stuttgart: 549, 1967.

59.   Wolf R. and Fischer J., Radionuklide in der
klinischen und experimentellen Onkologie, Zweite Jahrestagung
der Gesellschaft fur Nuklearmedizin, Heidleberg: 223, 1965.

60.   Wolf R., Rontgenkongress, Wesbaden 1964, G. Thieme,
Stuttgart: 57, 1965.

61.   Raynaund C. et al., J. Fr. Med. Chir. Thorac. 21:
735, 1967.

62.   Lamy P. et al., J. Fr. Med. Chir. Thorac. 23: 159, 1969.

63.   Pecorini V. et al., Rev. Biol. Med. Nucl. 2: 197, 1970.

64.   Isaac R. et al., J. Fr. Med. Chir. Thorac. 3:225, 1970.

65.   Isaac R., These de Medicine, Faculte de Medecine,
Paris, 1970.

66.   Rescigno B. et al., Riv. Patol. Clin. Tuberculosi
44: 149, 1971.

67.   Farrer P.A. et al., J. Nucl. Med. 15:490, 1974.

68.   Raynaud G. and Comar D., in Tumor Localization
with Radioactive Agents 1974 (Proc. Symp. Vienna 1974) 1,
IAEA Vienna: 57, 1976.

69.   Farrer P.A. et al., J. Nucl. Med. 15:489, 1974.

70.   Saha G.B. and Farrier P.A. in Radiopharmaceuticals
Subramania G., Rodes B.A., Cooper J.F. and Sodd V.J. Eds.
New York: Society of Nuclear Medicine, 1975, p.435.

71.   Raynaud C., J. Fr.Med. Chir. Thorac.

72.   Isaac R. et al., J. Fr. Med. Thorac.7:771, 1969.

73.   Gotta H. et al., Nucl. Medizin 12:275, 1974.

74.   Wagenr H.N. et al., Arch. Intern. Med. 113:696, 1964.

75.   Sodee D., Radioaktive Isotope in Klinik and Forschung 6:167, 1964.

76.   Johnston G.S. et al., J. Nucl. Med. 6: 549, 1965.

77.   Sodee D.B., J. Nucl. Med. 4: 194, 1963.

78.   Blau M. and Bender M., J. Nucl. Med. 3:83, 1962.

79.   Wolf R. and Fischer J. in 45th Dtsch. Rontgenkongress, Wiesbaden 1964, G. Thiem, Stuttgart: 57, 1965.

80.   Gotta H. et al., Nucl. Medizin. 12:285, 1974.

81.   Brooks W.H. et al., J. Nucl. Med. 15: 620, 1974.

82.   Krishinamurthy G.T. et al., J. Nucl. Med. 13: 373, 1972.

83.   Quinn J.L. et al., JAMA 194: 157, 1965.

84.   Soloway A.H., J. Pharm. Sci. 63: 647, 1974.

85.   Steinberg M. et al., J. Clin. Endocrin. 31:81, 1970.

86.   Sparagana M. et al., J. Nucl. Med. 11:224, 1970.

87.   Dos Remedios L.V. et al., J. Nucl. Med 12: 673, 1971.

88.   Cancroft E.T. et al., Radiol. 106: 441, 1973.

89.   Villarreal R.L. et al., Radiol. 111:657, 1974.

90.   Stebner F.C. et al., Am. J. Surg. 116: 513, 1968.

91.   Schall G.L. and Di Chiro G., Sem. Nucl. Med. 2:270, 1972.

92.   Baron J.M. and Rosen G., in Medical Radioisotope Scintigraphy 1972 (Proc. Symp. Monte Carlo, 1972) 2, IAEA, Vienna: 141, 1973.

93.   Hever H.E. and Ehilers N., Ann. Ocul 205: 283, 1972.

94.   Fazio C. et al., J. Nucl. Med. 10: 508, 1969.

95.   Whitley J.E. et al., Am. J. Roentgen. Rad. Nucl. Med. 67: 706, 1966.

96.   Gleen H.J. et al., in Tumor Localization with Radio-active Agents (Proc. Symp. Vienna 1974) 1, IAEA, Vienna: 63 1976.

97.   Usher M.S. et al., J. Nucl. Med. 12:136, 1971.

98.   Meighan J.W. and Dworkin H.J., J. Nucl. Med. 11: 173, 1970.

99.   Tonami N. and Hisada K., Clin. Nucl. Med. 2:75, 1977.

100.   Salvatore M. et al., radiol.121: 487, 1976.

101.   Kim, E.E. DeLand F.H., Maruayamay., Ho E., J. Nucl. Med. 19:64, 1978.

102.   Durbin P.W., et al., Proc. Soc. Exp. Biol. Med. 91: 78, 1956.

103.   Hayes R.L. et al., ORAU-123, 1973, p.56.

104.   Hisasa K. and Andio A.J. Nucl. Med. 14:615, 1973.

105.   Hisada K. et al. in Tumor Localization with Radioactive Agents (Proc. Symp. Vienna 1974) 1, IAEA, Vienna: 125, 1976.

106.   Hisada K. et al., Radiol. 116: 389, 1975.

107.   Thesingh C.W., Driessen O.M.J., Th. Daems W., Franken C., Pavwels E.K.J., Scheffer E., Vermeij J., Wisse E., J. Nucl. Med. 19: 28, 1978.

108.   Swartzendruber D.G., Nelson B., Hayes R.K., J. Natl. Cancer Inst 46:941, 1971.

109.   Brown D.H. et al., Cancer Res. 33: 2063, 1973.

110.   Haubold U. et al., in Medical Radioisotope Scintigra-phy 1972 (Proc. Symp. Monte Carlo, 1972) 2, IAEA Vienna 1973, p. 553.

111.   Brown D.H. et al., Cancer Res. 36: 956, 1976.

112.   Aulbert E. et al., Nuklear-Medizin 15:184, 1976.

113. Hammersley P.A.G. and Taylor D.M., in Radiopharmaceuticals, Rhodes G., Copper J.F., and Sodd V.J. Eds. New York: Society of Nuclear Medicine, 1975. p.447.

114. Menson S. et al., J. Nucl. Med. 19:44, 1978.

115. Tsan Min-Fu et al., J. Nucl. Med. 19:36, 1978.

116. Handmarker H. and O'Mara R.E., J. Nucl. Med. 18: 1057, 1977.

117. Larson S.M., Milder M.S., Johnston G.S. in Radiopharmaceuticals, Subramania G., Rhodes B.A., Copper F.J., and Sodd V.J. Eds. New York: Society of Nuclear Medicine, 1975, p.413.

118. New England Nuclear Gallium Citrate Ga67 Nuclear Department Reference, NEN, Mass 1976.

119. Patel A.R., Shah P.C., Sirpal S.C., Dulay C.C., Clin. Nucl. Med. 2:368, 1977.

120. Blei C.L., and Rollo F.D., J. Nucl. Med. 18: 445, 1977.

121. Gill S.P., Thrall J.H., Beauchamp M.L., J. Nucl. Med. 18: 312, 1977.

122. Hopkins G.B. et al., Clin. Nucl. Med. 2:345, 1977.

123. Bekerman C. Schulak J.A., Kaplan E.L., Shen K., J. Nucl. Med. 18:1096, 1977.

124. Myerson P.J. et al., J. Nucl. Med. 18: 893, 1977.

125. Park H.M., Clin. Nucl. Med. 1:269, 1976.

126. Myerson P. et al., Clin. Nucl. Med. 1 108, 1976.

127. Lyond K.P., Clin. Nucl. Med. 1: 134, 1976.

128. Luinia S., Chodas R.B., Sundaresh R., Clin. Nucl. Med. 1:263, 1976.

129. Kastl W.H., Soileau A.P., Prevot G.M., Clin. Nucl. Med. 2:245, 1977.

130. Berg G.R., Appl. Radiol. :127, 1976.

131. Lavender R.L. et al., Br. J. Radiol. 44:361, 1971.

132. Lunia S., Chadas R.B., Goel V., Clin. Nucl. Med. 1: 125, 1976.

133. Kaplan R.L. Griep R.J., Schuffler M.D., Silliman R.A., J. Nucl. Med. 18:448, 1977.

134. Perez J., Rivera J.V., Bermudez R.H., Radiol. 123:695, 1977.

135. Kumar B., Alderson P.O., Geisse G., J. Nucl. Med. 18: 534, 1977.

136. Lisbona R. and Rosenthall L., Clin. Nucl. Med. 2:337, 1977.

137. Siberstein E.B., A.J.M. 60: 226, 1976.

138. Larson S.M., Milder M.S., Johnston G.S., in Radio-pharmaceuticals, Subramania G.,Rhodes B.A., Copper J.F., Sodd V.J. Eds. New York Society of Nuclear Medicine, 1975 p.413.

139. Turner D.A., Pinsky S.M., Gottschalk A., Radio-logy 104: 97, 1972.

140. Johnston G., Benva R.S., Teates C.D., J. Nucl. Med. 15: 399, 1974.

141. Johnston G. Go M.A., Benva R.S., Larson S.M., Andrews G.A., Bubner K.F.,J. Nucl. Med. 18:692, 1977.

142. Greenlaw R.H., Weinstein M.B., Brill A.B., J. Nucl. Med. 15:404, 1974.

143. Waxman A.D., Lee G., Wolfstein R., J. Nucl. Med. 14: 903, 1973.

144. Wallner R.J., Croll M.N., Brady L.W., J. Nucl. Med. 15:308, 1974.

145. Henkin R.E., Polcyn R.E., Quinn J.L. III, Radiology 106: 595, 1973.

146. Waxman A.D., et al., Radiology 116:675, 1975.

147. Jones A.E. et al., Radiology 112:123. 1974.

148.   Midler M.S. et al., Cancer 32: 803, 1973.

149.   Grove R.B., Pinsky S.M., Brown T.L., J. Nucl. Med. 14: 402, 1973.

150.   Richman S.D., J. Nucl. Med. 46: 996, 1975.

151.   Bailey T.B., Pinsky S.M., Mittenmeyer B.T., Borski A.A., J. Urol. 110:387, 1973.

152.   Frankel R.S. et al., J. Nucl. Med. 15: 491, 1974.

153.   Silberstein E.B., Kornblut A., Shumrick D.A., Saenger E.L., Radiology 110: 605, 1974.

154.   Higashi T. et al., J. Nucl. Med. 18: 243, 1977.

155.   Frankel R.S., Radiol. 110: 597, 1974.

156.   Kaplan W.D. et al., J. Nucl. Med. 15: 424, 1974.

157.   Grove R.B. et al., J. Nucl. Med. 14:403, 1973.

158.   Van de Poll M.A.P.C., Versluis A., Rasker J.J., Jurjens H., Woldring M.G.,Nucl. Medizin. 15:86, 1976.

159.   Zimmermann M. and Hale T., Nucl. Medizin. 15: 176, 1976.

160.   Merrick M.V. et al., in Medical Radioisotope Scintigraphy, vol 2, Vienna, IAEA, 1972, p.721.

161.   Thakur M.V., Int. J. Appl. Radiat. Isot. 24: 357, 1973.

162.   Krohn A.K. Meyer J.M., De Nardo G.L., De Nardo S.J., J. Nucl. Med. 18: 276, 1977.

163.   Grove R.B., Madewell J.E., Rapp G.S., J. Nucl. Med. 14: 917, 1973.

164.   Taylor C.M. and Cottral M.F. in Radiopharmaceuticals, Subramania G., Rhodes B.A., Copper J.F. and Sodd V.J. Eds. New York: Sociatry of Nuclear Medicine, 1975 p.458.

165.   Coates G. et al., J. Nucl. Med. 15: 484, 1974.

166.   Hall J.N. and O'Mara R.F., J. Nucl. Med. 15: 498, 1974.

167.   Eckelman W.C. Rzeszotarski J., Siegel B.A., Kusota H., Meena C., Stevenson J., J. Nucl. Med. 15: 589, 1974.

168.   Thakur M.L. et al. in Radiopharmaceuticals and Labelled Compounds (Proc. Symp. Copenhagen, 1973) 2, IAEA, Vienna, 1973, p.183.

169.   Robbins P.J., Silberstein E.B., Fortman D.L., J. Nucl. Med. 15:338, 1974.

170.   Lin M.S., Goodwin D.A., Kruse S.L., J. Nucl. Med. 15:338, 1974.

171.   Orii H., Jap. J. Clin. Radiol. 18:211, 1973.

172.   Rayadu G.V.S. et al., J. Nucl. Med. 15:526, 1974.

173.   Leh F.K.V. and Wolf W., Int. J. of Pharm. 1:41, 1978.

174.   Renault H. et al., in Radiopharmaceuticals and Labelled Compounds, Vienna, IAEA, 1973, p.195.

175.   Nouel J.P. et al., Proc. First World Congr. Nucl. Med., Tokyo, 1973, p.129.

176.   Nanano S. et al., Ibid, p.700.

177.   Takasu A. et al., Ibid, p.706.

178.   Grove R.B. et al., J. Nucl. Med. 14: 917, 1973.

179.   Watanabe K. et al., Proc. First World Congr. Nuc. Med., Tokyo, 1973, p.937.

180.   Umezawa H. et al., J. Antibiot. 25: 409, 1972.

181.   Suzuki H. et al., J. Antibiot. 23: 473, 1970.

182.   Cheng C.C. and Zee-Cheng K.Y., J. Pharm. Sci. 61: 485, 1972.

183.   Mori T. et al., Proc. First World Congr. Nucl. Med., Tokyo, 1974, p.703.

184.   Nunn A.D., Eur. J. Nucl. Med. 2:53, 1977.

185.   Ganatra D. et al., in Medical Radioisotope Scinti-
graphy (Proc. Symp. Salzburg, 1968) 2, IAEA, Vienna, 1968,
p.25.

186.   Beirwaltes W.H. et al., J. Nucl. Med. 9:489, 1968.

187.   Boyd C.M. et al., J. Nucl. Med. 11:479, 1970.

188.   Boyd C.M. et al., J. Nucl. Med. 12:601, 1971.

189.   Knoll G.F., IEEE Trans Nucl. Sci. N.S. 19: 76, 1972.

190.   Rogers W.L. et al., 1974 Ultrasonic Symposium Pro-
ceedings, IEEE Catalogue #74CHO-896-ISU (IEEE Ultrasonics
Symp. Milwaukee, Nov. 11-15, 1974.

191.   Beirwaltes W.H. et al., Clin. Res. 22: 640, 1974.

192.   Seabold J.E. et al., in Nuclear Medicine in Clinical
Practice, Schneider D.B., Treves S. Eds., ASP Biological
and Medical Press B.V., Amsterdam, 1976.

193.   Bonnet R. in the Porphyrins Vol II, Dolpin D. Ed.,
New York, Academic Press, 1978, p.1.

194.   Auler H. and Banzer G., Z. Krebsforsch 53:65, 1942.

195.   Figge F., AAAS Research Conference on Cancer,
Science Press, 1945, p.117.

196.   Figge F., Weiland G.S., Manganiello L.O.J., Proc.
Soc. Exper. Biol. Med. 68: 640, 1948.

197.   Manganiello L.O.J. and Figge F., Bull. School.
Med. Univ. Maryland 36:3, 1951.

198.   Peck G.C., Mack H.P., Figge F.H.J., Bull. School. Med.
Univ. Maryland 38: 124, 1953.

199.   Ibid.

200.   Meyer-Betz F., Deut. Arch. Skin Med. 112: 476, 1913.

201.   Rassmussen-Taxdal D.S., Wand G.E., Figge F.H.J.,
Cancer Res. Jan-Feb, 1955.

202.   Winkelman J. and Rassmussen-Taxdal D.S., Bull.
John Hopkins Hosp. 107: 228, 1960.

203.   Derrien E. and Turchini P., Compt. Rend. Soc.
Biol. 91: 637, 1924.

204.   Altman K.I. in Porphyrin Biosynthesis and Metabo-
lism, Wolstenholme, G.E.W. and Millar, C.P. Eds, Boston:
Little Brown and Co., 1955, p.86.

205.   Kosaki T., Ikoda T., Kotani Y. Nakagawa S., Saka T.,
Science 127: 1176, 1958.

206.   Lipson R. and Baldes E.J., Arch. Dermat. 82: 508, 1960.

207.   Schwartz S., Absolon K., Vermund H., Conf. on
Porphyrins, X-rays, and Tumors, Univ. Min. June 2-3, 1956 Merk
and Co.

208.   Lipson R., Baldes E.J., Olsen A.M., J. Nat. Cancer
Inst. 26: 1, 1961.

209.   Lipson R., Baldes E.J., Olsen A.M., J. Thorac. Cardiovas.
Surg. 42: 623, 1961.

210.   Winkelman J. Cancer Res. 22: 589, 1962.

211.   With T.K., Scand. J. Clin. Lab. Invest. 10: 186, 1958.

212.   Winkelman J. and Jayes J.E., Nature 30: 903, 1963.

213.   Lipson R., Baldes E.J., Olsen A.M., Diseases of Chest
46: 676, 1964.

214.   Lipson R., Baldes E.J., Gray M.J., Cancer Dec: 2255,
1967.

215.   Leonard J.R. and Beck W.L., Laryn. 7: 365, 1971.

216.   Davis R. and Schwartz S., Nature 214: 186, 1967.

217.   Freeman R.G. and Troll O., Arch. Opthal. 78: 766, 1967.

218.   Sanderson D.R. Fontana R.S., Lipson R.L. Baldes E.J.,
Cancer Nov: 1368, 1972.

219.   McDonagh A.F. Biochem. Biophys. Res. Comm. 44: 1306,
1971.

220.   Diamond I., McDonagh A.F., Wilson O.B., Granelli
S.G., Nielsen S. Jaenicke R., Lancet Dec 2: 1175, 1972.

221.   Dougherty J.. Grindey G.B., Fiel R., Weishaut K.R.,
Boyle D.G., J. Natl. Cancer Inst. 55:115, 1975.

222.   Merkel P. and Kearns D., J. Am. Chem. Soc. 94: 7244, 1972.

223.   Wise B.L., Taxdal D.R., Brain Res. 4:387, 1967.

224.   Van Brunt E., Shepherd M.D., Wall J.R., Ganong W.F., Clegg M.T., Nat. Acad. Sci. 117:217, 1964.

225.   Granelli S.G., Diamond I., McDonagh A.F., Wilson C.B., Nielsen S.L., Cancer Res. 35:2567, 1975.

226.   Gutter B., Speck W.T., Rosenkranz H.S., Biochimica et Biophys. ACTA 475: 307, 1977.

227.   Podkaminsky N., Strahlentherapie 38: 98, 1930.

228.   Cohne L. and Schwartz S., Cancer Res. 26: 1769, 1966.

229.   Mack H.P., Diehl W.K., Peck G.C., Figge F.H.J., Cancer 10:529, 1957.

230.   Schwartz S., and Vermund H., Cancer 11:1119, 1958.

231.   Bases, R.E., Brodie S.S., Ruberfield S., Cancer 11: 259, 1958.

232.   Cittadine G. Lanfredini L., Mancini G., In Radiation Protection Sensitization, Moroson, H.L. and Quintiliani, M. Eds. New York: Barnes and Noble, 1969, p.295.

233.   Fiel R., Mark E.H., Datta Gupta N., Res. Commun. Chem. Path. Pharm. 10:65, 1975.

234.   Von Hemmen J.J., Meuling W.J.A., Bleichradt J.F., Radiation Res. 75: 410, 1978.

235.   Figge F.H.J., Weiland G.S., Mangariello L.O.J., Proc. Soc. Exp. Biol. Med. 68: 640, 1948.

236.   Basses R.E., BNL 326 Oct-Dec, 1954, p.45.

237.   Bases R.E., Brodie S.S., Rubenfeld D., Cancer 11: 259, 1967.

238.   Anghileri L.J., Heidreder M., Mathes R., Nucl. Medizin XV: 183, 1976.

239.   Smetana H., J. BIol. Chem. 125: 741, 1938.

240.   DiNello R.K., Phd thesis, Harward University, 1977.

241. DiNello R.K. and Chang C.K., in the Porphyrins, Dolphin D. Ed., New York: Academic Press, 1978, p.289 Vol 2.

242. Ellfolk N. and Diever G., J. Chromatog., 25: 373, 1966.

243. Morel D.B., Barrett J., Clezy P.S., Biochem. J. 78: 793, 1961.

244. Falk J.E., Porphyrins and Metalloporphyrins, New York: Elsevier, 1964.

245. Thudicum J.L.W., Rep. Med. Off. Privy. Counc. 10: 152 (Appendix 7) 1867.

246. DiNello R.K. and Dolphin D.H., unpublished obs.

247. Jones O.T.G., Biochem. J. 87: 186, 1963.

248. Caughey W.S., Alben J.O., Fujimoto W.Y., York J.L., J. Org. Chem. 31:2631, 1966.

249. Lemberg R., Bloomfield B., Caiger P., Lockwood W.H., Aus. J. Exp. Biol. Med. Sci. 33:435, 1955.

250. Morell D.B., Barret J., Clezy P.S., Biochem. J. 78: 793, 1961.

251. Morell D.B. and Stewart M., Aust J. Exp. Biol. Med. Sci. 34: 211, 1956.

252. Grinstein M., J. Biol Chem. 167: 515, 1947.

253. Carr R.P., Jackson A.H., Kenner G.W., Sach G.S., J. Chem. Soc. C, 1971, p.487.

254. Ellfolk P.S., and Sievers G., J. Chromatogr. 25: 373, 1966.

255. Fischer H. et al., J. Physiol Chem. 242: 131, 1938.

256. Barrett J., Nature 183:1185, 1959.

257. Inhoffen H.H., Bliesener C., Brockman H., Tetrahedron Lett. 31: 3779, 1966.

258. Inhoffen H.H. Brockmann H., Bliesener K.M., Justus Liebigs Ann. Chem. 730: 173, 1969.

259. Schwartz F.P., Gouterman M., Muljiani Z., Dolphin D., Bioinorg. Chem. 2: 1, 1972.

260. Asakura T. and Sono M.J., J. Biol. Chem. 249: 7087, 1974.

261. Clezy P.S. and Fookes C.J.R., Aust. J. Chem. 27: 371 1974.

262. O'Keefe D.H., Phd thesis, Arizona State University, 1974.

263. G.E. Chart of the Nuclides.

264. Anger H.O. and Van Dyke D.C., Science 144: 1587, 1964.

265. Van Dyke D.C., hkurin C., Price D., Yano Y., Anger H.O. Blood 30: 364, 1967.

266. Francois P.E. and Szur, L. Nature 181: 1665, 1958.

267. Yano Y. and Anger H.O., Int. J. Appl. Radiat. Isot., 16: 153, 1965.

268. Silvester D.J. and Sugden J. Nature 210: 1282, 1966.

269. Thakur M.L., Nunn A.D., Waters S.L., Int. J. Appl. Radiat. Isot. 22: 483, 1971.

270. Greene M.W., Lebouitz E., Richards P., Hillman M., Int. J. Appl. Radiation Isot. 21: 719, 1970.

271. Dahl J.R., and Tilbury R.S., Int. J. Appl. Radiation Isot. 23:431, 1972.

272. Garimella V.S., Shirazi S.P.H., Fordham E.W., Int. J. Appl. Radiation Isot. 24: 451, 1973.

273. Saha G.B. and Farrer P.A., Int. J. Appl. Radiation Isot. 22: 498, 1971.

274. Sodd V.J., Scholz K.L., Blue J.W., Medical Physics, 1:25, 1974.

275. Dropesky B.J. and O'Brien H.A. Rep. No. LA-5120-PR, U.S.A.E.C.

276. Cline J.E. and Nieshmidt E.B., Nucl. Phys. A169: 437, 1971.

277. J.B. Dropesky and O'Brien H.A., LA-5120-PR.

278. Rothe J.W. Stahl u. Eisen 12:1052, 1892.

279. Irvine in Solvent Extraction in Analytical Chemistry, Morrison, GH and Freiser, H. New York: John Wiley and Sons, 1957, p.118.

280. Dodson R.W., Forney G.J., Swift E.H., J. Am. Chem. Soc. 58:2573, 1936.

281. Nachtreib N.H. and Conway J.G., J. Am. Chem. Soc. 70: 3547, 3552, 1948.

282. Myers R.J., Metzler D.E., Swift E.H., J. Am. Chem. Soc. 72: 2573, 3767, 1950.

283. Wada I. and Ishii R., Bull. Inst. Phys. Chem. Res. Tokyo 13: 264, 1934.

284. Nachtreib N.H. and Conway J.G., J. Am. Chem. Soc. 70: 3552, 3547, 1948.

285. Sandell E.B., Colorimetric Determination of Traces of Metals, New York, Interscience Pub., 1959.

286. Specker H. and Doll W., Z. Anal. Chem. 152:178, 1956.

287. Steinbach J.F., U.S.A.E.C. Report No.NYO-6347, 1953 (University of Pittsburg).

288. McKaveney J.P., U.S.A.E.C. Report No. NYO-6507, 1957 (University of Pittsburg).

289. Reid J.C. and Calvin M., J. Am. Chem. Soc. 72: 2948, 1950.

290. Bolomy R.A. and Wish L., J. Am. Chem. Soc. 72: 4483, 1950.

291. Furman N.H. et al., Anal. Chem. 21: 1325, 1949.

292. Sandell E.B. and Cummings P.F., Anal. Chem. 21: 1356, 1949.

293. Diehl H. and Smith G.F., The Iron Reagents, G. Frederick Smith Chemical Co, Columbus, Ohio, 1960.

294. Krohnke F., Ber. 60:527, 1927.

295. Kraus C.A., U.S.A.E.C. Report No.A-1099, 1944.

296. Korpak W. and Deptuka C., U.S.A.E.C. Report No. NP-7238, 1958.

297.   Moore   G.E. and Kraus   K.A., J. Am. Chem. Soc. 72: 5792, 1950.

298.   Warren   G.W. and Fink   R.W., J. Inorg. Nucl. Chem. 2:176, 1956.

299.   Pollard   F.H., McOmie J.F.W., Stevens H.M., Maddock J.G., J. Chem. Soc. 1338, 1953.

300.   Bighi   C., Ann. Chim. (Rome)   45:532, 1955.

301.   Stevens   H.M., Anal. Chim. Acta   15: 538, 1956.

302.   Buchler   J.W. in the Porphyrins Vol II, Dolphin D. Ed., New York, Academic Press, 1978, p.389.

303.   Nunn   A.D., J. of Labelled Compounds and Radiopharmaceuticals, XVI: 140, 1979.

304.   W. Wiesehahn. SFU Dose Computer Program, Simon Frazer University, Burnaby.

305.   G. Rudstam, Zeitschrift fur Naturforschung 219: 1027, 1966.

306.   A. Siberberg and R. Taso.   The Astrophysical J. Suppl. 220   25: 315, 1973.

307.   Thaller   R.A., TRIUMF TSAC Report: Expected Radiation Levels from the Production of^{52}Fe by Ni Spallation, Jan 1979.

308.   TRIUMF Drawing D-4456 General Assembly.

309.   Thaller   R.A., TRIUMF TSAC Report: Application to Handle 1 Curie of Activity in the New Hot Cell in the Temporary Isotope Laboratory, 1979.

310.   Thaller, R.A., TRIUMF Temporary Isotope Laboratory Hot Cell Manual, 1979.

311.   Sephton   R.G., Hodgson   G.S., Abrew S.,Harris A.W., J. Nucl. Med. 19: 930, 1978.

312.   Loevinger   R. and Berman   N., NM/MIRD Pamphlet #1 Revised New York, Society of Nuclear Medicine, 1976.

313.   Snyder   W.S., Ford M.R., Warner   G.G., Watson   S.B., NM/MIRO   Pamphlet #11, New York, Society of Nuclear Medicine, 1975.